

To- Mom, Dad, Zadie and Sheryl whose encouragement, understanding and love made it all possible.

Acknowledgment

The author would like to express his sincere appreciation and gratitude to

Marshall Fixman, research advisor, teacher, scholar, and friend whose insight and inspiration made this work a reality,

Alfred Holtzer, professor and valued friend, whose contagious enthusiasm introduced me to the joys and excitement of science,

Ronald Lovett, teacher and savant who first taught me statistical mechanics,

The other members of my thesis committee, Tom Keyes and Don Crothers, for stimulating and useful discussions,

John Mercer and Glenn T. Evans, as well as all the occupants of the Theoretical Wing for many hours of exciting conversation and,

The National Institutes of Health for financial support.

Contents

Page

List of Tables

List of Illustrations

Chapter 1: General Introduction

0. Introductory Remarks

Chapter 2: Screened Coulomb Interactions on a Dielectric Cylinder
with Applications to Manning's Limiting Laws

I. Introduction

II. Charge Outside or on the Cylinder: Formal Theory

III. Numerical Results for Charges on the Cylinder

IV. Charge Inside a Cylindrical Low Dielectric Region

V. Helical Array of Charges

VI. Discussion of Results

Chapter 3: The Wormlike Polyelectrolyte

VII. Introduction

VIII. Calculation of the Electrostatic Persistence Length

VIII A. General Formalism

VIII B. Continuous Charge Distribution with No Rearrangements or Fluctuations

VIII C. Continuous Charge Model with Rearrangements but no Fluctuations

VIII D. Continuous Charge Distribution with Rearrangements and Fluctuations

IX. Comparison of Theoretical Electrostatic Persistence Length with Experiment

X. The Colligative Properties of a Wormlike Polyelectrolyte

Chapter 4: The Polyelectrolyte Excluded Volume Paradox

XI. Introduction

List of Tables

Table		Page
I.	Cylinder radius a versus the maximum salt concentration line of charge in bulk solvent adequately predicts the colligative properties of an infinite pitch helix	
II.	$4\pi\Delta h_n$ as a function of n and κ for an α helix, $P/a = .68$	
III.	$4\pi\Delta h_n$ as a function of n and κ for DNA like helix, $P/a = 3.45$	
IV.	$\beta^{-1} \Delta\psi^{\text{DNA}}$ versus κa	
V.	Comparison of Experimental and Theoretical Electrostatic Persistence Lengths	
VI.	Numerical values of the Integral $R(y)$ compared with the asymptotic large y formula	
VII.	Comparison of the Second Virial Coefficients of Orofino and Flory with Theoretical Results	

Chapter 1: General Introduction

0. Introductory Remarks

A fascinating aspect of the study of polyelectrolytes is the interplay between their chainlike nature and ionic character. On the one hand, we are interested in the electrochemical properties of polyelectrolyte solutions; e.g. the influence the polyion exerts on the osmotic and activity coefficients of the simple salt molecules. On the other hand, the charge density of the polymer greatly affects the expansion of the polyion and all related physical properties that depend on chain extension. Obviously, the two classes of problems are quite intertwined. The interaction of the polyelectrolyte with its ion atmosphere results in a modification of segment-segment repulsions and concomitant alteration of the coil's expansion. Conversely, both the geometry and charge of the polyion determine its effect on the mobile ions. All studies of the equilibrium properties must address themselves to the dual nature of polyelectrolyte solutions; our work, in particular, is no exception.

A considerable simplification in the calculation of polyelectrolyte properties results if the geometry of the polyion can be specified. Fortunately, a wide class of polyelectrolytes may be approximated, either locally or even globally, as low dielectric, salt excluding cylinders. Assuming the polyelectrolyte is a very long cylinder, we explore, in chapter two, a question of importance in polyelectrolyte theory: Precisely what is the influence of the low dielectric constant backbone on the interaction energy between a charge on a polymer and another ion? More generally, we treat various discrete and continuum charge distribution models to obtain insight into the effects of the dielectric cylinder.

For some polyelectrolytes such as DNA, a long low dielectric cylinder

is a quite reasonable representation of their actual conformation. However, if one considers semiflexible, random coil polyelectrolytes such as carboxymethylcellulose, while the global conformation is not a cylinder it seems quite likely that there are quasilinear stretches within a given contour length of the molecule. The preceding is highly suggestive that the wormlike polymer model of Kratky and Porod should be applicable to ionic as well as uncharged polymers. In chapter three, we calculate the electrostatic persistence length, P_{el} , and colligative properties of an unperturbed, stiff wormlike polyelectrolyte. An important and not unexpected qualitative result emerges from our study: if the ionic strength is sufficiently low, P_{el} may be quite large; in other words, the polyelectrolyte is locally quite rodlike.

Certainly one of the most annoying failures of equilibrium polyelectrolyte theories is their inability to predict the functional dependence of the expansion factors, α^3 , and second virial coefficients, A_2 , on molecular weight and simple salt concentration. This is a tantalizing problem, and in chapter four we present a possible guide to the resolution of it. As indicated previously, at low ionic lengths, a polyelectrolyte is locally rodlike. It, therefore, seems reasonable to treat the interacting segments as uniformly charged rods rather than "points". If the charge density is employed as an adjustable parameter, reasonably close agreement with experiment for α^3 and A_2 are obtained over a considerable range of degrees of ionization and ionic strength.

A further word is necessary before commencing with the body of the text: We have made extensive use of appendices. Where appropriate, the reader is urged to consult them if additional mathematical details or consideration of somewhat more general cases is desired.

Chapter 2 Screened Coulomb Interactions on a Dielectric Cylinder with Applications to Manning's Limiting Laws

I. Introduction

Although linear polyelectrolytes have been extensively studied for many years, the influence of the low dielectric constant backbone on the potential of mean force between a charge on the polymer and another ion is not well understood. We have studied this potential on the basis of classical electrostatic theory, which is supplemented by Debye-Hückel screening. One would like to know under what conditions, if any, the backbone behaves as if it were electrostatically invisible.

We cannot hope to summarize the vast body of polyelectrolyte literature which in one way or another models the low dielectric constant effect; rather a brief review emphasizing the ideas that influenced the present work will be undertaken.

An early consideration of the effect of a local dielectric constant appears in the work of Kirkwood and Westheimer^{1,2} on the electrostatic influence of substituents on the dissociation constants of organic acids. The organic acid is treated as a spherical, and subsequently ellipsoidal, low dielectric constant region within which an arbitrary discrete collection of charges is located. The molecule is assumed to be immersed in salt-free, bulk solvent. Kirkwood and Westheimer express the electrostatic free energy in two parts: one part represents the Coulomb interaction of charges immersed in an infinite medium of dielectric constant characteristic of the molecule, and the other part gives boundary corrections. Buff, Beveridge, et al^{3,4}, have recently noted many related problems, and devised several solutions for spherical boundaries.

A logical extension of the work of Kirkwood and Westheimer to polyelectrolyte systems was made by Harris and Rice.⁵ Each polyion is modeled as a spherical region of low dielectric constant, D , within which a fixed, discrete collection of charges reside. In addition, the mobile ions are assumed to permeate the entire polyion domain. Rice and Harris solve the linearized Poisson-Boltzmann equation and find the potential separates into two classes of terms: The first group is the spherically symmetric screened coulomb potential with a dielectric constant D . The second type of terms characterize the boundary effects.

While it may perhaps be appropriate to model some polyions as low dielectric constant spherical domains, there exist polyelectrolytes, such as short DNA, that are best approximated by cylinders. Additionally, the representation of the polyion backbone as a low dielectric constant cylinder may provide a more realistic description of the actual physical situation.

Hill⁶ has solved the linearized Poisson-Boltzmann equation in cylindrical coordinates for an isolated, uniformly charged cylinder immersed in bulk solvent. The electrostatic free energy, W , of such a cylinder is

$$W = \frac{Z^2 L}{D_2} \left\{ \frac{K_0(\lambda a)}{\lambda a K_1(\lambda a)} + \ln(a/b) \right\} \quad (1.1)$$

where: Z is the charge per unit length of the cylinder. κ^{-1} is the screening length. D_2 is the bulk dielectric constant. L is the length of the cylinder. $K_0(x)$ and $K_1(x)$ are modified cylindrical Bessel functions of the second kind, a is the distance closest approach and b is the radius

of the cylinder. It is of interest to observe that W is independent of the internal dielectric constant, D_1 , of the cylinder. There is, however, no reason to assume a priori that the potential for a more realistic charge distribution will remain independent of the interior dielectric constant. Indeed, the latter turns out to have large effects on the potential of discrete charge distributions.

For discussions of charge condensation, we refer to the literature⁷⁻¹⁴. Evidence exists that the linearized Poisson-Boltzmann equation describes the electrostatic potential outside the layer of condensed ions, and our use of that equation may therefore be consistent with condensation. In sections II to IV, we are concerned with a solution of the linearized equation and not with its domain of application. Only in section V do we employ condensation in the calculation of the colligative properties of colligative polyelectrolytes.

In section II, we obtain the formal solution, ψ_T , to the linearized Poisson-Boltzmann equation for a point source charge located on or outside a dielectric cylinder. The cylinder is supposed impermeable to the salt solution in which it is immersed and to have a dielectric D_1 different from the bulk value D_2 . Solution of this problem is equivalent to the determination of the interaction energy between two charges one of which is outside or on the cylinder. To obtain insight into the long range behavior of ψ_T , we analytically calculate ψ_T between two charges spatially far apart but near or on the cylinder. Finally, when the axial distance between two colinear charges on the surface of the cylinder is small, ψ_T is equivalent to the potential between two charges on a planar boundary separating two different dielectric media.

In section III, numerical results are given for the special case that

both charges are on the surface of the cylinder, either on the same or opposite sides, and are separated by an axial distance Z .

Section IV examines the potential, G_T , arising from a point charge located inside the low dielectric constant cylinder. The method of attack is similar to that of section II. In general one finds G_T is quite complicated. A considerable simplification in G_T arises if we assume there is no salt excluding region within the dielectric cylinder or equivalently if we assert a salt free solution is present. These situations are investigated in some detail. Analogous to the work of Harris and Rice⁵, we find that G_T can be expressed as the sum of the screened coulomb potential arising from a point charge in solvent of dielectric constant D_1 , and boundary effects. At the close of section IV, we consider the potential between two charges far apart from each other but within the low dielectric cylinder.

In section V, helical charge distributions are considered. The solution to this problem is relevant to the calculation of colligative properties, and possibly also to the question of structural stability.

As a first approximation, it seems reasonable to view the helical polyion as a thin helical stripe of charge embedded on the surface of a low dielectric, mobile ion free cylinder. α helices are represented by a single helical stripe of charge: DNA type double helices are modeled by two helical stripes of charge 180° out of phase with each other. When the pitch of the helix is infinite, the helix becomes a line of charge embedded on the surface of a low dielectric cylinder. Such a model is appropriate for linear, non-helical polyelectrolytes⁸ and is therefore examined.

The difference between the electrostatic free energy, F_{excess} of the

uniform charge distribution and the helical stripe is found to be rather small for either the α helix or for DNA, but increases with increasing pitch and increasing salt concentration. Possibly the difference might be significant for DNA at high salt concentrations. Furthermore, the severe effect of the dielectric cylinder on the interaction between two point charges has a different sign depending on whether the charges are on the same or opposite sides of the cylinder, and there is evidently a major cancellation for a helical distribution.

As the deviations from ideality of polyelectrolyte colligative properties depend on $(\partial F_{\text{excess}}/\partial K)_{T,V}$, we determine this quantity for the α helix, line of charge and DNA double helix. In each case, we delineate the conditions under which the line of charge in bulk solvent model is appropriate and when corrections become necessary. Finally, we formulate extended Manning limiting laws for the osmotic and activity coefficients of α helical and DNA polyelectrolytes.

II. Charge Outside or On The Cylinder: Formal Theory

In this section, we present a general treatment of the potential, ψ_T , due to a point charge located on or outside an infinitely long, low dielectric constant, salt-excluding cylinder immersed in a 1:1 aqueous salt solution. If the charge were situated in a homogeneous bulk medium, ψ_T would be given by the spherically symmetric, screened coulomb potential ψ_{DH}

$$\psi_{DH}(r) = q_j \frac{e^{-\kappa |r - r_j|}}{D_2 |r - r_j|} \quad (II-1)$$

q_j is the charge of the ionic species at r_j giving rise to the potential, D_2 is the bulk solvent dielectric constant and $\kappa^2 = (8\pi q^2 C_S N_A) / (1000 D_2 k_B T)$ q is the protonic charge, k_B is Boltzmann's constant and T is the absolute temperature. C_S is the 1:1 salt concentration in moles/liter, and N_A is Avogadro's number. However, due to the presence of the cylinder, two effects on ψ_T are expected: First of all, there should be an increase in ψ_T relative to ψ_{DH} because there is a low dielectric constant region near the point charge. Moreover, since simple salt is excluded from that portion of space occupied by the cylinder, an additional increase in ψ_T results. Finally, if the charge were moved from on the cylinder into the bulk solution, ψ_T should decrease. When both r and r_j are infinitely far from the cylinder $\psi_T = \psi_{DH}$.

We begin by employing Poisson's equation which relates the potential ψ_T to the charge density, ρ

$$\nabla^2 \psi_T(\underline{r}) = -\frac{4\pi\rho(\underline{r})}{D} \quad (\text{II-2})$$

D is the dielectric constant of the medium in which charges having total charge density ρ are immersed. Now, ρ is composed of three terms

$$\rho = \rho_+ + \rho_- + \rho' \quad (\text{II-3a})$$

ρ_+ and ρ_- refer to the charge density of the mobile positive and negative salt ions respectively.

$$\rho_+ = q_0 \rho_0 \exp[-q\psi/k_B T] \quad \rho_- = -q_0 \rho_0 \exp[+q\psi/k_B T] \quad (\text{II-3b})$$

ρ_0 is the equilibrium salt concentration in ions per unit volume. In addition, ρ' is the charge density resulting from the point charged fixed at \underline{r}' and is given by

$$\rho' = q \delta(\underline{r} - \underline{r}') \quad (\text{II-3c})$$

We shall treat the linearized version of Eq. II-2. Employing Eq. II-3a-c in Eq. II-2 and linearizing the exponential terms, the linearized Poisson-Boltzmann equation of Debye-Hückel is obtained,

$$(\nabla^2 - \kappa^2) \psi_T = -\frac{4\pi q}{D} \delta(\underline{r} - \underline{r}') \quad (\text{II-4})$$

Hence, ψ_T is the Green's function of the operator $\nabla^2 - k^2$.

By incorporating the effect of the salt excluding, low dielectric cylinder of radius a , we must solve

$$\nabla^2 \psi_T = -\frac{4\pi q_0}{D_1} \delta(r-r') \quad r \leq a \quad (\text{II-5})$$

(r is the distance in cylindrical coordinates from the principal axis of the cylinder)

$$(\nabla^2 - \chi^2) \psi_T = -\frac{4\pi q_0}{D_2} \delta(r-r') \quad r \geq a \quad (\text{II-5b})$$

Eq. II-5a merely states that within the cylinder there is a mobile ion-free, homogeneous medium of dielectric constant D_1 . By Eq. II-5b, outside the cylinder, mobile ions are present in a medium of dielectric constant D_2 . Thus, we want to determine ψ_T which satisfies Eq. II-5a and 5b subject to the appropriate boundary conditions.

Before determining ψ_T , let us briefly review the solution to the homogeneous Debye-Huckel equation in cylindrical coordinates, i.e.,

$$r^{-1} \frac{\partial}{\partial r} r \frac{\partial \Phi}{\partial r} + r^{-2} \frac{\partial^2 \Phi}{\partial \theta^2} + \frac{\partial^2 \Phi}{\partial z^2} - \chi^2 \Phi = 0 \quad (\text{II-6})$$

Setting $\Phi(r, \theta, z) = R(r)Q(\theta)Z(z)$ and requiring that Φ remains finite as $z \rightarrow \infty$ and $\Phi(r, \theta, z) = \Phi(r, \theta + 2\pi, z)$ it readily follows that

$$Q(\theta) = e^{\pm i n \theta} \quad (\text{II-7a})$$

$$Z(z) = e^{\pm i\ell z} \quad (\text{II-7b})$$

$$R_n(\lambda r) = A I_n(\lambda r) + B K_n(\lambda r) \quad (\text{II-7c})$$

n is an integer. In addition, the I_n and K_n are the modified Bessel functions of the first and second kind respectively, and

$$\lambda^2 = \ell^2 + \gamma^2$$

The Green's function, ψ_T , is the potential due to a point charge located at $\underline{r}' = (r', \theta', z')$ and satisfies Eq. II-5a and II-5b;

$\psi_T = \psi_T(r, r', \theta, \theta', z, z')$. We consider here the case of a point charge outside the cylinder; that is $r' \geq a$

Now,

$$\delta(z-z') = \pi^{-1} \int_0^\infty d\ell \cos \ell(z-z') = (2\pi)^{-1} \int_{-\infty}^\infty d\ell e^{i\ell(z-z')} \quad (\text{II-8})$$

$$\delta(\theta-\theta') = (2\pi)^{-1} \sum_{n=-\infty}^{+\infty} e^{in(\theta-\theta')}$$

Whereupon, it is possible to express $-4\pi q \delta(\underline{r}-\underline{r}')$ as

$$-4\pi q \delta(\underline{r}-\underline{r}') = -\frac{q}{\pi} \sum_{n=-\infty}^{+\infty} \int_{-\infty}^\infty d\ell \exp[i\{\ell(z-z') + n(\theta-\theta')\}] \frac{\delta(r-r')}{r} \quad (\text{II-9})$$

Furthermore, ψ_T is expanded in terms of the separated solutions of Eq. II-7a-c

$$\psi_T = \sum_{h=-\infty}^{+\infty} \int_{-\infty}^{+\infty} dl R_h(\lambda' r) \exp[i\{h\theta + lz\}] \quad (\text{II-10})$$

where

$$\chi^2 = \begin{aligned} & l^2 \quad \text{if } r \leq a \\ & l^2 + \kappa^2 \quad \text{if } r > a \end{aligned} \quad (\text{II-11})$$

i.e., salt is excluded from the space occupied by the cylinder. Substituting Eq. II-9 and II-10 into Eq. II-4 with II-5a and 5b, it follows that

$$\begin{aligned} \sum_{h=-\infty}^{+\infty} \int_{-\infty}^{+\infty} dl \left\{ \frac{d^2 R_h}{dr^2} + r^{-1} \frac{d R_h}{dr} - \left(\chi'^2 + \frac{h^2}{r^2} \right) R_h \right\} e^{i[h\theta + lz]} = \\ - \frac{q}{\pi D} \sum_{h=-\infty}^{+\infty} \int_{-\infty}^{+\infty} dl \frac{\delta(r-r')}{r} \exp[i\{l(z-z') + h(\theta-\theta')\}] \end{aligned} \quad (\text{II-12})$$

where for convenience we have written $R_h(\lambda' r)$ as R_h .

By equating the coefficients of $\exp[i(h\theta + lz)]$ on both sides of Eq. II-12,

we obtain,

$$\frac{d^2 R_n}{dr^2} + r^{-1} \frac{dR_n}{dr} - \left(\lambda'^2 + \frac{n^2}{r^2} \right) R_n = -\frac{q \delta(r-r')}{D(r)r} e^{-i(\ell z' + n\theta')} \quad (\text{II-13})$$

Here

$$D(r) = \begin{cases} D_1 & \text{if } r \leq a \\ D_2 & \text{if } r > a \end{cases} \quad (\text{II-14})$$

The $R_n(\lambda'r)$ must satisfy

$$A I_n(\lambda r) \quad r \leq a \quad (\text{II-15a})$$

$$R_n(\lambda'r) = B I_n(\lambda r) + C K_n(\lambda r) \quad a \leq r \leq r' \quad (\text{II-15b})$$

$$E K_n(\lambda r) \quad r' \leq r \quad (\text{II-15c})$$

A, B, C, E are constants to be determined from the boundary conditions of the problem. Eq. II-15a insures that the potential due to a point charge at r' , $r' \geq a$ remains finite at r equal to zero. Eq. II-15c guarantees that the potential goes to zero as r goes to infinity.

The following boundary conditions allow determination of A, B, C, and E:

$$A I_n(\lambda a) = B I_n(\lambda a) + C K_n(\lambda a) \quad (\text{II-16})$$

From Eq. II-15-b for $r=r'-\epsilon$, $x'=\lambda r'$ and in the limit $\epsilon \rightarrow 0$

$$R_n(x') = B I_n(x') + C K_n(x') \quad (\text{II-21})$$

Similarly, at $r=r'+\epsilon$, in the limit $\epsilon \rightarrow 0$

$$R_n(x') = E K_n(x') \quad (\text{II-22})$$

Inserting Eq. II-21 and Eq. II-22 into Eq. II-20

$$x' \{ E K_n'(x') - B I_n'(x') - C K_n'(x') \} = \frac{-q e^{-i[n\theta' + l z']}}{\pi D_2} \quad (\text{II-23})$$

the prime on I_n and K_n denotes the derivative with respect to x evaluated at $x=x'$. Consequently, we have four equations in four unknowns, the explicit calculation of A, B, C and E is found in Appendix A.

Since all the properties we shall subsequently calculate depend on ψ_T for $r \geq a$, we explicitly present our results for the potential outside or on the cylinder. The $r < a$ case is given in Appendix A.

For $r \geq a$

$$R_n(\lambda r) = (\pi D_2)^{-1} q \left\{ I_n(\lambda r_<) K_n(\lambda r_>) + M_n K_n(\lambda r_<) K_n(\lambda r_>) \right\} e^{-i[n\theta' + l z']} \quad (\text{II-24a})$$

$$R_n(\lambda r) = \frac{q}{\pi D_2} \Phi_n(\lambda r) e^{-i[n\theta + \ell z']} \quad (\text{II-24b})$$

where by Eq. A-4

$$M_n = \frac{D_1 \ell I_n(\lambda a) I_n'(\ell a) - D_2 \lambda I_n'(\lambda a) I_n(\ell a)}{D_2 \lambda K_n'(\lambda a) I_n(\ell a) - D_1 \ell I_n'(\ell a) K_n(\lambda a)} \quad (\text{II-25})$$

$r <$ is the minimum of (r, r') .

$r >$ is the maximum of (r, r') .

Note that M_n incorporates the boundary effects, i.e., the salt exclusion by the cylinder and the discontinuity in dielectric constant at $r=a$.

Placing Eq. II-24b into Eq. II-10, we find for all values of D_1 and D_2

$$\Psi_T = \frac{q}{\pi D_2} \sum_{n=-\infty}^{+\infty} \int_{-\infty}^{+\infty} d\ell \Phi_n(\lambda r) \exp[i\ell(z-z') + n(\theta-\theta')] \quad (\text{II-26})$$

which can be rewritten as

$$\begin{aligned} \Psi_T = \frac{2q}{\pi D_2} \left\{ \int_0^\infty dl \cos l(z-z') \left[I_0(\lambda r) K_0(\lambda r') + 2 \sum_{n=1}^\infty I_n(\lambda r) K_n(\lambda r') \cos n(\theta-\theta') \right] \right. \\ \left. + \int_0^\infty dl \cos l(z-z') \left[K_0(\lambda r) K_0(\lambda r') M_0 + 2 \sum_{n=1}^\infty K_n(\lambda r) K_n(\lambda r') M_n \cos n(\theta-\theta') \right] \right\} \end{aligned} \quad (II-27)$$

We now demonstrate in a heuristic way that

$$\frac{q}{D_2} \frac{e^{-\lambda |r-r'|}}{|r-r'|} = \frac{q}{\pi D_2} \left\{ \int_0^\infty dl \cos l(z-z') \left[I_0(\lambda r) K_0(\lambda r') + 2 \sum_{n=1}^\infty I_n(\lambda r) K_n(\lambda r') \cos n(\theta-\theta') \right] \right\} \quad (II-28)$$

A formal proof is found in Appendix B. Define

$$\Psi_S = \frac{2}{\pi D_2} \left\{ \int_0^\infty dl \cos l(z-z') \left[I_0(\lambda r) K_0(\lambda r') + 2 \sum_{n=1}^\infty I_n(\lambda r) K_n(\lambda r') \cos n(\theta-\theta') \right] \right\} \quad (II-29)$$

If we set $\lambda = \lambda$ and $D_1 = D_2$, the salt excluding, dielectric cylinder has been removed. Evaluating Eq. II-25 with $\lambda = \lambda$ and $D_1 = D_2$, one can readily demonstrate that $M_n = 0$ for all n . Whereupon, $\Psi_T(M_n = 0) = \Psi_S$. Moreover, in the absence of the dielectric cylinder, $\Psi_T(M_n = 0)$ must be spherically symmetric, i.e., Ψ_S satisfies

$$(\nabla^2 - \kappa^2) \psi_s = -\frac{4\pi q}{D_2} \delta(\underline{r} - \underline{r}') \quad (\text{II-30})$$

everywhere. This is precisely the Debye-Hückel equation for a point charge in bulk solvent. Consequently,

$$\psi_s = \frac{q}{D_2} \frac{e^{-\kappa |\underline{r} - \underline{r}'|}}{|\underline{r} - \underline{r}'|} = \psi_{DH} \quad (\text{II-31})$$

Substituting Eq. II-31 into Eq. II-27 for $r' \geq a, r \geq a$, and for any value of D_1, D_2, r and r' , we have

$$\psi_T(\underline{r}, \underline{r}') = \frac{q}{D_2} \frac{e^{-\kappa |\underline{r} - \underline{r}'|}}{|\underline{r} - \underline{r}'|} + \frac{2q}{\pi D_2} \int_0^\infty dl \cos l(z-z') M_0 K_0(\lambda r) K_0(\lambda r') + \quad (\text{II-32})$$

$$\frac{4q}{\pi D_2} \int_0^\infty dl \cos l(z-z') \left[\sum_{n=1}^\infty M_n K_n(\lambda r) K_n(\lambda r') \cos n(\theta - \theta') \right]$$

In Eq. II-32 the potential due to a point charge on or outside a salt excluding, dielectric cylinder is the sum of two types of terms: (1) the spherically symmetric, screened coulomb potential given by a point charge immersed in bulk solvent of dielectric constant D_2 , (2) a term incorporating boundary effects caused by the presence of a mobile ion free, dielectric cylinder. Since the boundary term is quite complicated, we shall restrict our investigation to various limiting cases of Eq. II-32.

Analytically accessible limiting cases of Eq. II-32 are $\lim_{Z-Z' \rightarrow \infty}$

and $(r=r'=a, \theta=\theta', Z-Z') \rightarrow (a, 0, 0)$. We proceed to demonstrate that in the former case ψ_T reduces to the Debye-Hückel form and that the latter situation is equivalent to two charges on a planar dividing surface between two regions of different dielectric constant.

Let

$$\begin{aligned} \psi_b = & \frac{2q_b}{\pi D_2} \int_0^\infty dl \cos l(Z-Z') M_0 K_0(\lambda r) K_0(\lambda r') \\ & + \frac{4q_b}{\pi D_2} \int_0^\infty dl \cos l(Z-Z') \left[\sum_{n=1}^\infty M_n K_n(\lambda r) K_n(\lambda r') \cosh n(\theta-\theta') \right] \end{aligned} \quad (\text{II-33a})$$

In the limit that $Z-Z' \rightarrow \infty$, (large $Z-Z'$ relative to a), only the small l component of the integrand in Eq. II-33 contributes to ψ_b . By assuming $Kr \gg 1$ and examining the asymptotic behavior of Eq. II-33, we show in Appendix C that if $D_1 \ll D_2$

$$\lim_{Z \rightarrow \infty} \psi_b = \frac{q_b e^{-KZ_\infty}}{2D_2 Z_\infty^2} (K + Z_\infty^{-1}) (2b r_\infty \cos(\theta-\theta') - b^2) \quad (\text{II-33b})$$

with $b = a^2/r_\infty$ and $Z_\infty = Z-Z'$. Hence, it follows from Eq. II-32 that

$$\begin{aligned} \lim_{Z \rightarrow \infty} \psi_T = & \frac{q_b e^{-KZ_\infty}}{D_2 Z_\infty^2} + \frac{q_b e^{-KZ_\infty}}{2D_2 Z_\infty^2} (K + Z_\infty^{-1}) (-r^2 - r'^2 - b^2) \\ & + \frac{q_b e^{-KZ_\infty}}{2D_2 Z_\infty^2} (K + Z_\infty^{-1}) (2 \cos(\theta-\theta') (2b r_\infty + r r')) \end{aligned} \quad (\text{II-33c})$$

The contribution of ψ_b to ψ_T is of the same order of magnitude as the contribution of the radial variation of ψ_S to ψ_T .

In general, it is evident that the dominant contribution to ψ_T at large $Z-Z'$ is the screened coulomb potential between two colinear charges immersed in bulk solvent. A detailed discussion of the radial variation of ψ_T is found in Appendix C; variations in ψ_T due to ψ_b and the radial components of ψ_S can be neglected in the $Z-Z' \gg a$ limit. We note in passing that Eq. III-9 is valid when $K=0$, i.e. salt free solutions. Moreover, intuitively our conclusions are quite reasonable. When $Ka \gg 1$, the range of the electrostatic interaction is large relative to the thickness of the low dielectric, salt excluding cylinder. Consequently, the perturbation of the lines of flux at large separations between the point and test charge due to the dielectric salt free cylinder should be quite small.

We now proceed to calculate ψ_T in the limit that $(Z-Z', r=r'=a, \theta=\theta') \rightarrow (0, a, 0)$. Rewriting Eq. II-27 as

$$Z\psi_T = \frac{2q}{\pi} \left\{ H_0 + 2 \sum_{n=1}^{\infty} H_n \cosh n(\theta - \theta') \right\} \quad (\text{II-34a})$$

with

$$H_n = Z \int_0^{\infty} dl \cos l(Z-Z') h_n \quad (\text{II-34b})$$

$$h_n = \frac{-K_n(\lambda a) I_n(\lambda a)}{\{D_2 \lambda a K'_n(\lambda a) I_n(\lambda a) - D_1 \lambda a K_n(\lambda a) I'_n(\lambda a)\}} \quad (\text{II-34c})$$

Setting $Z'=0$, $\theta'=0$, and $K=0$ and defining $y=\lambda Z$

$$H_n = \int_0^{\infty} dy \cos y h_n(y|Z) \quad (\text{II-35})$$

$$h_n(y|Z) = \frac{-K_n(y|Z) I_n(y|Z)}{y|Z \{D_2 K'_n(y|Z) I_n(y|Z) - D_1 K_n(y|Z) I'_n(y|Z)\}} \quad (\text{II-36})$$

Here, we have defined a , the cylindrical radius, as the unit of length.

For large n and to lowest order¹⁵

$$I_n(nx) = \frac{(2\pi n)^{\frac{1}{2}} e^{n\gamma}}{(1+x^2)^{1/4}} \quad (\text{II-37a})$$

$$I_n'(nx) = \frac{(2\pi n)^{\frac{1}{2}} e^{n\gamma} (1+x^2)^{1/4}}{x} \quad (\text{II-37b})$$

$$K_n(nx) = \sqrt{\frac{\pi}{2n}} \frac{e^{-n\gamma}}{(1+x^2)^{1/4}} \quad (\text{II-37c})$$

$$K_n'(nx) = -\sqrt{\frac{\pi}{2n}} \frac{e^{-n\gamma} (1+x^2)^{1/4}}{x} \quad (\text{II-37d})$$

$$\gamma = \sqrt{1+x^2} + \ln \left[\frac{x}{1+\sqrt{1+x^2}} \right] \quad (\text{II-37e})$$

Let $w = (y/z)n^{-1}$, then employing Equations II-37 in Eq. II-36

$$h_n = \frac{n^{-1}(1+w^2)^{1/2}z}{D_1 + D_2} \quad (\text{II-38})$$

Note that Eq. II-38 is a reasonable approximation to h_n for any value of w provided that n is large. The approximation is best for large w ; i.e. small z .

Placing Eq. II-38 into Eq. II-35

$$H_n = \frac{z}{D_1 + D_2} \int_0^\infty dw \frac{\cos(wnz)}{(1+w^2)^{1/2}} \quad (\text{II-39a})$$

$$H_n = \frac{z K_0(nz)}{(D_1 + D_2)} \quad (\text{II-39b})$$

Consider

$$z\psi_T = \frac{2q}{\pi} \left\{ H_0 + 2 \sum_{n=1}^{\infty} H_n \cos n\theta \right\} \quad (\text{II-40a})$$

In the limit that $Z \rightarrow 0$ and $\theta = 0$

$$\lim_{Z \rightarrow 0} Z \psi_T \sim \frac{4q_0}{\pi} \int_0^{\infty} dn H_n \quad (\text{II-40b})$$

$$\lim_{Z \rightarrow 0} Z \psi_T \sim \frac{4q_0}{\pi} \int_0^{\infty} dn \left\{ \frac{Z K_0(nZ)}{D_1 + D_2} \right\} \quad (\text{II-40c})$$

Evaluating the integral we find

$$\lim_{Z \rightarrow 0} Z \psi_T \sim \frac{2q_0}{D_1 + D_2} \quad (\text{II-40d})$$

Thus, when $K=0$, ψ_T is equivalent to the potential between two charges on a planar dividing surface between two different dielectric media.¹⁶ In fact, we demonstrate in Appendix D, that Eq. II-40c is valid independent of the value of K . Intuitively, our results for small Z appear quite reasonable. In the limit that $Z \rightarrow 0$, one would expect ψ_T to be independent of K due to ineffective charge screening. It also seems plausible that for small distances on the surface of the cylinder, the cylinder appears planar.

III. Numerical Results for Charges on the Cylinder

Since the major goal of this section is additional insight into the effects of the dielectric cylinder, rather than any specific applications, we have specialized our numerical work to a few special cases. The two charges under consideration, test and source charges, are located on the surface of the cylinder at $r=r'=1$ and are either on the same side of the cylinder at $\theta=0$, or opposite sides at $\theta=180^\circ$. The value of K is zero or unity; that is, the Debye screening length is either infinite or one cylinder radius. To maximize the low dielectric effect, D_1 and D_2 were taken as 2 and 80 respectively.

We begin by surveying the practical calculation of the potential from Equations II-34 to II-36. Throughout this section a unit source and test charge are assumed.

First of all, the coefficients of $\frac{2}{\pi} H_n$ must be obtained for large n . Values for large n are required only for small Z and are derived from the uniform asymptotic expansions in Appendix D. The $\frac{2}{\pi} H_n$ are given by

$$\frac{2}{\pi} H_n = \frac{2Z}{\pi(D_1+D_2)} \left[K_0(nZ) - \frac{(D_2-D_1)}{D_2+D_1} \left(\frac{\pi}{8n} \right) (1-n|Z|) e^{-n|Z|} \right] \quad (\text{III-1})$$

$a \equiv 1$

The details of the derivation of this formula from the original integral over λ in Eq. II-34b show that the leading terms in the expansion originate from large values of λ and that they are consequently independent of K .

For small z and n not too large, direct numerical integration of the integral expression for $\frac{2}{\pi} H_n$ in Eq. II-34b is practical. For large z a contour deformation of the path of integration is desirable. The path originally runs along the real axis, and deformation of it to run along the two sides of the positive imaginary axis gives exponential convergence of the integrand for large z . In justification of this deformation, we note first that the Bessel functions themselves are analytic throughout the λ plane. The square root functions that define λ and λ_0 ,

$$\lambda_0 = (\lambda^2 + K_0^2)^{\frac{1}{2}} \quad K_0 \rightarrow 0$$

in terms of λ have branchcuts along the imaginary axis, but the real parts of λ and λ_0 are never negative. Asymptotic forms for the Bessel functions in the right half of the λ or λ_0 planes indicate adequate convergence at infinity for the H_n integrand, and the only uncertainty remaining is whether the latter has any poles. We present a formal proof in Appendix E that asserts the absence of poles. A numerical proof of their absence lies in the agreement between the two expressions for H_n in the region of intermediate z (ca. $z=0.5$), where both are practical.

As is explicitly demonstrated in Appendix E, the result of contour deformation, appropriate transformation of the Bessel functions from real to imaginary arguments, and considerable rearrangement is

$$\pi^{-1} H_n = \frac{2|z|}{\pi} \int_{\lambda}^{\infty} dR e^{-R|z|} \left\{ \frac{BC - AE}{C^2 + E^2} \right\}$$

(III-2)

where

$$A = J_n(R)J_n(Sr) \quad S = (R^2 - K^2)^{1/2}; \quad a \equiv 1$$

$$B = -J_n(R)Y_n(Sr)$$

$$C = D_2 J_n(R) S J_n'(S) - D_1 J_n(S) R J_n'(R)$$

$$E = -D_2 J_n(R) S Y_n'(S) + D_1 Y_n(S) R J_n'(R)$$

$$BC - AE \rightarrow \frac{2D_2}{\pi} [J_n(R)]^2 \quad r \rightarrow a \equiv 1$$

Equation III-2 also requires certain precautions in the numerical integration, because of the rapid variation of the integrand in the vicinity of the zeroes of $J_n(R)$. For small z the integrand converges slowly, the integral must be extended to large z , and a great many zeroes require special treatment.

Our procedure was to use Eq. III-2 for n up to ten, and to supplement these values with asymptotic form, Eq. III-1 when necessary for the smaller values of z .

Numerical results are shown in Figures 1 and 2 for the ratio of the actual interaction potential ψ_T to the Debye-Huckel potential as a function of z for the two values of K and θ . The divergence of this ratio from unity indicates the effect of a dielectric discontinuity ($D_1=2$ and $D_2=80$) and salt exclusion ($K_0=0$).

The results for charges on opposite sides of the cylinder are quite

Figure 1. The divergence of the ratio ψ_T/ψ_{DH} from unity indicates the effect of a dielectric discontinuity and salt exclusion. We plot ψ_T/ψ_{DH} versus Z . The $\theta=0^\circ$ case is given with $K=0$, \bullet and $K=1$ \star .

*Does Z have
units?*

FIGURE 1

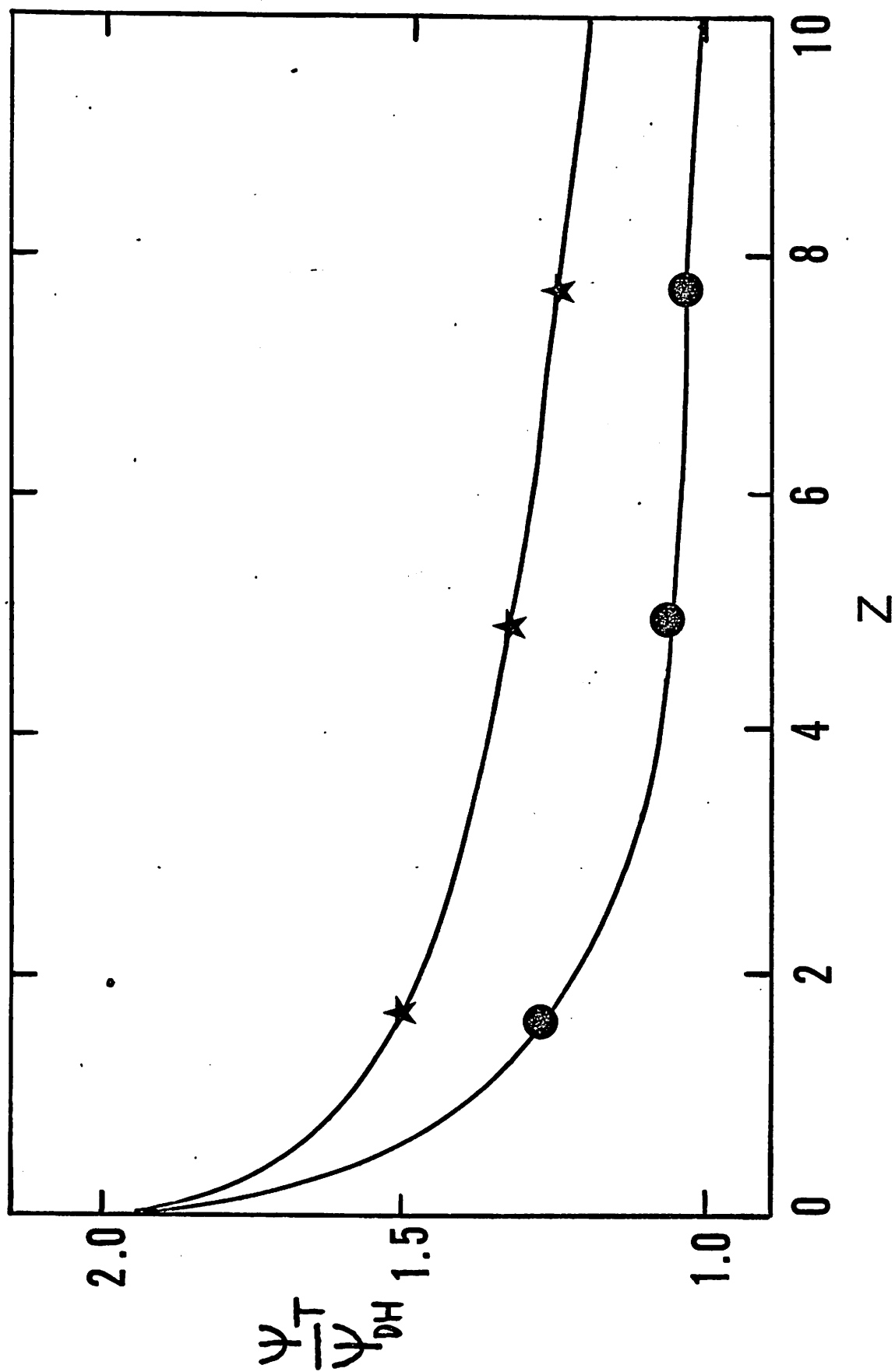


FIGURE 2.

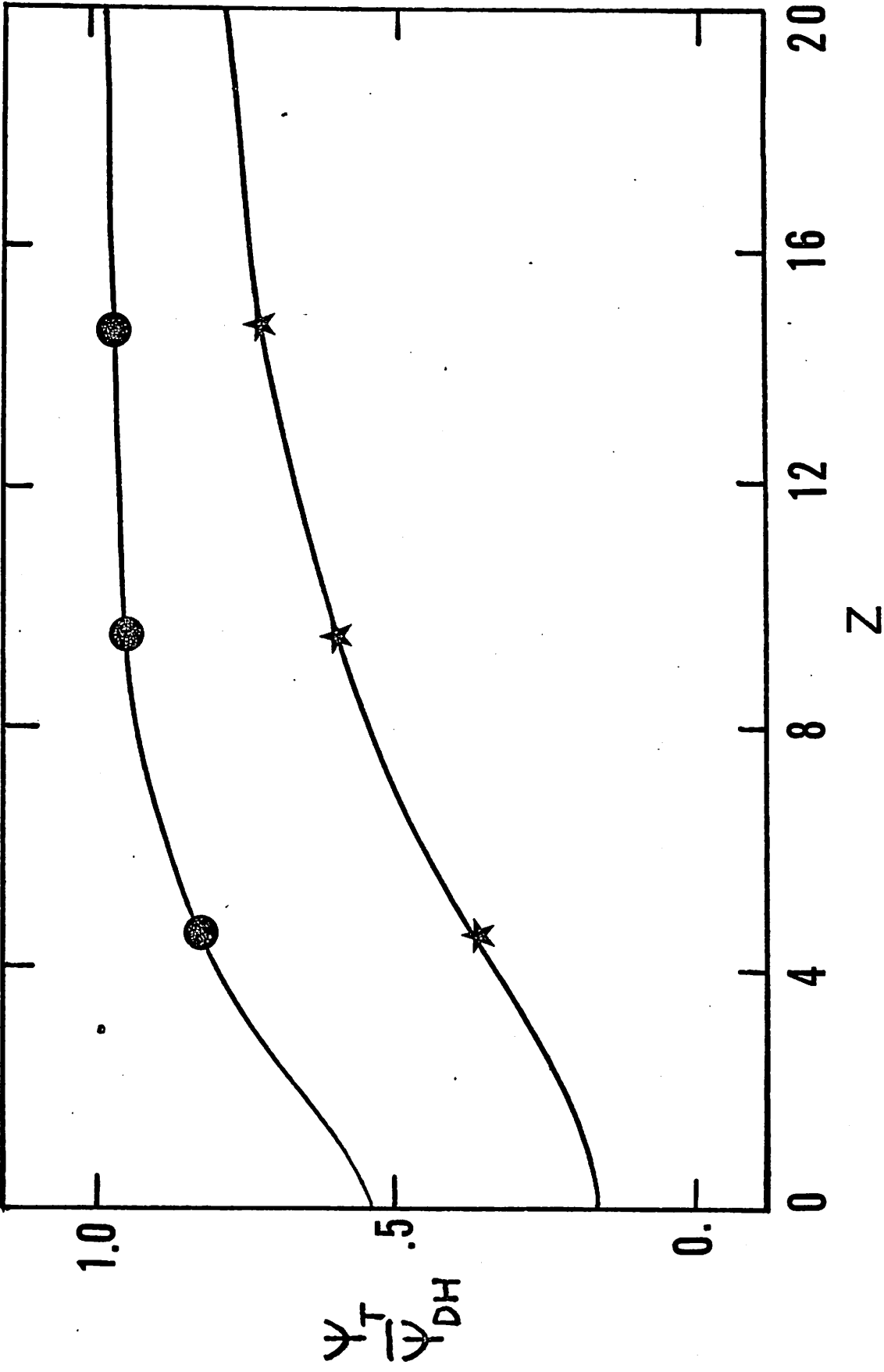




Figure 2. The $\theta=180^\circ$ case is given for ψ_T/ψ_{DH} vs Z with $K=0$,  ,
and $K=1$,  .

contrary to our naive expectations that the interaction would be greatly increased by the presence of a low dielectric constant region between the charges. On the contrary, the interaction is greatly decreased! We note that these results would not be changed by any small shift of the charges toward the interior of the cylinder, or toward the bulk solvent, because the potential is continuous across the dividing surface.

A rationalization along the following lines is probably acceptable. The lines of force from a charge avoid passing through the cylinder. If they passed through the interaction would indeed be increased over its value in bulk solution. Rather the lines of force avoid the cylinder, and travel through the solution to a charge on the opposite side of the cylinder. The greater distance leads to a decreased flux density from spreading of the lines of flux, and from their termination on counterions. If the two charges are close together on the same side of the cylinder, the lines of force bunch up somewhat, and thereby increase the interaction.

IV. Charge Inside a Cylindrical Low Dielectric Region

Suppose a point charge is fixed in a cylindrically symmetric, low dielectric constant medium at the center of which a salt excluding cylinder is located. We shall, in this section, briefly sketch the derivation of some limits of the potential arising from such a point charge. The mathematical approach is the same as section II, consequently, portions of the mathematical details will be omitted.

The potential $G_T(r, r')$ due to point charge at (r', θ', z') is given by

$$G_T(r, r') = \sum_{h=-\infty}^{\infty} \int_{-\infty}^{\infty} dl e^{i[n\theta + lz]} R_h(\lambda r) \quad (IV-1)$$

$$R_h(\lambda r) = \begin{array}{ll} A I_h(\lambda r) & r \leq a \\ B I_h(\lambda r) + C K_h(\lambda r) & a \leq r \leq r' \\ D I_h(\lambda r) + E K_h(\lambda r) & r' \leq r \leq c \\ F K_h(\lambda r) & c < r \end{array} \quad (IV-2)$$

with $\lambda^2 = \epsilon^2 + k^2$ and

$$D = \begin{cases} D_1 & r \leq c \\ D_2 & r > c \end{cases} \quad (\text{IV-3})$$

The radius of the salt excluding cylinder is a . Physically, Eq. IV-2 and IV-3 represent the fact that for $r \leq c$, the medium has dielectric constant D_1 . When $r < a$, the medium is also salt excluding. As explicitly demonstrated in Appendix F, by requiring continuity in $R_n(\lambda'r)$ at a, r' and c and by matching the normal component of the displacement vectors, For $a \leq r \leq c$

$$R_n(\lambda r) = \frac{q_b(1-M_n Q_n)^{-1}}{\pi D_1} \left\{ Q_n I_n(\lambda r) I_n(\lambda r') + K_n(\lambda r) I_n(\lambda r') \right\} f(\theta', z') \\ + \frac{q_b(1-M_n Q_n)^{-1}}{\pi D_1} \left\{ M_n Q_n I_n(\lambda r) K_n(\lambda r') + M_n K_n(\lambda r) K_n(\lambda r') \right\} f(\theta', z') \quad (\text{IV-4})$$

$$f(\theta', z') = e^{-i[\ell n \theta' + l z']}$$

for $r > c$

$$\begin{aligned}
 R_n(\lambda r) = & \frac{q_b (1 - M_n Q_n)^{-1}}{\pi D_2 K_n'(\lambda c)} \left\{ Q_n I_n(\lambda r') I_n'(\lambda c) K_n(\lambda r) \right\} f(\theta, z') \\
 & + \frac{q_b (1 - M_n Q_n)^{-1}}{\pi D_2 K_n'(\lambda c)} \left\{ Q_n I_n'(\lambda c) K_n(\lambda r) K_n(\lambda r') M_n \right\} f(\theta, z') \\
 & + \frac{q_b (1 - M_n Q_n)^{-1}}{\pi D_2} \left\{ I_n(\lambda r) I_n(\lambda r') + M_n K_n(\lambda r) K_n(\lambda r') \right\} f(\theta, z')
 \end{aligned} \tag{IV-5}$$

where $r_<$ is minimum of (r, r')

$r_>$ is maximum of (r, r')

$$M_n = \frac{\lambda I_n(la) I_n'(\lambda a) - l I_n'(la) I_n(\lambda a)}{l K_n(\lambda a) I_n'(la) - \lambda K_n'(\lambda a) I_n(la)} \tag{IV-6}$$

$$Q_n = \frac{(D_1 - D_2) K_n'(\lambda c) K_n(\lambda c)}{D_2 I_n(\lambda c) K_n'(\lambda c) - D_1 I_n'(\lambda c) K_n(\lambda c)} \tag{IV-7}$$

Several observations are appropriate at this time. If we set

$r' = c$, $c = a$, it is demonstrated in Appendix G that $G_T(r, r'=a) = \psi_T(r, r'=a)$ where ψ_T is given by Eq. II-32. In addition, if we define $a=0$, i.e., there is no salt excluding region and let $c \rightarrow \infty$, all $Q_n = 0$, and it follows that

$$G_T(r, r', a=0, c=\infty) = \frac{q e^{-\lambda |r-r'|}}{D_1 |r-r'|} = G_S(r, r') \quad (\text{IV-8})$$

Otherwise stated, we recover the result for a point charge immersed in bulk solvent with dielectric constant D_1 .

In general, Eq. IV-4-7 are quite complicated and do not separate simply into a term incorporating the boundary effects plus the screened coulomb potential. A considerable simplification results if we assume there is no salt excluding region, or equivalently if we assert a salt-free ($K=0$) solution is present. For these particular situations, all M_n given by Eq. IV-6 are zero; we shall concentrate strictly on these cases in what follows.

When $r \leq c$ and all $M_n = 0$, it can be shown from Eq. IV-1 and IV-4 that

$$G_T = \frac{q e^{-\lambda |r-r'|}}{D_1 |r-r'|} + \frac{2q}{\pi D_1} \int_0^\infty dl \cos l(z-z') [Q_0 I_0(\lambda r) I_0(\lambda r')] \\ + \frac{4q}{\pi D_1} \int_0^\infty dl \cos l(z-z') \left[\sum_{n=1}^{\infty} Q_n I_n(\lambda r) I_n(\lambda r') \cos n(\theta-\theta') \right] \quad (\text{IV-9})$$

If $r \geq c$ and $M_n = 0$ for all n , it follows from Eq. IV-1 and IV-5 that

$$\begin{aligned}
 G_T = & \frac{q e^{-\lambda |z-z'|}}{D_2 |z-z'|} + \frac{2q}{\pi D_2} \int_0^\infty d\lambda \cos \lambda (z-z') \left[\frac{Q_0 I_0(\lambda r') I_0'(\lambda c) K_0(\lambda r)}{K_0'(\lambda c)} \right] \\
 & + \frac{4q}{\pi D_2} \int_0^\infty d\lambda \cos \lambda (z-z') \left[\sum_{n=1}^\infty \frac{\cos n(\theta-\theta') K_n(\lambda r) I_n'(\lambda c) I_n(\lambda r') Q_n}{K_n'(\lambda c)} \right]
 \end{aligned}
 \tag{IV-10}$$

Notice that Eq. IV-9 and IV-10 hold for all values of D_1 , D_2 and r . See Appendix H for explicit evaluation of Eq. V-9 and 10 in the $\lim Z-Z' \gg c$, where as usual we assume $D_1 \ll D_2$ and $Kr \ll 1$. However, since we are mainly concerned with the potential in the vicinity of the charge we display the $r \leq c$ results. The reader is referred to Appendix H for further details.

For $r \leq c$

$$\begin{aligned}
 \lim_{z \rightarrow \infty} G_T = & \frac{q e^{-kz\infty}}{D_2 z\infty} + \frac{q e^{-kz\infty}}{2D_1 z\infty^2} (\chi + z\infty^{-1}) (r^2 + r'^2 - c^2 - \frac{r^2 r'^2}{c^2}) \\
 & + \frac{q e^{-\lambda z\infty}}{2D_2 z\infty^2} (\chi + z\infty^{-1}) \left[2rr' \cos(\theta-\theta') - r^2 - r'^2 - \frac{r^2 r'^2}{c^2} \right]
 \end{aligned}
 \tag{IV-11}$$

At this juncture, it is important to emphasize that the range of interaction, K^{-1} is large relative to the thickness of the low dielectric constant region. Moreover, because $D_2 \gg D_1$, the lines of flux will essentially see bulk D_2 plus a perturbation given by the second collection of terms on the rhs of Eq. IV-11. This concludes the examination of G_T , the potential of a point charge inside a cylindrically symmetric, low dielectric constant region.

V. Helical Array of Charges

In view of the quite large effect of a cylinder on the interaction between point charges on its surface, especially at high salt concentration, we have examined the self-energy of helical distributions of charges. Specifically, one of the questions put in this section is whether the effect of varying salt concentration on the self-energy differs between the helical array and a uniform charge distribution. The potential on the surface, that is, the self-energy is independent of D_1 for the uniform distribution.

Having determined the dependence of the self-energy on salt concentration, we then consider the influence of the helical charge distribution on the colligative properties of the polyelectrolyte solution; our treatment will be in the spirit of Manning's limiting laws.⁷⁻⁹ For α and DNA like continuous helical stripes, our numerical work indicates that the difference in electrostatic free energy between the helical and continuous distributions is rather small. Thus, at this juncture, we address ourselves to the range of applicability of the linearized Poisson-Boltzmann equation. Guided by the results of the MacGillvray and Winklemann¹² and MacGillvray¹³ on the potential of a uniformly charged cylinder in bulk solvent, we shall assume that the functional form of the excess electrostatic free energy is given by the linearized Poisson-Boltzmann equation and that the non-linearities manifest themselves as an effective charge per unit length.

The charges in a helical array are located at discrete values of z in the cylindrical polar coordinates (z, a, θ') , where $\theta' = 2\pi z / p$, and p is the pitch. For DNA p/a is about 3.45, and for an α -helix, p/a is about 0.68. As the pitch increases, a helical charge distribution goes over

to a line of charges parallel to the cylinder axis, and reaches the maximum degree of nonuniformity with respect to varying pitch.

The interaction ψ_T between two charges separated by a distance z along the cylinder axis is given in Eqs. II-32 or II-34a, and the potential ψ is defined as the sum of such pair interactions:

$$\psi = \sum_j \psi_T(x, z_j) \quad (V-1)$$

The sums could be handled straightforwardly with the aid of formulas for ψ_T given in sections II and III, but it would be much easier if the sums could be converted to integrals, and appropriate modifications of Eq. V-1 will be made to permit this simplification. As the equation stands, conversion to an integral would give the potential acting on a charge contained in a continuous helix, and this potential is infinite. We therefore add and subtract a comparison potential evaluated for vanishing salt concentration, and write

$$\psi_T = \Delta \psi + \psi^0 \quad (V-2)$$

$$\Psi^0 \equiv \sum_j \Psi_T^0(0, z_j) \quad (V-3)$$

$$\Delta \Psi \equiv \sum_j \left[\Psi_T(x, z_j) - \Psi_T^0(0, z_j) \right] \quad (V-4)$$

If Ψ^0 were simply the potential Ψ evaluated for $K=0$, the summand in Eq. V-4 would converge at $z=0$, but would diverge at large z , and the desired integral over z could not be extended to infinity. We therefore define Ψ^0 to be the potential for $K=0$, less the potential due to a uniformly charged cylinder at $K=0$. This subtraction will correspond to the omission of an $n=0$ term in Eq. II-34a. We now have a definition of $\Delta \Psi$ which allows the sum to be replaced by an infinite integral. The reference potential Ψ^0 is independent of salt concentration, and the effect of varying K is contained entirely in $\Delta \Psi$. The latter will separate naturally, in the continuous limit, into the potential of a continuous charge distribution, and corrections that depend on the pitch.

Equation II-34a in the continuous limit gives

$$\Delta \Psi = \frac{\beta}{\pi} \sum_{n=-\infty}^{+\infty} \int_{-\infty}^{\infty} dz (h_n - h_n^0) \exp[i\ell z + n\phi] \quad (V-5a)$$

where β is the charge density per unit length of axis and

$$\phi = \Theta + 2\pi z/p \quad (V-5b)$$

A phase shift Θ has been included in order to accomodate the effect of a double strand of charges on DNA. Either $\Theta=0^\circ$, in which case the term $z=0$ should be omitted, or $\Theta=180^\circ$, in which case all charges are to be included in the sum.

A delta function may be recognized to give

$$\Delta \Psi = 2\beta \left\{ h_0 + 2 \sum_{n=1}^{\infty} \Delta h_n \cos n\theta \right\} \quad (V-6a)$$

with

$$\Delta h_n = h_n(2\pi n/p) - h_n^0(2\pi n/p) \quad (V-6b)$$

$$h_0 = \frac{K_0(Ka)}{D_2 Ka K_1(Ka)} \quad (V-6c)$$

Here the displayed argument of h_n is the value for z . A superscript zero indicates that $K=0$; its absence indicates that the actual value of K should be used.

In the calculation of colligative properties, the quantity of interest is the difference in reversible work done in charging up a helical distribution of charge in the presence and absence of salt, F_{excess} and is related to $\Delta\psi$ by ⁷

$$F_{\text{excess}} = \int_0^L dz \int_0^\beta d\beta' \Delta\psi(\beta') \quad (\text{V-7})$$

Substitution of Eq. V-6a into Eq. V-7 and integration over Z gives

$$F_{\text{excess}} = \frac{\beta^2 L}{D_2} \left\{ \frac{K_0(\chi a)}{\chi a K_1(\chi a)} + 2 D_2 \sum_{n=1}^{\infty} \Delta h_n \cos n\theta \right\} \quad (\text{V-8})$$

The first term on the rhs of Eq. V-8 is the excess electrostatic free energy of a uniformly charged cylinder of radius a . The second class of terms contains corrections to the excess free energy due to deviations in the helical charge distribution from a uniform one. When the pitch p goes to zero, all $\Delta h_n = 0$ and we recover the uniformly charged cylinder result.

The colligative properties of the polyelectrolyte solution depend on

$$\left(\frac{\partial F_{\text{excess}}}{\partial K} \right)_{T,V}$$

$$\left(\frac{\partial F_{\text{excess}}}{\partial \chi} \right)_{T,V} = \frac{\beta^2 L}{D_2 \chi} \left\{ -1 + \frac{\kappa_0^2(\chi a)}{\kappa_1^2(\chi a)} + 2 D_2 \chi \frac{\partial}{\partial \chi} \left[\sum_{n=1}^{\infty} \Delta h_n \cos n\theta \right] \right\} \quad (\text{V-9a})$$

The first term, κ^{-1} , arises from the interaction of a line of charge immersed in bulk solvent with the mobile ions. The second term, $\kappa_0^2(Ka)[\kappa_1^2(Ka)]^{-1}$, contains corrections to $(\partial F_{\text{excess}}/\partial K)_{T,V}$ resulting from the fact the helix is wrapped around a salt excluding cylinder. For a fixed value of K , it is an increasing function of Ka . Increasing Ka gives rise to a larger excluded salt effect and a concomitant increase in F_{excess} . The third class of terms are the corrections to F_{excess} due to deviations in the helical distribution for a uniform one. Included in $p F_{\text{excess}}$,

$$p F_{\text{excess}} = 2 \chi \beta^2 L \left(\frac{\partial}{\partial \chi} \left[\sum_{n=1}^{\infty} \Delta h_n \cos n\theta \right] \right)_{T,V}$$

(V-9b)

are the effects of mobile ion screening. Hence, F_{excess} should be a decreasing function of Ka .

In the α helical case, $a=7.5\text{\AA}$, $p=5.1\text{\AA}$, and $\theta=0^\circ$. The required values of h_n are easily computed from Eq. II-34c. Consultation of table I verifies that to an excellent approximation

$$F_{\text{excess}}^{\alpha} = \frac{\beta^2 L K_0(Ka)}{D_2 Ka K_1(Ka)} ; \text{ all } Ka \leq 2 \quad (\text{V-10a})$$

and

$$\left(\frac{\partial F_{\text{excess}}^{\alpha}}{\partial K} \right)_{T,V} = \frac{\beta^2 L}{D_2 K} \left\{ -1 + \frac{K_0^2(Ka)}{Ka K_1^2(Ka)} \right\} \quad (\text{V-10b})$$

Thus, for an α continuous helical distribution of charge, the excess electrostatic free energy is well approximated by that of a uniformly charged cylinder. Moreover, it is only in the limit that $Ka \rightarrow \infty$ that the helical distribution is adequately represented as a line of charge.

In Figure 3, we plot $-C^{\alpha}(Ka)$ as a function of Ka

TABLE I *

 $4\pi\Delta h_{n/n}$

$\chi\alpha$	$4\pi h_0$	1	2	3	4	5	6
.1	3.869E-01	-8.475E-07	-1.109E-07	-3.338E-08	-1.420E-08	-7.304E-09	-4.241E-09
.2	2.882E-01	-3.389E-06	-4.435E-07	-1.335E-07	-5.679E-08	-2.922E-08	-1.696E-08
.3	2.352E-01	-7.622E-06	-9.979E-07	-3.004E-07	-1.278E-07	-6.573E-08	-3.817E-08
.4	2.004E-01	-1.354E-05	-1.774E-06	-5.340E-07	-2.271E-07	-1.169E-07	-6.785E-08
.5	1.753E-01	-2.115E-05	-2.771E-06	-8.344E-07	-3.549E-07	-1.826E-07	-1.060E-07
.6	1.562E-01	-3.042E-05	-3.989E-06	-1.201E-06	-5.110E-07	-2.629E-07	-1.527E-07
.7	1.411E-01	-4.136E-05	-5.428E-06	-1.635E-06	-6.955E-07	-3.578E-07	-2.078E-07
.8	1.288E-01	-5.396E-05	-7.088E-06	-2.135E-06	-9.083E-07	-4.674E-07	-2.714E-07
.9	1.186E-01	-6.819E-05	-8.967E-06	-2.702E-06	-1.149E-06	-5.915E-07	-3.434E-07
1.0	1.099E-01	-8.406E-05	-1.107E-05	-3.335E-06	-1.419E-06	-7.302E-07	-4.240E-07
1.1	1.024E-01	-1.015E-04	-1.338E-05	-4.035E-06	-1.717E-06	-8.834E-07	-5.130E-07
1.2	9.594E-02	-1.206E-04	-1.592E-05	-4.801E-06	-2.043E-06	-1.051E-06	-6.104E-07
1.3	9.025E-02	-1.413E-04	-1.868E-05	-5.633E-06	-2.397E-06	-1.234E-06	-7.164E-07
1.4	8.521E-02	-1.635E-04	-2.165E-05	-6.531E-06	-2.780E-06	-1.431E-06	-8.308E-07
1.5	8.072E-02	-1.872E-04	-2.483E-05	-7.495E-06	-3.190E-06	-1.642E-06	-9.536E-07
1.6	7.668E-02	-2.125E-04	-2.824E-05	-8.525E-06	-3.629E-06	-1.868E-06	-1.085E-06
1.7	7.304E-02	-2.392E-04	-3.186E-05	-9.621E-06	-4.097E-06	-2.109E-06	-1.225E-06
1.8	6.973E-02	-2.674E-04	-3.569E-05	-1.078E-05	-4.592E-06	-2.364E-06	-1.373E-06
1.9	6.672E-02	-2.971E-04	-3.973E-05	-1.201E-05	-5.115E-06	-2.634E-06	-1.530E-06
2.0	6.396E-02	-3.282E-04	-4.399E-05	-1.330E-05	-5.667E-06	-2.918E-06	-1.695E-06

* $4\pi\Delta h_n$ as a function of n and K for an α helix, $P/a = .68$



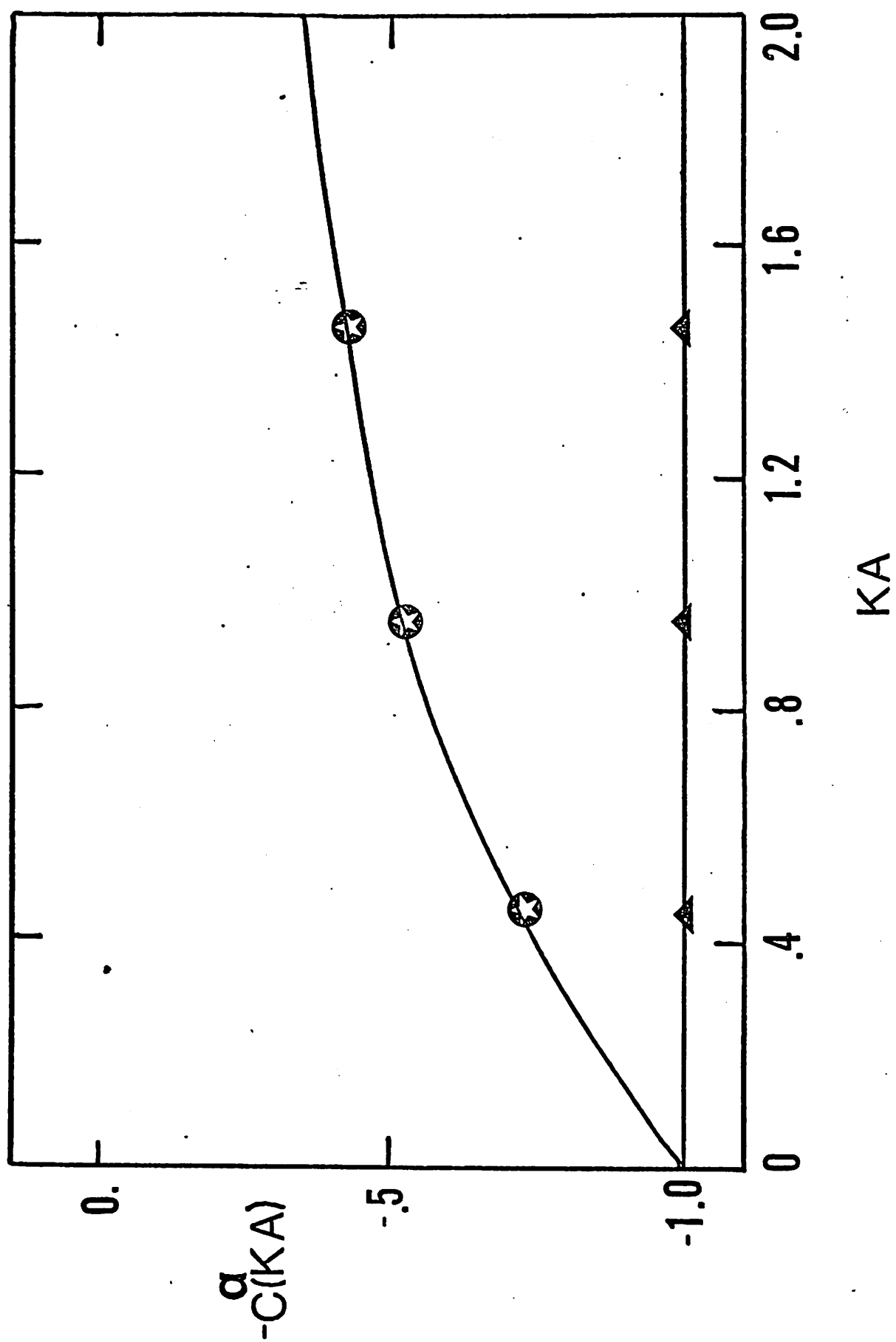
Figure 3.  is the value of $-C^\alpha(Ka)$ as a function of Ka if the α helix were a line of charge. $-C^\alpha(Ka)$ given by Eq. V-11b,  , is the corrected value incorporating the backbone effect on the colligative properties. We have used $p = 5.1\text{\AA}$ and $a = 7.5\text{\AA}$.

FIGURE 3



$$-C^{\alpha}(\chi a) = \frac{D_2 \chi}{\rho^2 L} \left(\frac{\partial F_{\text{excess}}^{\alpha}}{\partial \chi} \right)_{T, V,} \quad (\text{V-11a})$$

$$-C^{\alpha}(\chi a) = -1 + \frac{\kappa_0^2(\chi a)}{\kappa_1^2(\chi a)} \cdot \quad (\text{V-11b})$$

For $Ka \geq .15$ or $C_s \geq 3.7 \times 10^{-3} M$, there are experimentally observable deviations in colligative properties from the line of charge model.

It is straightforward to following Manning's original treatment⁷ and obtain the colligative properties of the α helical polyelectrolyte. Corrections to Manning's theory will be presented after DNA double helical polyelectrolytes are examined.

If pitch is set equal to infinity, the helix reduces to a line of charge embedded on the surface of a low dielectric, salt excluding cylinder. This model may be relevant to linear, non-helical polyelectrolytes such as poly(acrylic-acid).

It follows from Appendix J that

$$\Delta \psi^{line} = 2\beta \left\{ \frac{K_0(ka)}{ka K_1(ka)} + 2 \sum_{n=1}^{\infty} \Delta h_n^{line} \right\} \quad (V-12a)$$

with

$$\Delta h_n^{line} = \left\{ \left[(D_2 + D_1)n + \frac{D_2 ka K_{n-1}(ka)}{K_n(ka)} \right]^{-1} - (D_2 + D_1)^{-1} n^{-1} \right\} \quad (V-12b)$$

Hence, by Eq. V-7

$$F_{excess}^{line} = \frac{\beta^2 L}{D_2} \left\{ \frac{K_0(ka)}{ka K_1(ka)} + 2 D_2 \sum_{n=1}^{\infty} \Delta h_n^{line} \right\} \quad (V-13)$$

As previously, the first term on the rhs of Eq. V-13 is the free energy associated with the reversible work done in charging up a uniformly charged cylinder. The second class of terms appears due to the angular asymmetry in the lines of flux induced by the presence of the low dielectric, mobile ion free cylinder.

Similarly,

$$\left(\frac{\partial F_{\text{excess}}^{\text{line}}}{\partial \kappa} \right)_{T,V} = \frac{\beta^2 L}{D_2} \left\{ -1 + \frac{\kappa_0^2(\kappa a)}{\kappa_1^2(\kappa a)} + 2D_2 \kappa \left(\frac{\partial \left[\sum_{n=1}^{\infty} \Delta h_n^{\text{line}} \right]}{\partial \kappa} \right)_{T,V} \right\} \quad (\text{V-14})$$

Define

$$-C^{\text{line}}(\kappa a) = -1 + \frac{\kappa_0^2(\kappa a)}{\kappa_1^2(\kappa a)} + 2D_2 \left(\frac{\partial \left[\sum_{n=1}^{\infty} \Delta h_n^{\text{line}} \right]}{\partial \ln \kappa} \right)_{T,V} \quad (\text{V-15})$$

In Figure 4, we plot $-C^{\text{line}}(Ka)$ as a function of Ka . As expected when $Ka \ll 1$, the dominant contribution to $\left(\frac{\partial F_{\text{excess}}^{\text{line}}}{\partial K}\right)_{T,V}$ arises from the line of charge in bulk solvent. Provided that the cylinder's radius is very small relative to K , the mobile ions essentially interact with a line of charge with a slight perturbation caused by the dielectric cylinder. However, when $Ka > .15$ there are measurable deviations in $-C^{\text{line}}(Ka)$ from a line of charge in bulk solvent model. In Table II, we present the maximum salt concentration versus cylinder radius for which the line of charge model in bulk solvent adequately characterizes the colligative properties of an infinite pitch helix.

Note that $-C^{\text{line}}(Ka)$ is a decreasing function of Ka for a fixed value of K . This may perhaps be rationalized by a qualitative argument analogous to that for the two point charges (see the discussion at the close of section III.) First of all, it is those terms which reflect the angular asymmetry in the potential,

$$2 D_2 \left(\frac{\partial \left[\sum_{n=1}^{\infty} \Delta h_n^{\text{line}} \right]}{\partial \ln x} \right)_{T,V}$$

that dominate the difference in $\left(\frac{\partial F_{\text{excess}}^{\text{line}}}{\partial K}\right)_{T,V}$ from -1. (The line of charge in bulk solvent result). As previously, we argue that the lines of flux will tend to avoid the cylinder, the avoidance increasing with increasing Ka . Whereupon, over a region of space opposite the line of charge ($\theta=180^\circ$), there is a decreased flux density from both the spread-




Figure 4.  is $-C^{\text{line}}(Ka)$ given by Eq. V-15 as a function of Ka for a line of charge embedded on the surface of a low dielectric, $D_1 = 2$, cylinder. -1,  , is the value if the line of charge were immersed in bulk solvent.  gives the uniformly charged cylinder contribution to $-C^{\text{line}}(Ka)$.

FIGURE 4

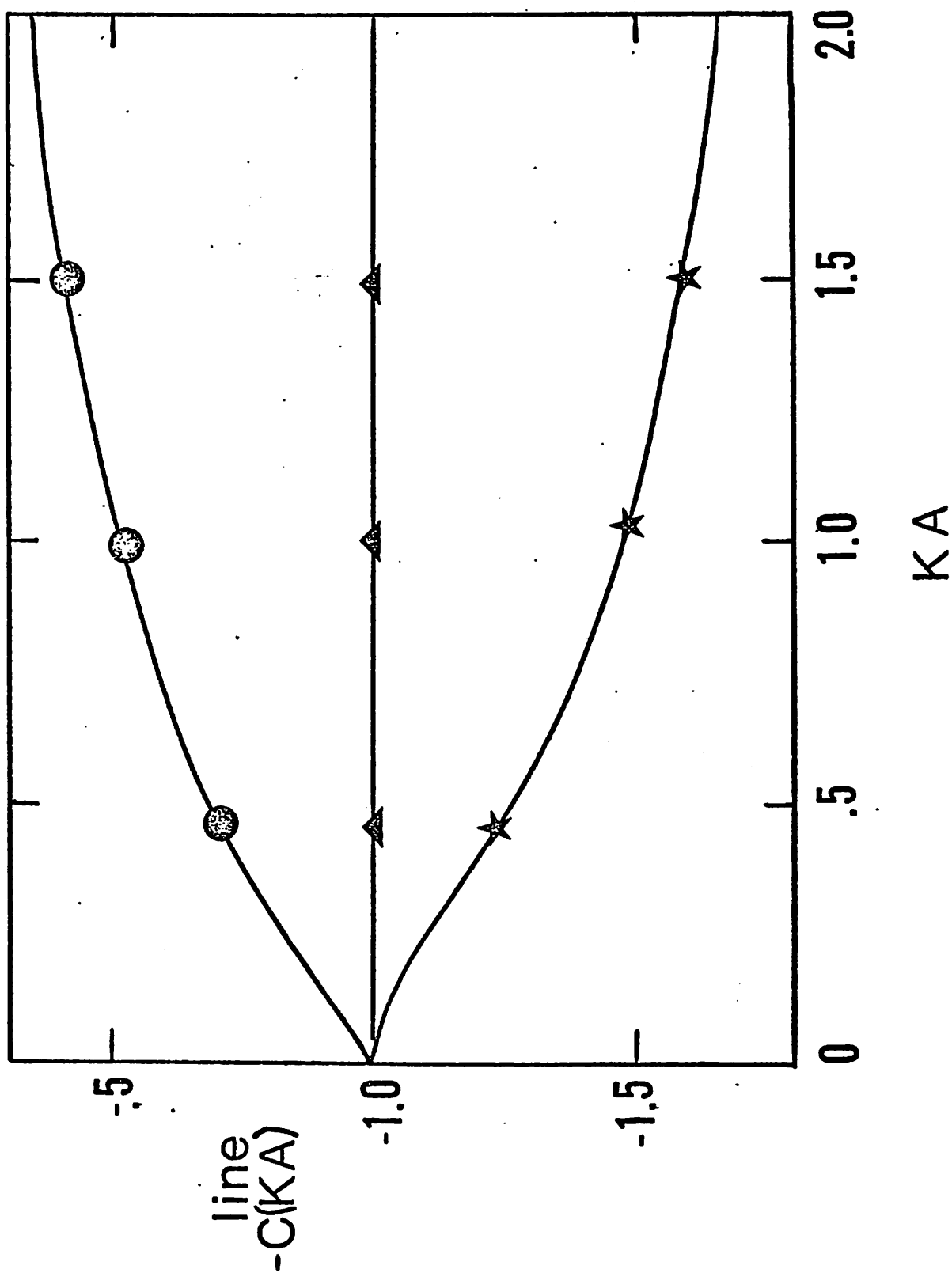


TABLE II

a vs C_S^{\max}

a in A°	C_S^{\max} in moles/liter
1.25	.133
1.75	.069
3.0	.023
13	.0012

* a versus the maximum salt concentration a line of charge in bulk solvent adequately predicts the colligative properties of a helix of infinite pitch.

ing of the lines of flux and their termination on counterions. Conversely, in that portion of space near ($\theta=0^\circ$) the line of charge, there is an increase in flux density vis a vis the absence of the dielectric cylinder. With respect to the line of charge in bulk solvent, the net effect appears to be a decrease in the reversible work required to charge up a helix of infinite pitch. Thus, the reversible work decreases with increasing asymmetry i.e., increasing Ka .

We continue this section with an examination of the colligative properties of a DNA type double helix. The charge distribution is modeled as two helical stripes of charge, 180° out of phase with respect to each other. The stripes of charge lie on the surface of a low dielectric, salt excluding cylinder. Thus, by Eq. V-6a

$$\Delta \Psi^{DNA} = 2\beta \left\{ h_0 + 2 \sum_{n=1}^{\infty} \Delta h_n^{DNA} (1 + \cos n\pi) \right\} \quad (V-16a)$$

β is the charge density per unit length of axis; in DNA the unit of length of axis is 1.7\AA . Clearly only the even n contribute to the sum in Eq. V-16a.

$$\Delta \Psi^{DNA} = 2\beta \left\{ h_0 + 4 \sum_{n=1}^{\infty} \Delta h_{2n}^{DNA} \right\} \quad (V-16b)$$

We have computed the Δh_{2n} from Eq. V-6b. The corrections to the uniform charge distribution are extremely small for $Ka < 1.0$ as a brief consultation of Tables III and IV will verify.

Inserting Eq. V-16b into V-7 gives

$$F_{\text{excess}}^{\text{DNA}} = \frac{\beta^2 L}{D_2} \left\{ \frac{K_0(Ka)}{Ka K_1(Ka)} + 4 D_2 \sum_{n=1}^{\infty} \Delta h_{2n}^{\text{DNA}} \right\} \quad (\text{V-17})$$

Hence,

$$\left(\frac{\partial F_{\text{excess}}^{\text{DNA}}}{\partial K} \right)_{T,V} = - \frac{\beta^2 L}{D_2 K} C(Ka)^{\text{DNA}} \quad (\text{V-18a})$$

TABLE III*

$$\frac{4\pi\Delta h_n}{n}$$

K	$4\pi h_0$	1	2	3	4	5	6
.1	3.869E-01	-6.523E-05	-9.204E-06	-2.843E-06	-1.225E-06	-6.348E-07	-3.704E-07
.2	2.882E-01	-2.596E-04	-3.677E-05	-1.136E-05	-4.897E-06	-2.539E-06	-1.482E-06
.3	2.352E-01	-5.791E-04	-8.255E-05	-2.555E-05	-1.101E-05	-5.710E-06	-3.333E-06
.4	2.004E-01	-1.017E-03	-1.463E-04	-4.535E-05	-1.956E-05	-1.015E-05	-5.923E-06
.5	1.753E-01	-1.566E-03	-2.277E-04	-7.074E-05	-3.053E-05	-1.584E-05	-9.250E-06
.6	1.562E-01	-2.215E-03	-3.264E-04	-1.017E-04	-4.392E-05	-2.280E-05	-1.331E-05
.7	1.411E-01	-2.954E-03	-4.418E-04	-1.380E-04	-5.969E-05	-3.100E-05	-1.811E-05
.8	1.288E-01	-3.770E-03	-5.734E-04	-1.798E-04	-7.784E-05	-4.045E-05	-2.364E-05
.9	1.186E-01	-4.652E-03	-7.206E-04	-2.268E-04	-9.834E-05	-5.114E-05	-2.989E-05
1.0	1.099E-01	-5.588E-03	-8.827E-04	-2.790E-04	-1.212E-04	-6.305E-05	-3.687E-05
1.1	1.024E-01	-6.568E-03	-1.059E-03	-3.362E-04	-1.463E-04	-7.618E-05	-4.457E-05
1.2	9.594E-02	-7.580E-03	-1.249E-03	-3.984E-04	-1.737E-04	-9.052E-05	-5.298E-05
1.3	9.025E-02	-8.615E-03	-1.451E-03	-4.654E-04	-2.033E-04	-1.061E-04	-6.210E-05
1.4	8.521E-02	-9.664E-03	-1.665E-03	-5.371E-04	-2.351E-04	-1.228E-04	-7.193E-05
1.5	8.072E-02	-1.072E-02	-1.890E-03	-6.133E-04	-2.690E-04	-1.407E-04	-8.247E-05
1.6	7.668E-02	-1.178E-02	-2.125E-03	-6.939E-04	-3.051E-04	-1.597E-04	-9.369E-05
1.7	7.304E-02	-1.283E-02	-2.369E-03	-7.787E-04	-3.433E-04	-1.799E-04	-1.056E-04
1.8	6.973E-02	-1.387E-02	-2.621E-03	-8.676E-04	-3.834E-04	-2.012E-04	-1.182E-04
1.9	6.672E-02	-1.490E-02	-2.881E-03	-9.603E-04	-4.256E-04	-2.236E-04	-1.315E-04
2.0	6.396E-02	-1.592E-02	-3.148E-03	-1.057E-03	-4.697E-04	-2.471E-04	-1.454E-04

* $4\pi\Delta h_n$ as a function of n and K for a DNA like double helix, $P/a = 3.45$

TABLE IV
 $\beta^{-1} \Delta\psi^{\text{DNA}}$ vs Ka

Ka	uniform cylinder	$\theta=0$	$\theta=\pi$	average of $\theta + \pi$, i.e. $\Delta\psi^{\text{DNA}}$
.1	.38690	.38674	.38701	.38688
.2	.28823	.28759	.28869	.28814
.3	.23515	.23372	.23618	.23495
.4	.20037	.19785	.20217	.20001
.5	.17532	.17144	.17810	.17477
.6	.15624	.15073	.16016	.15544
.7	.14112	.13375	.14634	.14005
.8	.12881	.11936	.13546	.12741
.9	.11856	.10685	.12674	.11679
1.0	.10987	.09574	.11968	.10771
1.1	.10242	.08573	.11391	.09982
1.2	.09594	.07658	.10916	.09287
1.3	.09025	.06812	.10523	.08668
1.4	.08521	.06025	.10197	.08111
1.5	.08072	.05286	.09925	.07605
1.6	.07668	.04589	.09697	.07143
1.7	.07304	.03928	.09507	.06717
1.8	.06973	.03299	.09346	.06323
1.9	.06672	.02699	.09212	.05955
2.0	.06396	.02124	.09098	.05611

where

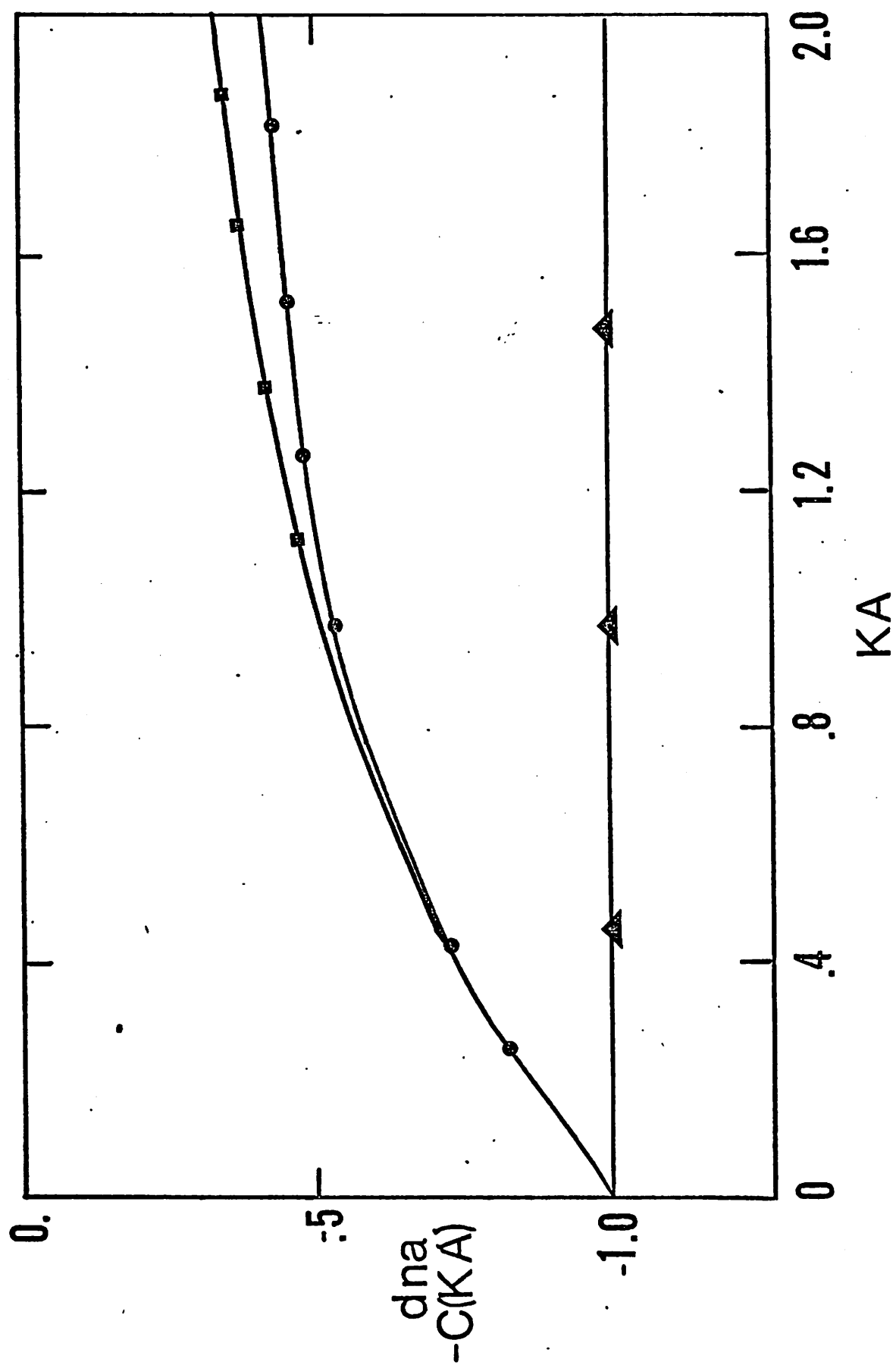
$$-C^{DNA}(Ka) = -1 + \frac{K_0^2(Ka)}{Ka K_1(Ka)} + 4D_2 \left(\frac{\partial \left[\sum_{n=1}^{\infty} \Delta h_{2n}^{DNA} \right]}{\partial \ln Ka} \right)_{T,V} \quad (V-18b)$$

In figure 5 we plot $-C^{DNA}(Ka)$ as a function of Ka . Whenever $Ka \geq .15$ or $C_S \geq 2.1 \times 10^{-3}$ M for DNA, appreciable corrections to the colligative properties as predicted by Manning are necessary. If $Ka > .5$, we find a contribution to $C^{DNA}(Ka)$ due to deviations in the double helical charge distribution from cylindrical symmetry. Such effects are to be expected when the screening length is of the order of the pitch or smaller. Furthermore, corrections to cylindrical symmetry must also depend on the ratio of the pitch to the cylindrical radius. That is, for fixed KP , whether or not the charge distribution appears uniform depends on how tightly wound the helical stripes are. In the case of DNA double helix, P/a is 3.45 and $KP=1$ when $Ka=.3$. Thus, corrections to the uniform charge result are observed in $C^{DNA}(Ka)$. On the other hand, an α helix has a pitch to radius ratio of .68, and $KP=1$ when $Ka=1.5$. It is therefore, not surprising that for $Ka < 2$ corrections to the uniform charge distribution are negligible in the α helical case.

This section is concluded with a brief presentation of some corrected

Figure 5. ● is the value of $-C^{\text{DNA}}(Ka)$ given by Eq. V-18b as a function of Ka . ■ is the contribution of the uniformly charged cylinder to $-C^{\text{DNA}}(Ka)$. -1, ▲ , is the value of $\frac{D_2 K}{\beta^2 L} \left(\frac{\partial F_{\text{excess}}}{\partial K} \right)_{T,V}$ for a line of charge of equivalent charge density. The parameters of the DNA helix were $p = 34.5^\circ$, $a = 10.0\text{\AA}$.

FIGURE 5



colligative properties for α helical and DNA type double helical charge distributions. We shall employ Manning's notation⁷ and assume only monovalent mobile ions are present.

Define

$$\xi = \frac{q^2}{D_2 k_B T b}$$

b is the linear spacing along principal axis of the charges.

When $\xi < 1$, the activity coefficients of the mobile ions are⁷

$$\ln \gamma_i = \left(\frac{\partial F_{\text{excess}}^{\delta}}{\partial n_i} \right)_{T, V, n_{j \neq i}} \quad (\text{V-19a})$$

Here " i " equal to 1 refers to counterion and 2 to coion, n_i is the number density of mobile ions of species " i "; and $\delta = \alpha$, line or DNA refers to the α helix, line of charge on the dielectric cylinder, and DNA double helical polyelectrolytes respectively.

Now

$$\left(\frac{\partial F_{\text{excess}}^{\delta}}{\partial n_i} \right)_{T, V, n_{j \neq i}} = \left(\frac{\partial F_{\text{excess}}}{\partial \kappa} \right)_{T, V} \left(\frac{\partial \kappa}{\partial n_i} \right)_{n_{j \neq i}} \quad (\text{V-19b})$$

Consequently, we can write if $\xi < 1$

$$\ln \gamma_i = -\frac{\xi}{2} X(X+2)^{-1} C^\delta(Ka) ; \quad i = 1, 2$$

(V-19c)

Here $C^\alpha(Ka)$ is given by Eq. V-11b, $C^{line}(Ka)$ is given by Eq. V-15 and $C^{DNA}(Ka)$ is obtained from Eq. V-18b.

X is the ratio of the concentration of counter ions from the polyelectrolyte n_e , to the concentration of counter ions from the simple salt, n_s .

The mean activity coefficient γ_{\pm}^δ is:

$$\ln \gamma_{\pm}^\delta = \frac{1}{2} [\ln \gamma_1 + \ln \gamma_2]$$

(V-20a)

$$\ln \gamma_{\pm}^\delta = -\frac{\xi}{2} X(X+2)^{-1} C^\delta(Ka) ; \quad \xi < 1$$

(V-20b)

The osmotic coefficient ϕ^δ is related to the mean activity coefficient by

$$\phi^\delta = 1 + \ln \gamma_{\pm}^\delta$$

(V-21a)

Employing Eq. V-20b, we have

$$\phi^\delta = 1 - \frac{\xi}{2} X (X+2)^{-1} C^\delta(Xa) \quad ; \quad \xi < 1 \quad (V-21b)$$

In the limit that $n_s \rightarrow 0$, $x \rightarrow \infty$ and $C^\delta(Ka) \rightarrow 1$. Denoting the salt free osmotic coefficient by ϕ_p^δ we have

$$\phi_p^\delta = 1 - \frac{\xi}{2} \quad ; \quad \xi < 1 \quad (V-22)$$

in agreement with Manning.⁷

For $\xi > 1$, we proceed in an identical fashion as Manning does⁷ to find

$$\gamma_1^\delta = \frac{(\xi^{-1}x+1)}{(x+1)} \exp \left[- \frac{\xi^{-1}x C^\delta(x'a)}{2(\xi^{-1}x+2)} \right] ; \quad \xi > 1 \quad (V-23a)$$

$$\gamma_2^\delta = \exp \left[- \frac{\xi^{-1}x C^\delta(x'a)}{2(\xi^{-1}x+2)} \right] ; \quad \xi > 1 \quad (V-23b)$$

$$x'^2 = \frac{4\pi q^2 (\xi^{-1}n_e + n_s)}{2k_B T} ; \quad \xi > 1 \quad (V-23c)$$

$$\phi^{\delta} = \left[\frac{-\frac{1}{2} \xi^{-1} X C^{\delta}(K'a) + \xi^{-1} X + 2}{(X + 2)} \right] ; \quad \xi > 1 \quad (V-24a)$$

$$\phi_p^{\delta} = (2\xi)^{-1} ; \quad \xi > 1 \quad (V-24b)$$

By analogy to simple electrolyte theory, it seems appropriate to designate Equations V-19c to V-24b as extended Manning limiting laws.

It follows from Eq. V-21b, V-22, and Eq. V-24a and b, that the so-called additivity rule⁷

$$\phi^{\delta}(n_e + 2n_s) = \phi_p^{\delta} n_e + 2n_s \quad (V-25)$$

holds only in the limit that $Ka \rightarrow 0$, i.e. $C^{\delta}(Ka) \rightarrow 1$. This conclusion casts further doubt on the interpretation of Eq. V-25) which states that a fraction $(1 - \phi_p)$ of the counterions from the polyelectrolyte salt are bound to the polyion. Strictly speaking Eq. V-25 is valid for helical polyelectrolytes when they appear as a line of charge, in other words at infinite dilution. However, as a matter of practical application, Eq. V-25 is a useful approximation whenever $Ka \leq 15$. This completes the discussion

of the helical array of charges.

VI. Discussion of Results

The linearized Poisson-Boltzmann has been solved to obtain the potential arising from a point charge in, on, or outside a dielectric cylinder. The cylinder is assumed to exclude the salt solution in which it is immersed, to have a dielectric constant D_1 , that may be different from that of the solution, namely D_2 , and to be infinitely long. Numerical results are given for the special case in which both the source and test charge reside on the surface of a low dielectric cylinder; they are on either the same or opposite sides and are separated by an axial distance Z . When the two charges are on the same side and colinear, the potential is significantly increased, over a considerable distance, above that if the charges were in bulk solvent. In the limit that $Z \rightarrow 0$, the potential is equivalent to that of charges on a planar dividing surface between two different dielectric constant regions. Placing the charges on opposite sides of the cylinder gave results, which are, at first glance, indeed surprising. The low dielectric cylinder decreases the interaction energy between the charges! Moreover, the potential between source and test charges spatially very far apart, but near the cylinder is given by the screened coulomb potential characteristic of charges in bulk solvent plus boundary corrections that are on the order of the radial variation in the screened coulomb potential.

In the context of a continuous charge model, we have extended Manning's limiting laws to helical polyelectrolytes. The actual polyion charge distribution is replaced by a thin, helical stripe(s) of charge on the surface of a mobile ion free, low dielectric cylinder. More explicitly, we treat α helical, DNA type double helical charge distributions, and a helix of infinite pitch. A helix of infinite pitch is a line of

charge on the surface of the dielectric cylinder. When $Ka \geq 15$, appreciable corrections to the colligative properties as predicted by a line of charge model become necessary. In the spirit of simple salt solutions, we denote the colligative properties calculated for the α and DNA helices as extended Manning limiting laws.

Until now, a has been defined as the radius of the low dielectric salt excluding cylinder; no explicit relationship to the molecular geometry of the linear, non-helical polyelectrolyte was discussed. As a first approximation, it seems reasonable to associate a with the distance of closest approach to the backbone of the polyelectrolyte; i.e., van der Waals radius of the backbone plus mobile ion. We observe that our theory can be straightforwardly extended to include the finite size of the ions; for small K the corrections should be of minor consequence. In addition, our qualitative results should remain unchanged.

At a fixed axial distance, our numerical results indicate that the interaction energy of two charges on the surface of a dielectric cylinder is quite angle dependent. When $\theta = 0^\circ$ and the magnitude of Z is less than several cylindrical radii, the interaction energy increases greatly with respect to that of charges in bulk solvent. At the other extreme, $\theta = 180^\circ$, the interaction energy decreases appreciably vis a vis charges in bulk solution. One cannot but wonder if the angular dependence of the potential is perhaps at least partially responsible for the large expansions observed in semiflexible polyelectrolytes. Let us, for a moment, view the semiflexible polyelectrolyte as a locally cylindrically symmetric dielectric region with its charges on the dielectric surface. Our numerical results imply that the trans configuration of the backbone,

($\theta=180^\circ$ between the charges), will be enhanced over and above that if the low dielectric region were ignored. In other words, the chain expansion should be larger than that predicted by a line of charge model such as is discussed in the next chapter. While the above is mere speculation, further investigations into the low dielectric effect on polyelectrolyte conformational statistics is clearly warranted.

We conclude our discussions with several observations on Manning's counterion condensation theory.⁷⁻⁹ In his investigations, Manning replaces the actual flexible, linear polyelectrolyte by an infinitely thin line of charge. To the uninitiated and perhaps naive, ignoring the influence of the cylinder on the excess electrostatic free energy seems to be an approximation of questionable validity. Such a query provided part of the original motivation for this work. We therefore examined the colligative properties of helical polyelectrolytes and found when $Ka \geq 1.5$ a line of charge model is inadequate. On the other hand, when the screening length is large relative to a , the helical polyion appears as a line of charge and Manning's original treatment is appropriate. Consequently, we formulated a series of extended Manning limiting laws valid for all values of Ka .

Chapter 3. The Wormlike Polyelectrolyte

VII. Introduction

In the previous chapter, the influence of a low dielectric cylinder on the potential of various charge distributions was examined. We now turn our attention to a particular limiting case of that discussion, the line of charge in bulk solvent. While cognizant of its restricted range of applicability, we shall treat the semiflexible, linear polyelectrolyte as a structureless, charged space curve, i.e. a wormlike polymer with a continuous charge distribution.²² Calculation of the equilibrium dimensions and the colligative properties of a wormlike polyelectrolyte occupies our attention throughout this chapter.

Polyelectrolyte excluded volume theories assume that the unperturbed mean-square end-to-end distance $\langle h_0^2 \rangle$, is independent of the supporting electrolyte concentration, C_s .^{23,24,25} The basis of this assumption comes either from the use of Stockmayer-Fixman, S-F, plots, which give a slight ionic strength dependence for the unperturbed dimensions,²⁵ even though S-F plots assume $\langle h_0^2 \rangle$ is independent of solvent, or from direct measurements in relatively high salt concentration theta solvents.^{27,28} However, for sufficiently low C_s , one would intuitively expect that local electrostatic forces exert a significant influence on $\langle h_0^2 \rangle$. The model of Rice and Harris takes account of local electrostatic interactions by considering an equivalent Kuhn chain with charges concentrated at the midpoints of the statistical elements; if nearest neighbor segment interactions are assumed, the polymer behaves as a random chain. Thus, in the absence of long range interactions, the somewhat artificial Rice-Harris model gives unperturbed chain dimensions that depend in a complicated fashion on C_s .

In section VIII, we calculate the electrostatic persistence length, P_{el} ,

of a charged, wormlike polymer which is sufficiently rigid that there are no excluded volume effects. The total persistence length, P_T , is a measure of chain stiffness and, qualitatively, can be regarded as the distance along the polymer for which a given vector direction persists. Hence, the more rigid a polymer is, the larger is P_T . We can relate, P_{el} to $\langle h_0^2 \rangle$ by³⁰

$$\langle h_0^2 \rangle = 2L(P_0 + P_{el}) = 2LP_T \quad \text{(VII-1)}$$

where L = contour length of the chain

$P_0 \equiv$ persistence length in the absence of electrostatic forces,
(i.e. $C_s \rightarrow \infty$).

$P_T \equiv$ total persistence length.

P_{el} is obtained for (i) a continuous, uniform charge distribution

without charge rearrangements due to bending and without fluctuations due to thermal motion. We then consider two additional calculations relating to P_{el} : (ii) the continuous charge distribution with charge rearrangements, but no fluctuations; (iii) the continuous charge distribution with charge rearrangements and fluctuations. Cases (ii) and (iii) are found to agree with the results of case (i), if the polymer is assumed to be locally stiff; the exact definition of local stiffness will be given in the body of the paper.

Having obtained a theoretical prediction for P_{el} , we compare our results with experimental data on carboxymethylcellulose in section IX. Reasonably good agreement between theory and experiment is demonstrated.

Pursuant to the calculation of P_{el} , the increase in electrostatic free energy due to bending of the polymer is obtained. Whereupon, it is straightforward to determine the total excess electrostatic free energy, F_{excess}^T ; i.e., the difference in reversible work required to charge up the polymer in the presence and absence of salt. Clearly, F_{excess}^T consists of two terms: (1) the excess electrostatic free energy of a line of charge and (2) the excess bending electrostatic free energy averaged over all configurations of the molecule.

As in chapter 2, we then proceed to examine the colligative properties of the wormlike polyelectrolyte. In particular, Manning's assumption⁷ that the dominant contribution to the colligative properties arises from the rod-like configuration is investigated. Within the context and limitations of our model, his supposition is found to be correct.

VIII. Calculation of the Electrostatic Persistence Length

VIIIA. General Formalism

Consider a charged space curve whose infinitesimal elements interact via a screened Coulomb potential. We wish to calculate the electrostatic persistence length, P_{el} . V , the increase in potential energy per unit length due to electrostatic repulsions relative to the reference configuration of a straight rod, is given by³⁰:

$$V = \frac{1}{2} \epsilon R_c^{-2}$$

(VIII-1)

ϵ = bending constant of the rod

R_c is the radius of curvature of the element of space curve at which V is evaluated.

It then follows immediately from the worm model that³⁰

$$\frac{\langle h_o^2 \rangle}{L} - 2 P_o = 2 P_{el} = \frac{2 \epsilon(K)}{k_B T}$$

(VIII-2)

k_B is Boltzmann's constant.

Thus, we direct our attention to determining the explicit form of $\epsilon = \epsilon(K)$ in Equation VIII-2.

Let us choose the origin at an arbitrary point somewhere in the middle of the space curve, and let us parameterize the space curve by s , the contour length relative to the origin. If $\underline{r}(s)$ is the location of

a point on the space curve relative to the origin, then

$$\underline{F}(s) = f(s)\hat{i} + g(s)\hat{j} + h(s)\hat{k} \quad (\text{VIII-3})$$

where \hat{i} , \hat{j} , \hat{k} are unit vectors in the x, y, z directions respectively.

Define $\underline{F}_0(s)$ to be the location of the point in the straight rod reference configuration. We shall choose the reference configuration to lie along \hat{i} so that we can write

$$\underline{F}_0(s) = s\hat{i} \quad (\text{VIII-4})$$

Now, the length of the space curve must remain invariant, i.e.,

$$\begin{aligned} s(b) &= \int_0^b [(f'(s))^2 + (g'(s))^2 + (h'(s))^2]^{1/2} ds \\ s(b) &= \int_0^b [(f'_0(s))^2]^{1/2} ds \end{aligned} \quad (\text{VIII-5})$$

for arbitrary b. The prime denotes differentiation with respect to s.

Hence,

$$(f'(s))^2 + (g'(s))^2 + (h'(s))^2 = (f'_0(s))^2 = 1 \quad (\text{VIII-6})$$

Setting $f'(s) = 1 - \delta(s)$, where $\delta(s) \geq 0$, we find on direct substitution into Eq. VIII-6 and on solving the quadratic that results

$$\delta(s) = 1 - \left\{ 1 - [(g'(s))^2 + (h'(s))^2] \right\}^{1/2} \quad (\text{VIII-7})$$

We now introduce the concept of local stiffness; i.e., $g'(s)^2 + h'(s)^2 \ll 1$ (We see later this is equivalent to neglecting terms of order R_c^{-4}).

$$f'(s) = 1 - \delta(s) = 1 - \frac{1}{2} \{ (g'(s))^2 + (h'(s))^2 \} \quad (\text{VIII-8})$$

Furthermore, the unit tangent vector $\underline{u}(s)$ is given by

$$\underline{u}(s) = (f'(s), g'(s), h'(s)) \quad (\text{VIII-9})$$

A general property of unit tangent vectors and their derivatives follows from $\underline{u}(s) \cdot \underline{u}(s) = 1$.

$$\underline{u}(s) \cdot \frac{\partial \underline{u}(s)}{\partial s} = f'(s)f''(s) + g'(s)g''(s) + h'(s)h''(s) = 0 \quad (\text{VIII-10})$$

From Eq. VIII-8, it follows that

$$f''(s) = -\{g'(s)g''(s) + h'(s)h''(s)\}$$

and Eq. VIII-10 becomes

$$\{g'(s)g''(s) + h'(s)h''(s)\} \{ (g'(s))^2 + (h'(s))^2 \} = 0$$

(VIII-11a)

This implies that

$$f''(s) = 0$$

(VIII-11b)

Furthermore, the radius of curvature is related to $\frac{\partial^2 u}{\partial s^2}$ by

$$R_c^{-2} \frac{\partial^2 u}{\partial s^2} = (h''(s))^2 + (g''(s))^2$$

(VIII-12)

the last expression follows from Eq. VIII-11a.

A general property of $g(s)$, $h(s)$, $h'(s)$, $g'(s)$ is that they must vanish at $s=0$; i.e., the reference and given configurations have the same tangent vector at the origin. By expanding $g(s)$, $g'(s)$, $h(s)$, $h'(s)$ in a Taylor series about $s=0$ and using Eq. VIII-12 we find

$$\underline{F}(s) = \left(s - \frac{s^3}{6R_c^2(0)}, \frac{g''(0)s^2}{2}, \frac{h''(0)s^2}{2} \right)$$

(VIII-13)

VIIIB. Continuous Charge Distribution with No Rearrangements or Fluctuations

At this point, a brief discussion of the appropriate electrostatic potential is necessary. According to MacGillvray and Winklemann¹², and MacGillvray^{13,14} if $\xi = \alpha q / (Dk_B T a) < 1$, the Debye Huckel approximation to the potential, ψ_{DH} , for a line of charge is the asymptotic solution of the nonlinear Poisson-Boltzmann equation. When $\xi > 1$, the asymptotic solution to the Poisson-Boltzmann equation is $\xi^{-1} \psi_{DH}$. Note that the backbone charge density σ is still equal to σ_0 . Physically, the decrease in potential may be interpreted as an increasing in clustering of mobile ions near but not on the line of charge. For small deviations from cylindrical symmetry, it seems reasonable that these qualitative conclusions remain valid; we shall assume such is the case. As a matter of completeness, however, when $\xi > 1$, we shall also employ ψ_{DH} to calculate P_{el} .

Let $V^* \equiv$ potential at origin, per unit charge, due to electrostatic repulsion relative to the straight rod configuration. We shall neglect intermolecular interactions and assume the polyelectrolyte is a polyacid. The $\xi < 1$ case is treated explicitly.

$$V^* = \frac{\sigma_0}{D} \left[\int_0^{L_1} ds \left\{ \frac{e^{-\kappa |F(s)|}}{|F(s)|} - \frac{e^{-\kappa s}}{s} \right\} + \int_0^{L_2} ds \left\{ \frac{e^{-\kappa |F(s)|}}{|F(s)|} - \frac{e^{-\kappa s}}{s} \right\} \right] \quad (\text{VIII-14})$$

where

$\sigma_0 \equiv$ charge per unit length

$\sigma_0 = \alpha q/a = \alpha \Gamma_0$

$\alpha =$ degree of ionization

$q =$ charge per monomer unit

$a =$ length of monomer unit

$$\frac{1}{K} = \frac{1000 D k_B T^{\frac{1}{2}}}{4 \pi e^2 N \sum_i c_i z_i^2}$$

$e =$ protonic charge

$c_i =$ concentration of ionic species "i" in solution

$z_i =$ valence of i^{th} species

$D =$ solvent dielectric constant.

L_1 and L_2 are the arc lengths of the curve from the origin to the ends.

We shall assume a 1:1 supporting electrolyte is present.

In what follows, we assume that the interaction is sufficiently short-ranged that letting $L_1, L_2 \rightarrow \infty$ doesn't affect the result, i.e., $K \ll L$.

$$V^* = \frac{2\sigma_0}{D} \int_0^\infty ds \left\{ \frac{e^{-\kappa |F(s)|}}{|F(s)|} - \frac{e^{-\kappa s}}{s} \right\} \quad (\text{VIII-15})$$

Now,

$$|F(s)| = s \left\{ 1 - \frac{s^2}{12 R_c^2(0)} \right\}^{1/2} \quad (\text{VIII-16})$$

The last step follows from Eq. VIII-12.

We expand $|F(s)|$ and $e^{-\kappa |F(s)|}$ in a Taylor series about $s=0$ to terms of order $1/R_c^2$. (This is the local stiffness approximation). Hence,

$$\frac{e^{-\kappa |F(s)|}}{|F(s)|} = e^{-\kappa s} \left\{ s^{-1} + \frac{s}{24 R_c^2(0)} + \frac{\kappa s^2}{24 R_c^2(0)} \right\} \quad (\text{VIII-17})$$

Substitution of Eq. VIII-17 into Eq. VIII-15 yields

$$V^* = \sigma_0 \{ 4 \kappa^2 D R_c^2(0) \}^{-1} \quad (\text{VIII-18})$$

Therefore, the potential of an element of length dx is

$$V dl = \frac{V^*}{2} dq = \frac{1}{2} V^* \sigma_0 dl$$

or

$$V = \frac{\alpha^2 \Gamma_0^2}{8 \chi^2 D R_c^2(\xi)} \quad (\text{VIII-19})$$

The factor of 1/2 is introduced to avoid overcounting; i.e., we wish to consider the potential acting on each infinitesimal element only once.

Furthermore, we have substituted $\alpha \Gamma_0$ for σ_0 .

Comparing Eq. VIII-19 with Eq. VIII-1, it is readily seen that

$$\epsilon = \frac{\alpha^2 \Gamma_0^2}{4 \chi^2 D} \quad (\text{VIII-20})$$

Substituting the value of ϵ in Eq. VIII-20 into Eq. VIII-2 we find if $\xi < 1$

$$2 P_{el}^{theo} = \frac{\alpha^2 \Gamma_0^2}{2 \chi^2 k_B T D} \quad (\text{VIII-21a})$$

for the uniformly charged rod without charge rearrangements due to binding and without fluctuations. In appendix K, we demonstrate that the result

for a discrete charge model without rearrangements or fluctuations reduces to Eq. VIII-21 in the limit $Ka \rightarrow 0$.³¹ Moreover, we note if $\xi > 1$,

$$2P_{el}^{theo} = \frac{\xi^{-1} \alpha^2 \Gamma_0^2}{2 \kappa^2 k_B T D}$$

(VIII-21b)

In all that follows, we shall for convenience write Γ_0 as

$$\Gamma_0 = q/a \text{ if } \xi < 1$$

$$\Gamma_0 = \xi^{-1/2} q/a \text{ if } \xi > 1$$

VIIIC. Continuous Charge Model with Charge Rearrangements but No Fluctuations

We now consider case (ii): the continuous charge distribution with charge rearrangements, but no fluctuations. The change in free energy of the charged space curve relative to the straight rod configuration, ΔG , can be decomposed into three parts: First, there is the term arising from the excess electrostatic interaction due to bending between various parts of the polyelectrolyte. For definiteness, we shall assume the polymer is a polyacid. Then, there is an entropic contribution arising from the mixing of occupied and unoccupied sites. A site is said to be occupied if it has a net negative charge and unoccupied if the site has no net charge. When the polymer is bent, the fraction of occupied sites will perhaps change; this gives rise to the entropy of mixing term and the third contribution to ΔG , the addition of hydrogen ions from the solution to the polyelectrolyte which acts to reduce the repulsive force

between segments.

Before presenting an expression for ΔG , we shall derive an expression for the entropy of mixing. Random mixing is assumed.

For a discrete array of charges

$$\Delta S_{\text{mixing}} = -k_B \{ N_1^f \ln X_1^f + N_2^f \ln X_2^f - N_1^i \ln X_1^i - N_2^i \ln X_2^i \} \quad (\text{VIII-22})$$

Here i and f refer to the initial and final states. N_1 is the net number of sites occupied by a negative charge whose valence is determined by the nature of the individual polyacid. N_2 is the number of sites occupied by H^+ ions.

$$X_j = \frac{N_j}{N_1 + N_2}$$

Let

$$\frac{N_1^f}{L} = \sigma ; \quad \frac{N_2^f}{L} = \omega - \sigma ; \quad \text{and} \quad \frac{N_1^i}{L} = \sigma_{\text{ref}}$$

(the straight rod configuration is the reference configuration)

where ω is the total number of sites per length.

Thus

$$X_1^f = \frac{\sigma}{w} ; \quad X_2^f = 1 - \sigma/w ; \quad \frac{\sigma_{ref}}{w} = \alpha$$

The continuous version of Eq. VIII-22 becomes

$$\Delta S_{mixing} = -k_B \left[\int_0^L ds \left\{ \sigma \ln(\sigma/w) + (w-\sigma) \ln\left(\frac{w-\sigma}{w}\right) \right\} \right] + \\ + k_B \left[\int_0^L ds \left\{ \sigma_{ref} \ln \alpha + (w-\sigma_{ref}) \ln(1-\alpha) \right\} \right] \quad (\text{VIII-23})$$

Here we have parameterized the arc length from one end of the worm.

Thus, ΔG is given by

$$\Delta G = \frac{\Gamma_0^2}{2w^2D} \int_0^L \int_0^L ds ds' \left\{ \sigma(s) \sigma(s') U(|s-s'|) - \sigma_{ref}^2 \frac{e^{-ks}}{s} \right\}$$

$$- T \Delta S_{mixing} + k_B T \int_0^L ds \left\{ \sigma(s) - \sigma_{ref} \right\} \ln a_{H^+}$$

(VIII-24)

where

$$U(|s-s'|) = e^{-\kappa|s-s'|} \left\{ |s-s'|^{-1} + \frac{|s-s'|}{24R_c^2(s)} + \frac{\kappa|s-s'|^2}{24R_c^2(s)} \right\}$$

a_{H^+} is the activity of the hydrogen ion in solution; i.e., at an infinite distance from the polyelectrolyte.

The last term in Eq. VIII-24 arises from the free energy contribution due to H^+ addition caused by the bending of the chain.

We shall now assume that the charge distribution varies slowly on the scale of the range of the interaction, κ^{-1} . At least to lowest order, $\sigma(s)$, $\sigma(s')$ are functionals of and change on the scale of the variation in R_c^{-2} . In the local stiffness approximation, $R_c^{-2}(s)$ is approximately constant, and as in the derivation of case (i), we implicitly assume the distance over which R_c^{-1} is constant $> \kappa^{-1}$. Hence, setting $\sigma(s) \approx \sigma(s')$ should be a valid approximation. Thus,

$$\Delta G = \frac{\pi_0^2}{2w^2D} \left[\int_0^L ds \sigma^2(s) \int_0^L ds' U(|s-s'|) - \int_0^L ds \int_0^L ds' \sigma_{ref}^2 \frac{e^{-\kappa|s-s'|}}{|s-s'|} \right]$$

$$- T \Delta S_{mixing} + k_B T \int_0^L ds (\sigma(s) - \sigma_{ref}) \ln a_{H^+}$$

(VIII-25)

Set

$$I = \frac{1}{2} \int_0^L ds' \frac{e^{-\kappa|s-s'|}}{|s-s'|} = \frac{1}{2} \int_{L_1}^{L_2} ds'' \frac{e^{-\kappa|s-s''|}}{|s-s''|}$$

$$I \approx \int_{0^+}^{\infty} ds'' \frac{e^{-\kappa|s-s''|}}{|s-s''|}$$

(VIII-26)

s'' denotes the arc length from an origin defined at a point s along the curve. Note that the lower limit of the integral in Eq. VIII-26 is really not zero, but a ; the real lower limit arises from consideration of the discrete nature of the chain. The integral, I , may be large but it is finite. Furthermore, that the lower limits of the other integrals in VIII-25 may be replaced by zero follows from our discussion in Appendix K.

Similarly,

$$H(s) = \frac{1}{2} \int_0^L ds' e^{-\kappa|s-s'|} \left\{ \frac{|s-s'|}{24R_c^2(s)} + \frac{\kappa|s-s'|^2}{24R_c^2(s)} \right\}$$

$$H(s) \approx \{8\kappa^2 R_c^2(s)\}^{-1}$$

For convenience we shall write $R_c^{-2}(s)$ as R_c^{-2} . Substituting the expressions for I and $H(s)$ into Eq. VIII-25, we obtain

$$\Delta G(\sigma) = \frac{\Gamma_0^2}{w^2 D} \int_0^L ds \sigma^2(s) H(s) + \frac{\Gamma_0^2}{w^2 D} \int_0^L ds I(\sigma^2(s) - \sigma_{\text{ref}}^2) - T \Delta S_{\text{mixing}} + k_B T \int_0^L ds (\sigma(s) - \sigma_{\text{ref}}) \ln a_H^+$$

(VIII-27)

Now, ΔG is a functional of $\sigma(s)$; it can therefore be expanded about the most probable value of σ , $\bar{\sigma}$, as follows:

$$\Delta G(\sigma) = \Delta G(\bar{\sigma}) + \frac{1}{2} \int_0^L ds \left. \frac{\delta^2 \Delta G}{\delta \sigma^2} \right|_{\sigma = \bar{\sigma}} (\sigma - \bar{\sigma})^2$$

(VIII-28)

Here $\frac{\delta^2 G}{\delta \sigma^2}$ is the second functional derivative of G with respect to σ .

The second term on the rhs of Eq. VIII-28 is related to charge fluctuations; we shall consider it further under case (iii). Furthermore,

$$\left. \frac{\delta \Delta G}{\delta \sigma} \right|_{\sigma = \bar{\sigma}} = 0$$

Thus, $\bar{\sigma}$ can be calculated from

$$\left. \frac{\delta \Delta G}{\delta \sigma} \right|_{\sigma = \bar{\sigma}} = \frac{2\bar{\sigma} \Gamma_0^2}{w^2 D} \{ H(s) + I \} + k_B T \ln a_H^+ +$$

(VIII-29)

$$k_B T \ln(\bar{\sigma}/(w - \bar{\sigma})) = 0$$

If we let $R_c^{-2} \rightarrow 0$, $\bar{\sigma} = \sigma_{ref}$ and it follows from Eq. VIII-29 that

$$I = \frac{2.303 R_B T W pK_{app}}{2\alpha \Gamma_0^2}$$

$$pK_{app} = pH - \log(\alpha/(1-\alpha)) \quad (VIII-30)$$

Let

$$\bar{\sigma} = \sigma_{ref} - A R_c^{-2} \quad (VIII-31a)$$

where A is a constant to be determined.

Substituting Eq. VIII-31a into Eq. VIII-29 and expanding out logarithmic terms in $\bar{\sigma}$ to order R_c^{-2} , we find that

$$\bar{\sigma} = \sigma_{ref} - \frac{\alpha^2(1-\alpha)\Gamma_0^2}{4DX^2R_B T \{ (1-\alpha)2.303 pK_{app} + 1 \}} \quad (VIII-31b)$$

Note that $\bar{\sigma} \rightarrow \sigma_{ref}$ as $\alpha \rightarrow 0$ and $\alpha \rightarrow 1$ as would be intuitively expected.

Using Eq. VIII-31b in Eq. VIII-25 for $\sigma = \bar{\sigma}$ and taking the derivative of $\Delta G(\bar{\sigma})$ with respect to s, one finds to order R_c^{-2} , the local stiffness approximation,

$$\frac{\partial \Delta G(\bar{\sigma})}{\partial s} = \frac{\partial V(\bar{\sigma})}{\partial s} - T \frac{\partial \Delta S_{mixing}(\bar{\sigma})}{\partial s} + R_B T (\bar{\sigma} - \sigma_{ref}) \ln a_{H^+} \quad (VIII-32a)$$

$$\frac{\partial V(\bar{\sigma})}{\partial s} = \frac{\alpha^2 \Gamma_0^2}{8DX^2 R_c^2} - \frac{2.303 \alpha^2 (1-\alpha) \Gamma_0^2 pH_{app} R_c^{-2}}{4DX^2 \{ 2.303 (1-\alpha) pH_{app} + 1 \}} \quad (\text{VIII-32b})$$

$$\frac{-T \frac{\partial \Delta S(\bar{\sigma})}{\partial s}}{\text{mixing}} = \frac{-\alpha^2 \Gamma_0^2 (1-\alpha) \ln(\alpha/(1-\alpha)) R_c^{-2}}{4DX^2 \{ 2.303 (1-\alpha) pH_{app} + 1 \}} \quad (\text{VIII-32c})$$

$$K_B T (\bar{\sigma} - \sigma_{ref}) \ln a_{H^+} = \frac{2.303 \alpha^2 (1-\alpha) pH R_c^{-2} \Gamma_0^2}{4DX^2 \{ 2.303 (1-\alpha) pH_{app} + 1 \}} \quad (\text{VIII-32d})$$

Substituting the explicit forms of $\frac{\partial V}{\partial s} - \frac{T \partial \Delta S}{\partial s} \text{mixing}$, $K_B T (\bar{\sigma} - \sigma_{ref}) \ln a_{H^+}$ to order R_c^{-2} , into $\frac{\partial \Delta G(\bar{G})}{\partial s}$,

$$\frac{\partial \Delta G(\bar{\sigma})}{\partial s} = \frac{\alpha^2 \Gamma_0^2}{8X^2 D R_c^2} \quad (\text{VIII-33})$$

Thus, the result of case (ii) is identical to the result of case (i) to terms of order R_c^{-2} .

VIIID. Continuous Charge Distribution with Rearrangements and Fluctuations

We now examine case (iii): the continuous charge model with charge rearrangements and fluctuations. If we do not assume $\sigma(s) = \sigma(s')$, Eq. VIII-28 can be rewritten as

$$\Delta G(\sigma) = \Delta G(\bar{\sigma}) + \frac{1}{2} \int_0^L \int_0^L ds ds' \left. \frac{\delta^2 \Delta G}{\delta \sigma(s) \delta \sigma(s')} \right|_{\sigma = \bar{\sigma}} (\sigma(s) - \bar{\sigma}(s)) (\sigma(s') - \bar{\sigma}(s')) \quad (\text{VIII-34})$$

It follows directly from Eq. VIII-24 that

$$\left. \frac{\delta^2 \Delta G}{\delta \sigma(s) \delta \sigma(s')} \right|_{\sigma = \bar{\sigma}} = \frac{\Gamma_0^2 e}{w^2 D} \left\{ |s-s'|^{-1} + \frac{|s-s'|}{24 R_c^2(s)} + \frac{\chi |s-s'|^2}{24 R_c^2(s)} \right\} + \frac{k_B T \delta(s-s')}{2 w (1-\alpha)} \quad (\text{VIII-35})$$

So that

$$\Delta G(\sigma) - \Delta G(\bar{\sigma}) = \frac{\Gamma_0^2}{2 D} \int_0^L \int_0^L ds ds' e^{\chi |s-s'|} \left\{ |s-s'|^{-1} + \frac{|s-s'|}{24 R_c^2(s)} + \frac{\chi |s-s'|^2}{24 R_c^2(s)} \right\} \gamma(s) \gamma(s') + \frac{k_B T w}{2 \alpha (1-\alpha)} \int_0^L ds \gamma^2(s) \quad (\text{VIII-36})$$

where

$$\gamma(s) = \frac{\{\sigma(s) - \bar{\sigma}(s)\}}{\omega}$$

and $\Delta G(\sigma)$ is approximated by the value obtained when $\sigma(s) \approx \sigma(s')$; i.e.,

$$\Delta G(\bar{\sigma}) = \int_0^L ds \frac{\alpha^2 \Gamma_0^2}{8K^2 D R_c^2(s)}$$

(VIII-37a)

Furthermore, we approximate

$$\int_0^L \int_0^L ds ds' \frac{e^{-\chi|s-s'|}}{|s-s'|} \gamma(s)\gamma(s') \approx 2 \int_0^L ds I \gamma^2(s)$$

(VIII-37b)

since this term is very short ranged.³² Hence,

$$\begin{aligned} \Delta G(\sigma) - \Delta G(\bar{\sigma}) &= \frac{\Gamma_0^2}{2D} \int_0^L \int_0^L ds ds' \frac{\gamma(s)\gamma(s')}{24R_c^2(s)} e^{-\chi|s-s'|} \{ |s-s'| + \chi|s-s'|^2 \} \\ &+ \frac{\Gamma_0^2}{D} \int_0^L ds \gamma^2(s) I + \frac{K_B T \omega}{2\alpha(1-\alpha)} \int_0^L \gamma^2(s) ds \end{aligned}$$

(VIII-38)

We now expand $\gamma(s)$ and $\phi(r) = \bar{e}^{Kr}(r+Kr^2)$ in a truncated Fourier series

$$\gamma(s) = \sum_{j=0}^{Lw} C_j \cos\left(\frac{2\pi j s}{L}\right) + C'_j \sin\left(\frac{2\pi j s}{L}\right)$$

$$C_j = \frac{2}{L} \int_0^L \gamma(s) \cos\left(\frac{2\pi j s}{L}\right) ds; \quad C'_j = \frac{2}{L} \int_0^L \gamma(s) \sin\left(\frac{2\pi j s}{L}\right) ds$$

$$\phi(s) = \sum_{j=0}^{Lw} \phi_j \cos\left(\frac{2\pi j s}{L}\right)$$

$$\phi_j = \frac{2}{L} \int_0^L \phi \cos\left(\frac{2\pi j s}{L}\right) ds$$

(VIII-39)

If we assume $L \gg$ range of interaction of $\phi(r)$, it follows that^{33,34}

$$\Delta G(\sigma) - \Delta G(\bar{\sigma}) = \frac{\Gamma_0^2 L^2}{96 D R_c^2} \sum_{j=0}^{Lw} (C_j^2 + C_j'^2) \phi_j + \frac{L}{2} \left\{ \frac{k_B T w}{2\alpha(1-\alpha)} + \frac{\Gamma_0^2 I}{D} \right\} \left[\sum_{j=0}^{Lw} C_j^2 + C_j'^2 \right]$$

(VIII-40)

Futhermore, the excess electrostatic free energy due to bending, G_b , is given by³⁵

$$\exp [-\beta \{G - \Delta G(\bar{c})\}] = L^N \int_{-\infty}^{\infty} \dots \int_{-\infty}^{\infty} d c_0 \prod_{j=1}^{Lw} d c_j \dots d c_j' \exp W$$

$$W = -\beta \left\{ \frac{\Gamma_0^2 L^2}{96 D R_c^2} \sum_{j=0}^{Lw} (c_j^2 + c_j'^2) \Phi_j + \frac{L}{2} \left[\frac{k_B T w}{2 \alpha (1-\alpha)} + \frac{\Gamma_0^2 I}{D} \right] \sum_{j=0}^{Lw} c_j^2 + c_j'^2 \right\}$$

(VIII-41)

Evaluating the integrals and taking the logarithm of both sides, we find

$$G = \Delta G(\bar{c}) + k_B T \sum_{m=0}^{Lw} \ln (Z + \Phi_m R_c^{-2})$$

$$-k_B T L w \ln (4 \pi k_B T)$$

(VIII-42)

where

$$Z = \frac{k_B T}{\alpha (1-\alpha)} + \frac{2 \Gamma_0^2 I}{D}$$

$$\Phi_m = \frac{L \Gamma_0^2 \phi_m}{12}$$

To obtain G_{net} , the net electrostatic free energy due to bending, we must let $R_c^{-2} \rightarrow 0$ and subtract that result from Eq. VIII-42. Hence,

$$G_{\text{net}} = \int_0^L ds \left\{ \frac{\alpha^2 \Gamma_0^2}{8K^2 D R_c^2} + \frac{\Gamma_0^2 \alpha (1-\alpha) T(L\omega, K) R_c^{-2}}{12\omega D \{ 2.303 (1-\alpha) p\kappa_{\text{app}} + 1 \}} \right\}$$

$$T(L\omega, K) = \sum_{m=0}^{L\omega} \frac{3K^4 - m^4 - 6K^2 m^2}{(K^2 + m^2)^3}$$

(VIII-43)

Here, the explicit expression for Φ_m has been substituted.

Furthermore, the sum can be evaluated by approximating it as an integral. Then,

$$\frac{\partial G_{\text{net}}}{\partial L} = \frac{\alpha^2 \Gamma_0^2}{8K^2 D R_c^2} + \frac{\alpha (1-\alpha) \Gamma_0^2 (3K^2 + 4\pi^2 \omega^2) R_c^{-2}}{12D \{ 2.303 p\kappa_{\text{app}} (1-\alpha) + 1 \} \{ K^2 + 4\pi^2 \omega^2 \}^2}$$

(VIII-44)

However, $1/K \gg a = 1/\omega$ or $\omega \gg K$ so that

$$\frac{\partial G_{\text{net}}}{\partial L} \approx \frac{\alpha^2 \Gamma_0^2}{8K^2 D R_c^2} + \frac{\alpha (1-\alpha) \Gamma_0^2 R_c^{-2}}{12D \{ 2.303 p\kappa_{\text{app}} (1-\alpha) + 1 \} 4\pi^2 \omega^2}$$

(VIII-45)

$$2 P_{e1}^{\text{theo}} = \frac{\alpha^2 \Gamma_0^2}{2 \kappa^2 D k_B T} + \frac{\alpha(1-\alpha) \Gamma_0^2 (4\pi^2 \omega^2)^{-1}}{3 D k_B T \{2.303 pK_{app}(1-\alpha) + 1\}} \quad (\text{VIII-46})$$

By comparing typical experimental data³⁶⁻³⁸ for the fluctuating term with calculated values of $\alpha^2 \Gamma_0^2 / 2 \kappa^2 k_B T D$, it is readily seen that the charge fluctuation contribution to P_{e1} is negligible.

IX. Comparison of Theoretical Electrostatic Persistence Length with Experiment

In the development of the wormlike polyelectrolyte model, it is assumed that

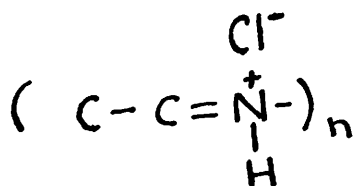
(1) $1/K > a$

(2a) excluded volume effects are negligible

(2b) the polyelectrolyte is locally stiff

Condition (1) can be relaxed by an explicit consideration of the discrete charge nature of the chain (see Appendix K). However, the region where P_{el} contributes significantly to P_T is precisely that domain where (1) is valid. Furthermore, condition (1) puts restraints on the range of ionic strengths, I , where (2a) is applicable. For (2a) to hold in general, we must examine the polyelectrolyte in low I , θ solvents. Unfortunately, the existing measurements are in θ solvents at relatively high I ; our theory predicts a very slight dependence on I , as is observed.^{27,28} Hence, we must choose a system at low I in which the polyelectrolyte is sufficiently stiff that excluded volume effects are negligible anyway. Finally, since light scattering gives an unambiguous determination of polyelectrolyte dimensions, it is the method of choice.

One of the surprising results of our literature search to find suitable data is the lack of light scattering measurements on polyelectrolytes at low ionic strength. Moreover, we were unable to find any light scattering data on polyethylene imine hydrochloride PEI(HCl):²⁹



PEI(HCl) conforms perfectly to the charged worm model; it has no side chains and all the charges are located on the polymer backbone. Clearly, more experimental work is required to fully test the applicability of the proposed model.

On the basis of the above, we decided to compare the experimentally determined dimensions of carboxymethylcellulose, CMC,^{39,40} in aqueous NaCl solutions with those of our theory in the following way: Schneider and Doty determined b^{exptl} by light scattering.

$$b^2 = \langle h^2 \rangle / N \quad (\text{IX-1})$$

N is the degree of polymerization; the measurements were corrected for polydispersity.

b^{theo} is obtained from Eq. VII-1, IX-1, and $L = Na$ by equating

$$2P_T = \frac{b^2}{a} \quad (\text{IX-2})$$

We then plot the experimentally determined b^{exptl} vs $I^{-1} \cdot 2P_0^{\text{exptl}}$ is related to the zero intercept of b^{exptl} by Eq. VIII-1 and IX-2. Employing Eq. VIII-1 and VIII-21b and recognizing that $\xi = 1.53$ for CMC, we have

$$\frac{(b^{\text{theo}})^2}{a} = 2P_0^{\text{exptl}} + 2P_{el}^{\text{theo}} \quad (\text{IX-3a})$$

where if MacGillivray's results are used¹³

$$2P_{el}^{theo}(\xi) = \frac{\xi^{-1} \alpha^2 q^2}{2\kappa^2 k_B T D a^2}$$

(IX-3b)

On the other hand, if classical Debye Hückel theory is assumed valid,

$$2P_{el}^{theo}(\xi=1) = \frac{\alpha^2 q^2}{2\kappa^2 D k_B T a^2}$$

(IX-3c)

As seen in Table V, Eq. IX-3c agrees quite well with $2P_{el}^{exptl}$, and Eq. IX-3b gives somewhat poorer agreement. We are thus left with the dilemma that the Debye Hückel potential gives results that accurately predict $2P_{el}^{exptl}$ and the supposedly "correct" potential does not. Several explanations come to mind: first of all, the charges in CMC reside on the side chains; it is possible, though unlikely, that the charge density of the equivalent line of charge is such that $\xi < 1$. Conversely, ξ may in fact be greater than one and we are observing a manifestation of the low dielectric backbone and salt exclusion effect on the potential as discussed in section V. Moreover, the presence of excluded volume effects would also serve to make $2P_{el}^{exptl} > 2P_{el}^{theo}$. To explore this possibility further, we suggest both experimental measurement of

TABLE V
Comparison of $2P_{el}$ with $2P_{el}^{theo}$ *

I	I^{-1}	b	$2P_T$	$2P_{el}^{exptl}$	$2P_{el}^{theo}(\xi \equiv 1)$	$2P_{el}^{theo}(\xi)$
.5	2	40.2A°	—	—	3.03	
.05	20	43.1A°	360.7A°	27.9A°	30.4	19.8
.01	100	49.8A°	481.6A°	148.5A°	151.8	99.0
.005	200	58.1A°	655.4A°	335.6A°	303.62	198.1

* For CMC $a = 5.15A^\circ$, the degree of substitution was 1.15, $\alpha = .96$, $M_w = 4.4 \times 10^5$ and $\xi = 1.53$ (Schneider and Doty)³⁹. Rice and Harris⁴⁰ give $2P_0 = 335A^\circ$ in agreement with our value of $2P_0 = 332.8$. A value of 80 is used for the dielectric constant D.

the dependence of b^2 on N and the incorporation of $\langle h_0^2 \rangle = \langle h_0^2(C_s) \rangle$ into polyelectrolyte excluded volume theory. Thus, while we have established that the contribution of electrostatic effects to P_T^0 may be sizeable, when $\xi > 1$ more work is necessary to test the range of validity of the proposed model.

X. The Colligative Properties of a Wormlike Polyelectrolyte

In this section, we proceed to calculate the excess electrostatic free energy, F_{excess}^T , of a wormlike polyelectrolyte and examine the influence of bending on the colligative properties of our hypothetical polymer. Within the limitations of the model, it turns out that bending contributes negligibly. As such, it is only necessary to explicitly consider the $\xi < l$ case.

Let us divide F_{excess}^T into two parts:

$$F_{\text{excess}}^T = F_{\text{excess}}^{\text{Rod}} + F_{\text{excess}}^{\text{Bending}}$$

(X-1)

$F_{\text{excess}}^{\text{Rod}}$ is the excess electrostatic free energy of the reference straight rod configuration. Proceeding in a manner analogous to that in section V, we find

$$F_{\text{excess}}^{\text{Rod}} = - \frac{\alpha^2 \Gamma_0^2 L \ln \chi}{D}$$

(X-2)

$F_{\text{excess}}^{\text{Bending}}$ is the difference in reversible work, over and above that of the reference configuration, required to charge up the polyelectrolyte backbone in the presence and absence of salt. $F_{\text{bending}}^{\text{excess}}$ is given by

$$F_{\text{excess}}^{\text{Bending}} = \left\langle \int_0^L ds \frac{\epsilon_0(x) R_c^{-2}}{2} \right\rangle - \left\langle \int_0^L ds \frac{\epsilon_0(0) R_c^{-2}}{2} \right\rangle$$

(X-3)

$\langle \rangle$ denotes the appropriate average over all configurations

$\epsilon_0(K)$ is the bending constant of the space curve in an ionic solution with a Debye length K^{-1} .

$\epsilon_0(0)$ is the bending constant of the wormlike polyelectrolyte in a salt free, $K=0$, solution.

Now,

$$\epsilon_0(K) = \epsilon(K) + \epsilon_\infty$$

(X-4a)

where ϵ_∞ is the bending constant in the absence of electrostatic interactions, ($K=\infty$), and $\epsilon(K)$ is that portion of the bending constant arising from electrostatic repulsions in a solution having screening length K^{-1} .

Provided that $L \gg K^{-1}$ $\epsilon(K)$ is given by Eq. VIII-20

$$\frac{\epsilon(K)}{R_B T} = \frac{\alpha^2 l_0^2}{4 K^2 R_B T D}$$

(X-4b)

In a similar fashion,

$$\epsilon_0(0) = \epsilon(0) + \epsilon_\infty$$

We note as $K \rightarrow 0$ and for finite sized polymers, L will eventually be less than K and Eq. X-4b will be invalid. We can, however, get $\epsilon(0)$ by recognizing that in the limit of infinite dilution, the polyelectrolyte assumes a rodlike configuration. It follows from Yamakawa that the bending constant becomes infinite³⁰ or

$$\lim_{K \rightarrow 0} \left[\frac{R_B T}{2 \epsilon_0(K)} \right] \rightarrow 0 \quad (X-5)$$

It therefore follows from Eq. X-1, X-2 and X-3 that

$$F_{\text{excess}}^T = - \frac{\alpha^2 \pi_0^2 L}{D} \ln K + \left\langle \int_0^L ds \frac{\epsilon_0(K)}{2} R_c^{-2} \right\rangle - \left\langle \int_0^L ds \frac{\epsilon_0(0)}{2} R_c^{-2} \right\rangle \quad (X-6)$$

$\epsilon_0(0)$ is to be treated in $\lim_{K \rightarrow 0} \epsilon_0(K)$.

At this point the ensemble average over all configurations of the chain must be calculated. An approximate evaluation will be undertaken in the context of wormlike polymer theory.^{30,41}

Let $\bar{U}(\underline{u}(L))$ be the potential energy of a chain of contour length L subject to the constraint that the unit tangent vector, $\underline{u}(L)$, at one

of the ends remains fixed.

$$U_{\epsilon}(\underline{u}(L)) = \frac{1}{2} \int_0^L ds \epsilon R_c^{-2}$$

(X-7)

ϵ is either $\epsilon_0(K)$ or $\epsilon_0(0)$.

Now, $Z(\underline{u}(L), L)$ the configurational partition function with $\underline{u}(L)$ fixed, may be written as³⁰

$$Z(\underline{u}(L), L) = \int d\{\underline{r}\} \exp \left\{ -\beta \frac{1}{2} \int_0^L ds \epsilon R_c^{-2}(s) \right\}$$

$$\beta = (k_B T)^{-1}$$

(X-8)

where the integration over $\{\underline{r}\}$ is carried out over all possible configurations of the chain consistent with the constraint that $\underline{u}(L)$ remains fixed

$$\beta \langle U_{\epsilon}(\underline{u}(L)) \rangle = \frac{\int d\{\underline{r}\} \beta \frac{1}{2} \int_0^L ds \epsilon R_c^{-2} \exp \left[-\beta \frac{1}{2} \int_0^L ds \epsilon R_c^{-2} \right]}{\int d\{\underline{r}\} \exp \left[-\beta \frac{1}{2} \int_0^L ds \epsilon R_c^{-2} \right]}$$

(X-9)

Setting $Z(\underline{u}(L), L) = Z$, we note that

$$-\beta \frac{\partial Z}{\partial \beta} = \beta \int d\underline{r} \left\{ \frac{1}{2} \int_0^L ds R_c^{-2} \exp \left\{ -\beta \epsilon \int_0^L ds R_c^{-2} \right\} \right.$$
(X-10)

So that

$$\beta \langle U_\epsilon(\underline{u}) \rangle = -\beta \frac{\partial Z}{Z \partial \beta}$$
(X-11)

An explicit expression for Z can be found in the work of Yamakawa³⁰

$$Z = \sum_l \frac{(2l+1)}{4\pi} e^{-\frac{(l)(l+1)}{2} \frac{\beta \epsilon}{P_T} L} P_l(\cos \theta) P_l(1)$$
(X-12)

The $P_l(\cos \theta)$ are the Legendre Polynomials and (θ, ϕ) is the position of $\underline{u}(L)$ in spherical coordinates.

$$\frac{\beta \epsilon}{P_T} = \frac{1}{2P_T}$$
(X-13)

P_T is the total persistence length of the chain under consideration.

$$\frac{\partial Z}{\partial \beta} = \frac{\Theta L}{\beta} \sum_l (l)(l+1)(2l+1) e^{-\Theta L(l)(l+1)} P_l(\cos \theta) \quad (X-14)$$

$$\beta \langle U_{\epsilon}(\underline{u}) \rangle = \frac{-\Theta L \sum_l (l)(l+1)(2l+1) e^{-\Theta L(l)(l+1)} P_l(\cos \theta)}{\sum_{l'} (2l'+1) e^{-\Theta L(l')(l'+1)} P_{l'}(\cos \theta)} \quad (X-15)$$

Note that in the limit of a rigid rod, $\Theta L \rightarrow 0$ and $\beta \langle U_{\epsilon=\infty}(\underline{u}) \rangle = 0$. Moreover, if the polymer were infinitely long Eq. X-4b would be valid and we could obtain $\beta \langle U_{\epsilon_0(0)}(\underline{u}) \rangle$ by

$$\beta \langle U_{\epsilon_0(0)}(\underline{u}) \rangle = \lim_{\kappa \rightarrow 0} \frac{-2\kappa^2 k_B T D L f(\theta)}{\alpha^2 \Gamma_0^2} = 0 \quad (X-16)$$

where $f(\theta)$ is the quantity in Eq. X-15 to the right of $-\Theta L$. Similarly, for a finite length rod, we have $\lim_{\kappa \rightarrow 0} \Theta L \rightarrow 0$ and

$$\beta \langle U_{\epsilon_0(0)}(\underline{u}) \rangle = \lim_{\kappa \rightarrow 0} \Theta L f(\theta) = 0 \quad (X-17)$$

Since space is isotropic, the probability of observing a given value of $U(L)$ is $\frac{1}{4\pi}$. Consequently, $U_{\epsilon_0(K)}$ the average value of $\langle U(u) \rangle_{\epsilon_0(K)}$ is given by

$$\begin{aligned} \beta U_{\epsilon_0(K)} &= \int d\Omega \frac{\beta}{4\pi} \langle U(u) \rangle_{\epsilon_0(K)} \\ &= \frac{1}{4\pi} \int_0^{2\pi} d\phi \int_0^\pi d\theta \sin\theta \beta \langle U(u) \rangle_{\epsilon_0(K)} \end{aligned} \quad (X-18)$$

$$\begin{aligned} \beta U_{\epsilon_0(K)} &= -\frac{\Theta L}{4\pi} \int_0^{2\pi} d\phi \int_0^\pi d\theta \sin\theta \frac{\sum_l (l)(l+1)(2l+1) e^{-\Theta L(l)(l+1)} P_l(\cos\theta)}{\sum_{l'} (2l'+1) e^{-\Theta L(l')(l'+1)} P_{l'}(\cos\theta)} \end{aligned} \quad (X-19)$$

Eq.(X-19) is formally exact; we can now make the physically reasonable assumption that $\Theta L \gg 1$ so we can expand the denominator of Eq. X-19 and invert

$$\begin{aligned} \left[\sum_{l'=0}^{\infty} (2l'+1) e^{-\Theta L(l')(l'+1)} P_{l'}(\cos\theta) \right]^{-1} &= 1 - \left\{ \sum_{l'=1}^{\infty} (2l'+1) e^{-\Theta L(l')(l'+1)} P_{l'}(\cos\theta) \right\} \\ &= g(\theta) \end{aligned} \quad (X-20)$$

$$\beta U_{\epsilon_0(x)} = -\frac{\Theta L}{2} \int_0^\pi d\theta \sin\theta \left[\sum_{l=0}^{\infty} (2l+1)(l)(l+1) e^{-\Theta L(l)(l+1)} P_l(\cos\theta) \right] g(\theta)$$

$$\beta U_{\epsilon_0(x)} = \frac{\Theta L}{2} \int_0^\pi d\theta \sin\theta \left[\sum_{l=1}^{\infty} (2l+1)^2 (l)(l+1) e^{-2\Theta L(l)(l+1)} P_l^2(\cos\theta) \right]$$

$$\beta U_{\epsilon_0(x)} = \Theta L \sum_{l=1}^{\infty} (2l+1)(l)(l+1) e^{-2\Theta L(l)(l+1)}$$

(X-21)

In Eq. X-21 we have used the fact that

$$\int_0^\pi d\theta \sin\theta P_l(\cos\theta) P_{l'}(\cos\theta) = \delta_{ll'} \frac{2}{(2l+1)}$$

We now examine X-21 to obtain an approximate expression in the

(H) $L \gg 1$ limit.

Consider

$$F(w) = \sum_{l=1}^{\infty} (2l+1) e^{-w(l)(l+1)}$$

(X-22)

$$\frac{-dF(w)}{dw} = \sum_{l=1}^{\infty} (2l+1)(l)(l+1) e^{-w(l)(l+1)}$$

(X-23)

Converting the sum in Eq. X-22 to an integral, integrating with respect to l and then differentiating with respect to w , we find $F'(w) = -1/w^2$. Hence,

$$\beta U_{\epsilon_0(x)} = \frac{(\Theta)L}{(2(\Theta)L)^2} = \frac{1}{4(\Theta)L} \quad (X-24a)$$

$$\beta U_{\epsilon_0(x)} = \left(\frac{2\beta\epsilon_0(x)}{4L} \right) = \frac{2\beta\epsilon_{\infty}}{4L} + \frac{2Pe_1}{4L} \quad (X-24b)$$

Similarly, by Eq. X-17, it follows for finite rods that

$$\beta U_{\epsilon_0(0)} = 0 \quad (X-25)$$

Substituting Equations X-25 and X-24b into Eq. X-6 gives

$$F_{\text{excess}}^T = -\frac{\alpha^2 \Gamma_0^2}{b} \ln x + \frac{2\beta\epsilon_{\infty}}{4L} + \frac{\alpha^2 \Gamma_0^2}{8x^2 k_B T L}$$

(X-26)

Whereupon, the excess electrostatic free energy of a polyelectrolyte solution of non-interacting molecules, \bar{F}_{excess} , is⁴²

$$\frac{\bar{F}_{\text{excess}}}{V k_B T} = -\xi n_e \ln \kappa + \frac{N_p}{V} \left[\frac{2\beta\epsilon_\infty}{4L} + \frac{\alpha^2 \Gamma_0^2}{8\kappa^2 k_B T D L} \right] \quad (\text{X-27})$$

Here $\frac{a\xi}{\alpha} = \frac{\alpha \Gamma_0^2}{D k_B T}$.

n_e is the concentration of polyelectrolyte counterions and is given by $\frac{PN_p}{V}$.

P is the number of charged groups per polyion, $P = \frac{L}{a}$

N_p is the number of polyions in a solution of volume V .

We can rewrite Eq. X-27 as

$$\frac{\bar{F}_{\text{excess}}}{V k_B T} = \xi n_e \left[-\ln \kappa + \frac{L}{8\kappa^2 L^2} \right] + \frac{N_p \beta \epsilon_\infty}{2V L} \quad (\text{X-28})$$

As discussed in section V, the relevant colligative properties in $\xi < 1$ case depend on

$$\left(\frac{\partial [\bar{F}_{\text{excess}} / V k_B T]}{\partial \kappa} \right)_{T, V} \quad (\text{X-29a})$$

By Eq. X-28

$$\left(\frac{\partial [F_{\text{excess}}/V k_B T]}{\partial \kappa} \right)_{T, V} = -\frac{\xi n_e}{\kappa} \left\{ 1 + \frac{\kappa^{-2} L^{-2}}{4} \right\} \quad (\text{X-29b})$$

Let n_i be concentration of species "i". $i=1$ is the counter ion; $i=2$, the coion.

$$\left(\frac{\partial \kappa}{\partial n_i} \right)_{T, V, n_{j \neq i}} = \frac{\lambda}{2\kappa} \quad (\text{X-30a})$$

where

$$\lambda = \frac{4\pi q_b^2}{D k_B T} \quad (\text{X-30b})$$

and

$$\kappa^2 = \lambda(n_1 + n_2) = \lambda(n_e + 2n_s) \quad (\text{X-30c})$$

Furthermore, n_s is the simple salt concentration. Proceeding a la Manning⁷, we have for $\xi < 1$

$$\ln \gamma_i = \left(\frac{\partial [\bar{F}_{\text{excess}}/V k_B T]}{\partial n_i} \right)_{T, V, n_{j \neq i}} = -\frac{\xi n_e \lambda}{2\kappa} \left[1 + \frac{\kappa^{-2} L^{-2}}{4} \right] \quad (\text{X-31})$$

Observe that an increase in salt concentration results in a decreased bending constant and a concomitant decrease in \bar{F}_{excess} . Let us define $X = n_e/n_s$; then by Eq. X-31

$$\ln \gamma_i = -\frac{\xi X}{2(X+2)} \left[1 + \frac{1}{4K^2L^2} \right]; \quad i=1, 2 \quad \xi < 1 \quad (\text{X-32a})$$

$$\ln \gamma_{\pm} = \ln (\gamma_1 \gamma_2)^{1/2}$$

$$\ln \gamma_{\pm} = -\frac{\xi X}{2(X+2)} \left[1 + \frac{1}{4K^2L^2} \right] \quad \xi < 1 \quad (\text{X-32b})$$

The osmotic coefficient ϕ , is related to $\ln \gamma_{\pm}$ by

$$\phi = 1 + \ln \gamma_{\pm} = 1 - \frac{\xi X}{2(X+2)} \left[1 + \frac{1}{4K^2L^2} \right] \quad (\text{X-33})$$

Now the Donnan salt exclusion factor Γ is defined by

$$\Gamma = \lim_{n_e \rightarrow 0} \left[\frac{n_s' - n_s}{n_e} \right] \quad (\text{X-34a})$$

Γ arises from consideration of a system in Donnan equilibrium in which the external compartment has a fixed salt concentration n_s' .

It can be shown that⁴³

$$\Gamma \approx \frac{1}{2} + n'_s \left(\frac{\partial \ln \gamma_{\pm}}{\partial n_e} \right)_{n_e \rightarrow 0} \quad (X-34b)$$

Placing Eq. X-32b into Eq. V-34b and using the definition of K in Eq. X-30c, we obtain

$$\Gamma = \frac{1}{2} \left[1 - \frac{1}{2} \xi \left(1 + \frac{1}{4K_s^2 L^2} \right) \right] \quad (X-34c)$$

with $K_s^2 = 2\lambda n_s$.

For $\xi > 1$, we can follow Manning⁷ and relate the various quantities in Eq. X-31 to X-34c to their values when $\xi=1$ and $r_0 \rightarrow \xi^{-1} r_0$. Clearly, if $KL \gg 1$ the contribution of bending to the limiting laws are negligible.

In conclusion, we have in the context of a worm model calculated the approximate contribution of the excess bending electrostatic free energy to some colligative properties. Within the range of validity of our present treatment, such effects are negligible. Thus, provided that $L \gg K^{-1}$ and excluded volume effects are absent, we have demonstrated the plausibility of Manning's fundamental assumption that bending effects can be ignored in the calculation of polyelectrolyte colligative properties.

Chapter 4. The Polyelectrolyte Excluded Volume Paradox

XI. Introduction

The expansion of polyelectrolyte chains due to repulsion between backbone charges is much less than most theories predict. The evidence and theories have been reviewed by Nagasawa, Takahashi, et al.^{23,44} It seems fair to conclude that those theories which do agree with experiment do so only at high charge densities and at the expense of ad hoc assumptions of uncertain merit. We certainly do not exclude from this comment a contribution to one of us.⁴⁵ What seems especially paradoxical is the apparent failure of Debye-Hückel theory to give even a qualitative explanation of the degree of expansion as a function of salt concentration. We propose to show here that the Debye-Hückel theory actually works reasonably well, and that its apparent failure in the usual method of application is due to other approximations made in conventional excluded volume theory. Our focus is on the paradox, and there are many aspects of the problem that we treat superficially, especially the charge condensation and internal conformations of a segment. So we still fall short of a conclusive theory.

One aspect of a complete theory, in the context of a worm model, is the variation of persistence length with ionic strength and linear charge density (real or effective). This has been considered elsewhere by ourselves and others.⁴⁶⁻⁵⁰ We allow this variation here only to the limited extent that the length of a segment is allowed to depend adjustably on the charge density, but not on the ionic strength. A more careful treatment is omitted for several reasons: (1) The qualitative failure of Debye-Hückel theory is so striking as to require consideration separate

from relatively minor corrections. (2) We are not content with the current theory of electrostatic effects on the persistence length (in regard to the applicability of the worm model, the effect of polymer dielectric constant and salt exclusion on the charge interactions,⁵¹ and the nature of the effective charge correction.) (3) Within the limits of current theory, the effect of a variable persistence length on excluded volume theory has already been analyzed clearly by Odijk and Houwaart.⁵⁰

Several calculations of the electrostatic potential of rods and cylinders^{7,8,12-14,52} indicate that the linearized Poisson-Boltzmann equation gives the correct potential out in the solvent if an effective charge density is used to describe the backbone. For fully charged native DNA the effective charge may be only a fourth of the actual charge, but for chain polymers the fraction will be higher, and for poly (acrylic acid) a maximum decrease of one-half should be about right. And at a degree of ionization of one-half the correction would vanish. But the failure of the Debye-Hückel interaction in excluded volume theory is still gross and we therefore conclude, with Nagasawa and Takahashi,⁴⁴ that something has gone wrong in its application.

The simplest use of the Debye-Huckel interaction adequately shows the problem. In this use the interaction is substituted into the theory of uncharged polymers, for which the degree of expansion is a function of z . This parameter will be considered fully below. For the present, it suffices to say that z is proportional to \sqrt{M} , where M is the molecular weight, and to X , where X is the excluded volume that two segments of the chain present to each other. Since the whole theory of the excluded volume effect for nonelectrolytes, and especially its modern versions based on scaling and renormalization, has considered the limits where M

is large and X is small, it is natural to suppose that a segment is a single monomer unit, and that the interaction between two segments is just the screened Coulomb or Debye-Huckel interaction. For large Debye screening lengths this at once makes X inversely proportional to the salt concentration C , and $z \propto \sqrt{M/C}$. But experiment indicates that z is proportional to $\sqrt{M/C}$, which is, of course, a qualitatively different scaling.

The observed proportionality of z to the Debye length has motivated, we presume certain plausible recalculations²⁴ of X that in effect replace the segment by a long cylinder of effective exclusion radius proportional to the Debye length. This model may seem reasonable enough at high charge densities, but requires ad hoc adjustments for low charge densities. Moreover, the only work known to us that comes close to a justification of the model is Onsager's calculation of the osmotic second virial coefficient for charged colloidal particles.⁵³ And that work we find insufficient to our needs for several reasons: First, the electrostatic part of the calculation was based on the interaction between infinite charged planes. Second, the modification made to that interaction to make it applicable to thin rods was ad hoc (but correct of course!), and left unspecified a basic multiplicative constant for the interaction energy. And third, the calculation yields no insight into the apparent failure of Debye-Huckel theory for the excluded volume effect.

The present treatment begins with a division of the chain into segments which consist of many monomer units and with an excluded volume potential that is simply the sum of all screened Coulomb interactions between backbone charges. The use of a large segment makes the application of conventional excluded volume theory³⁰ somewhat questionable, be-

cause of the implied limits of large M and small X . Unfortunately, it is not possible to observe these limits for any polyelectrolyte, as the value of X computed for even a single pair of discrete charges may become large. That is, X may become comparable to or larger than the cube of the distance between adjacent backbone charges. Hence, an assumption of excluded volume theory that a segment has negligible interaction with its immediate neighbors and only interacts with segments distant along the backbone is no longer valid. To salvage the validity of this assumption, which seems quite essential in the two-parameter (or "scaled") excluded volume theory, we choose very large segments and hope that any new problems thereby incurred are not too serious. One of these problems is that the enlarged segment has a conformational distribution that can depend on the degree of ionization and salt concentration. Here we shall simply make a bald simplification that has much precedence in polyelectrolyte theory. We take the segment to be, more or less, a stiff rod with an adjustable length, and see whether lengths inferred from previous thermodynamic applications of the same model can be transferred to the current problem. In time, of course, this neglect of conformational fluctuations could be remedied. However, it seemed reasonable to us to deal first with the basic question concerning the Debye-Huckel theory.

In section XII the values of X and z are computed for the given model, and it is shown that the usual result, $X \propto 1/C$, is recovered exactly for very low charge densities. However, an application to experiment in section XIII shows that the actual charge densities, even at a degree of ionization of one tenth, are so large that the usual result is inapplicable. Although the electrostatic potential at any point may be small enough in practice to justify the Debye-Huckel approximation, the

total interaction between segments is too large to be linearized in the calculation of χ . Of course, for this remark to be meaningful it is necessary, as in the rest of the calculation, that the segments are small enough to be modeled as rods. A certain amount of bending would not be serious, but even so, a few persistence lengths is all one would wish to allow. In fact, we must use somewhat longer segments for chains with low degrees of ionization. Although it is never necessary to specify their exact length, they must be a bit longer than the Debye length to justify neglect of interactions between neighbors.

XII. The Segment Excluded Volume

The excluded volume parameter X is the effective volume of exclusion that one segment presents to another, and has the general form

$$X \equiv \int \langle 1 - e^{-v} \rangle d\mathbf{r} \quad (\text{XII-1})$$

where v is the interaction potential in units of KT , \mathbf{r} is the difference between center of mass positions, and the angle brackets represent an average over internal coordinates. The complete potential is conveniently divided into contributions

$$V = V_c + V_a + V_e \quad (\text{XII-2})$$

from a core potential v_c , an attractive potential v_a , and a screened Coulomb potential v_e . The core potential is infinite or zero, and may be used immediately to separate off a positive core contribution X_c ,

$$X = X_c + \int' \langle 1 - \exp[-(v_a + v_e)] \rangle d\mathbf{r} \quad (\text{XII-3})$$

where the primed integral sign designates an integral over those values of the relative coordinates that do not violate the region of exclusion. An additional formal subdivision of X gives

$$X = X_c + X_e + X_a$$

(XII-4)

where

$$X_e = \int' \langle 1 - e^{-v_e} \rangle d\mathbf{r}$$

(XII-5)

and

$$X_a = \int' \langle e^{-v_e} (1 - e^{-v_a}) \rangle d\mathbf{r}$$

(XII-6)

In practice, X_e , the purely electrostatic part of X , will swamp other contributions at low salt concentrations unless the backbone charge is very low. The attractive part X_a is formally dependent on salt concentration, since v_e is dependent, but at the short distances where v_a is significant this dependence is not large, and X_a may be taken independent of salt concentration in first approximation. Our work is consequently restricted to a calculation of X_e .

XIIA. The Electrostatic Interaction

For the calculation of v_e and X_e a rather schematic model is adopted. The segment is treated as a rigid rod of length L , and L is assumed to be much larger than the Debye screening length. We may argue, following Onsager,⁵³ that the results should also apply to flexible segments, if L

is taken to be somewhat less than the contour length, unless the flexibility is so great or the segments so long that several close contacts between a given segment pair are allowed. But even if this possibility is allowed by chain flexibility, we expect it to be excluded by energetic factors except at low degrees of ionization I , and there the additional contributions will be minimized by a coefficient I^2 . Consequently the model may serve, at least as a rough approximation, for any I .

A uniform charge distribution along the axis of each segment, or rod, gives

$$V_e = \iint u(r_{ij}) di dj \quad (XII-7)$$

where

$$u(r) = \beta^2 a_0 r^{-1} e^{-\beta r} \quad (XII-8)$$

In these expressions di and dj are elements of length measured along the two rods, and $a_0 = 7.136 \text{ \AA}$ for an aqueous solution at 25°C . β is the number of electron charges per unit length, and has units $(\text{length})^{-1}$. It is convenient for the evaluation of the integral⁵³ to set up a coordinate system in which the first rod is oriented along the z -axis and centered on the origin, and the second rod makes a polar angle θ with the z axis. The value of the other orientational angle turns out to be irrelevant. The projection of the second rod on the xy plane will have length $L \sin \theta$. We define p to be the perpendicular distance from this projection to the origin, and require $|p| > d$, where d is the diameter of either rod. How-

ever, it is helpful in visualization and consistent with the model to regard p as infinitesimal on the scale of L . If the perpendicular intersects the projection outside its end points, the two rods are taken to have negligible interaction. Then

$$V_e = \iint_{-\infty}^{\infty} u([p^2 + i^2 + j^2 - 2ij\cos\theta]^{1/2}) di dj$$

(XII-9)

Extension of the limits to infinity is justified by the assumption that L is much greater than the Debye length. Introduction of polar coordinates for i and j and completion of the integrals gives

$$V_e = 2\pi\beta^2 a_0 (\chi \sin\theta)^{-1} \exp\{-\chi|p|\}$$

(XII-10)

This is the result put forward by Onsager, except for a proportionality constant previously left unspecified.⁵³

XIIB. The Excluded Volume

For the computation of X there remains an integration over relative center of mass coordinates and an average over the angle θ . The three orthogonal displacements for the center of mass of rod 2 are taken along the axis of p , along the z axis, and along a third orthogonal axis. The latter two displacements are restricted to values that do not eliminate the intersection defined above, and do not alter v_e within their allowed

range. Their integrals give factors L and $L \sin \theta$, respectively. Then

$$X_e = 2L^2 \left\langle \sin \theta \int_0^\infty (1 - e^{-ve}) dp \right\rangle \quad (\text{XII-11})$$

The factor of two accounts for negative p ; the average over θ must be taken with weight $\sin \theta$.

The remaining integrations in Eq. XII-11 cannot be completed in closed form. The simplest expression seems to be

$$X_e = (2L^2/\chi) R(y); \quad y \equiv 2\pi\beta^2 a_0 \chi^{-1} e^{-\chi d} \quad (\text{XII-12})$$

where

$$R(y) = \int_0^{\pi/2} d\theta \sin^2 \theta \int_0^{y/\sin \theta} dx \, x^{-1} (1 - e^{-x}) \quad (\text{XII-13})$$

or

$$R(y) = \int_0^{\pi/2} d\theta \sin^2 \theta \left[E_1(y/\sin \theta) + \ln(y/\sin \theta) + \gamma \right] \quad (\text{XII-14})$$

A numerical tabulation of $R(y)$ is given in Table VI, and limiting forms are easily obtained. For small y

$$\lim_{y \rightarrow 0} y^{-1} R(y) = 1 \quad (\text{XII-15})$$

and for large y the asymptotic form,¹⁵

$$R(y) \sim (\pi/4) \cdot (\ln y + \gamma - \frac{1}{2} + \ln 2) \quad (\text{XII-16})$$

is accurate to within two percent for $y > 2$, and to within one-half percent for $y > 3$.

XIIC. The Low Charge Limit

We now wish to verify that our results are consistent with conventional ones for chains of very low charge density. Of course there is no point in a direct comparison of values for X_e , because the usual calculation implies a somewhat different "segment" than used here. However, if a two parameter theory is to be used, corresponding values of

$$Z = \left(\frac{3}{2\pi h_0^2} \right)^{3/2} n^2 X \quad (\text{XII-17})$$

can be compared. Here h_0 is the root mean square end to end distance, and

TABLE VI

Numerical Values of the Integral $R(y)$ are Given and Compared with the
Asymptotic Formula for Large y

y	$R(y)/y$	y	$R(y)$	$R(y)$ (asymptotic)
.1	.9633	1.5	.9795	.9235
.2	.9301	2.0	1.1754	1.1494
.3	.8996	2.5	1.3373	1.3247
.4	.8714	3.0	1.4742	1.4679
.6	.8205	3.5	1.5922	1.5890
.8	.7757	4.0	1.6955	1.6938
1.0	.7359	5.0	1.8696	1.8691

is to be considered an experimentally determined quantity. So the comparison of electrostatic contributions to z comes down to $n^2\chi_e$. The same quantity, along with z , enters the theory of the osmotic second virial coefficient.

In the usual calculation, reduced to its essentials, there are n_0 small segments which can be identified with individual monomer units. Each has excluded volume X_0 calculated from

$$X_0 = \beta_0^2 a_0 \int r^{-1} e^{-\chi r} d\tau = 4\pi a_0 \beta_0^2 / \chi^2$$

(XII-18)

where β_0 is the charge on a segment. That is, one assumes, as was discussed in the Introduction, a weak potential and linearizes the Boltzmann expression. Comparison of $n_0^2 X_0$ with $n^2 \chi_e$ under conditions of low charge density, where $R(y)$ can be replaced by y , shows that agreement is found if $n_0 \beta_0 = nL\beta$. Since each of these quantities is an expression for the total charge, agreement is indeed found.

XIII. Comparison with Experiment

Disclaimers regarding the finality of this comparison have already been entered in the Introduction. We repeat that our object is to resolve the fundamental paradox, and not to deal with every ramification.

XIIIA. Intrinsic Viscosity

The intrinsic viscosity data of Noda et. al.²³ will serve to illustrate the theory. They analyzed their data on the basis of

$$[\eta]/\sqrt{M} = K_0 + 0.51 \Phi_0 B \sqrt{M}$$

(XIII-1)

where $\Phi_0 = 2.87 \times 10^{21}$, K_0 is a constant related to h_0 but of no present interest, and B is inferred from the data. The origin of this equation will be quite briefly reviewed. It relies on the assumption that the chain is non-draining, and on a semiempirical form for the expansion.

$$[\eta] = \Phi_0 h_0^2 \alpha_\eta^3 / M$$

(XIII-2)

$$\alpha_\eta^3 = 1 + A_\eta Z$$

(XIII-3)

where A_η is a coefficient inferred from an excluded volume perturbation theory. To the somewhat questionable extent that Eqs. XIII-2 and XIII-3

provide an adequate basis for an understanding of Eq. XIII-1, they imply, together with the definition of z , Eq. XII-17, that the electrostatic part of B is

$$B_e = a X_e / m_s^2 = A_\eta (3/2\pi)^{3/2} X_e / 0.51 m_s^2$$

$$m_s = M/n \quad (\text{XIII-4})$$

where the value of a is to be inferred from A_η , and m_s is the molecular weight of a segment. Noda et al chose $A_\eta = 1.55$, on the basis of theoretical estimates available at the time for nonelectrolyte polymers. More recent estimates⁵⁴ put A_η in the vicinity of 1.1, for nonelectrolytes, and as light scattering data on polyelectrolytes suggest a still smaller value, we have used $a=0.5$, corresponding to $A_\eta = .775$.

Equation XII-12 now gives

$$B_e = (L^2 / m_s^2 \kappa) R(y) = R(y) / m_\ell^2 \kappa \quad (\text{XIII-5})$$

where m_ℓ is the molecular weight (i.e., the mass in Daltons), per unit length. In what follows m_ℓ and β will be referred to a single monomer of effective length ℓ ,

$$m_\ell = m_s / L = m_0 / \ell$$

$$\beta = I / \ell \quad (\text{XIII-6})$$

where m_0 is the molecular weight of a monomer unit and I is the mean

number of elementary charges on a monomer unit, i.e., I is the degree of ionization. An effective charge can be used if one wishes, but it would have little effect because of the logarithmic dependence on I through most of the relevant range of y . Then

$$B_e = \left(\frac{\ell^2}{\kappa m_0^2} \right) R(y)$$

(XIII-7)

where

$$y = (2\pi a_0 I^2 / \ell^2 \kappa) e^{-\kappa d} \approx 136.4 I^2 / \ell^2 \sqrt{C}$$

$$\kappa^{-1} = 3.043 / \sqrt{C}$$

(XIII-8)

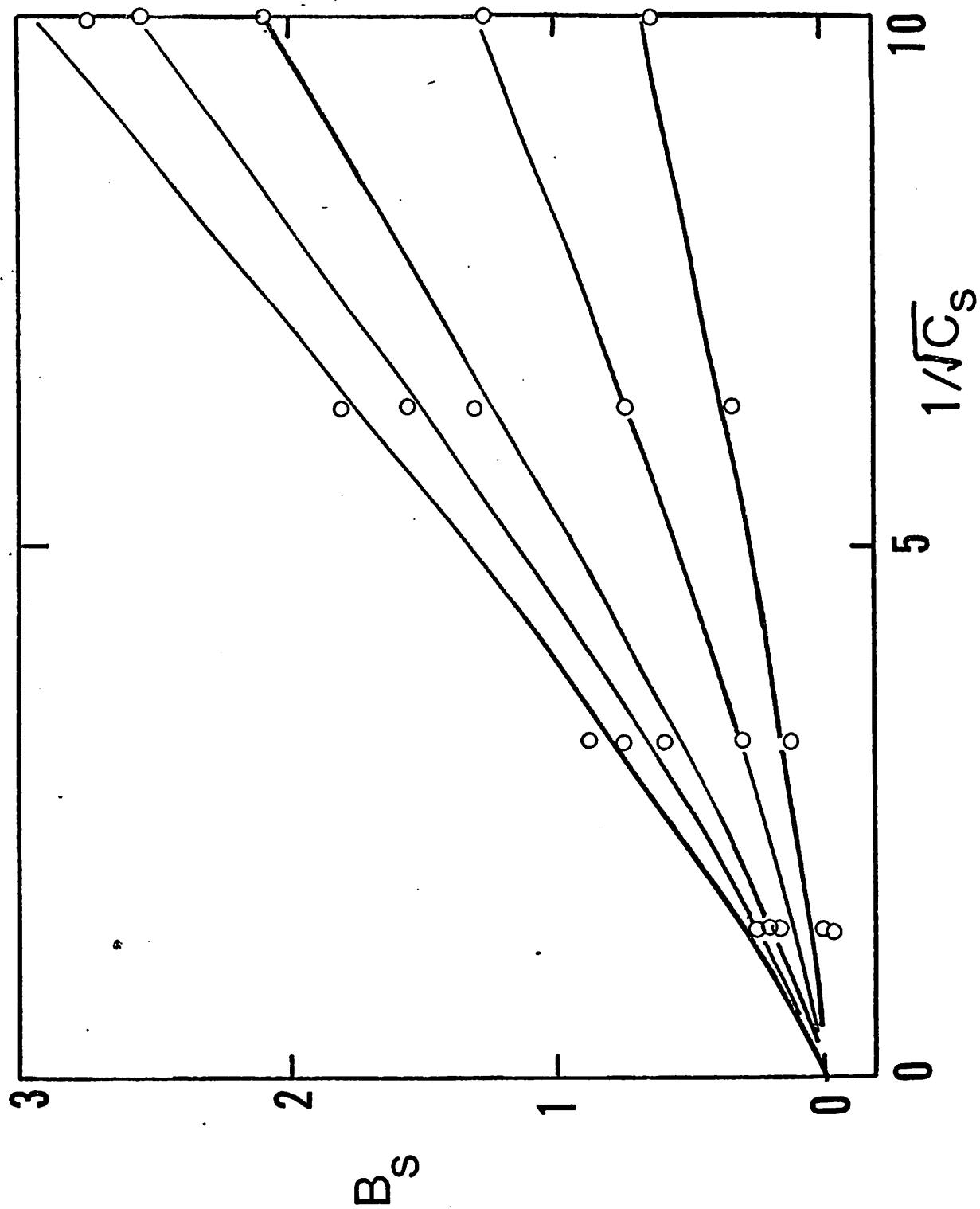
and ℓ is expressed in \AA , C in mol/liter. The numerical expressions involving C apply to a 1-1 salt, and imply the neglect of K_d .

Equation XIII-7 is compared with the data of Noda et al.²³ in Fig. 6. A value $m_0 = 94 \text{ g/mol}$ has been used, and the value of ℓ has been allowed to vary somewhat from its structural value of 2.51\AA . For $I=1$ the value chosen, $\ell = 1.2 \text{\AA}$, is close to the value inferred from titration and thermodynamic studies.^{55,56} We have used values, listed in the caption for Fig. 6 down to 0.8\AA for $I=0.1$. The largest value of y occurs at $I=1$ and $C=0.01$ where $y=947$, $R(y)/y=0.06$. In other words, the actual segment excluded volume is 0.6 percent of the Donnan value. For $I=0.1$ at $C=0.01$, $y=4.58$ and $R(y)/y=0.39$.

The agreement between theory and experiment seems good enough to justify the fairly modest conclusion put forward in the Introduction, that

Figure 6. The scaled excluded volume parameter, $B_s = 10^{26} B_e$, versus $1/\sqrt{C_s}$, where C_s is the salt concentration in mol/liter. Points are experimental results of Noda, et al,²³ and the curves are theoretical. The values of (I, ℓ) , where I is the degree of ionization and ℓ is the effective length of a monomer unit in Angstroms are, from bottom to top: (0.103, 0.8), (0.2, 1.0), (0.4, 1.15), (0.6, 1.2), (1.0, 1.2).

FIGURE 6



the Debye-Huckel approximation is reasonably adequate for the study of excluded volume problems, instead of being paradoxically bad.

IIIB. Osmotic Second Virial Coefficient

The osmotic second virial coefficient is given by theory³⁰ as

$$\begin{aligned} A_2 &= (N_{AV} n^2 X / 2 M^2) h(\bar{z}) \\ &= N_{AV} R(y) h(\bar{z}) / \kappa m_l^2 \end{aligned} \quad (\text{XIII-9})$$

where X has again been approximated by X_e , the latter from Eq. XII-12, and $h(\bar{z})$ is a decreasing function of z that has been much studied but is still, like α or α_n , not known exactly. However, for our present purposes, we may refer to the discussion of Nagasawa and Takahashi,⁴⁴ where it is shown that $h(\bar{z})$ decreases rather rapidly from unity to ca. 0.5 as z increases, and thereafter decreases quite slowly, or perhaps even levels off, depending on which theoretical formula is used to fit the data. We have simply put $h(\bar{z})=0.5$. The parameter y is calculated from Eq. XIII-8.

A comparison with the data of Orofino and Flory⁵⁷ for poly (acrylic acid) is given in Table VII. The agreement between theory and experiment is about as good as the intrinsic viscosity comparison.

TABLE VII

Experimental Osmotic Second Virial Coefficients from Orofino and Flory⁵⁷
 Compared with Theoretical Results

I	C	$10^4 A_2$ (exp)	χ	$10^4 A_2$ (theory)
.102	.10	5.95	.8	7.6
.335	.10	22.2	1.1	23.6
.344	.01	69.5	1.1	94.5
.947	1.00	10.0	1.2	10.4
.959	.10	43.9	1.2	40.3
.994	.01	196.	1.2	152.0

Appendix A: Evaluation of Radial Coefficients

In this appendix, we determine A, B, C, and E subject to the boundary conditions expressed in Eq. II-16, 17, 18 and 23.

From Eq. II-16, it readily follows that

$$A = \{B I_n(\lambda a) + C K_n(\lambda a)\} I_n^{-1}(\ell a) \quad (A-1)$$

Substituting Eq. A-1 into Eq. II-17, we have

$$D_1 \left[\frac{\{B I_n(\lambda a) + C K_n(\lambda a)\} \ell I_n'(\ell a)}{I_n(\lambda a)} \right] = D_2 \lambda [B I_n(\lambda a) + C K_n(\lambda a)] \quad (A-2)$$

On rearranging,

$$C = M_n B \quad (A-3)$$

where

$$M_n = \frac{D_1 \ell I_n(\lambda a) I_n'(\ell a) - D_2 \lambda I_n'(\lambda a) I_n(\ell a)}{D_2 \lambda K_n'(\lambda a) I_n(\ell a) - D_1 \ell K_n(\lambda a) I_n'(\ell a)}$$

(A-4)

From Eq. II-18, it is apparent that

$$B I_n(\lambda r') + (M_n B - E) K_n(\lambda r') = 0 \quad (A-5)$$

Substituting Eq. A-3 into Eq. II-23, if $x' = \lambda r'$

$$x' E K_n'(x') - B x' I_n'(x') - M_n B x' K_n'(x') = -\frac{q_0}{\pi D_2} e^{-i[n\theta' + l z']} \quad (A-6)$$

The relevant equations for B and E become

$$\begin{aligned} B I_n(x') + (M_n B - E) K_n(x') &= 0 \\ B x' I_n'(x') + x' (M_n B - E) K_n'(x') &= \frac{q_0}{\pi D_2} e^{-i[n\theta' + l z']} \end{aligned} \quad (A-7)$$

The determinate of the system of equations is

$$\begin{vmatrix} I_n(x') & -K_n(x') \\ x' I_n'(x') & -x' K_n'(x') \end{vmatrix} = -x' (I_n K_n' - K_n I_n') \quad (A-8)$$

By Kraut,¹⁷ we have

$$-X' \{ I_n K_n' - K_n I_n' \} = 1$$

From Cramers Rule, it follows that

$$B = \frac{q}{\pi D_2} K_n(x') e^{-i[n\theta' + lz']} \quad (A-9a)$$

$$E - M_n B = \frac{q}{\pi D_2} I_n(x') e^{-i[n\theta' + lz']} \quad (A-9b)$$

$$E = \frac{q}{\pi D_2} \{ I_n(x') + M_n K_n(x') \} e^{-i[n\theta' + lz']} \quad (A-9c)$$

Now if $a \leq r \leq r'$, by Eq. II-15b and A-3

$$R_n(x) = B I_n(x) + M_n B K_n(x) \quad (A-10)$$

Thus, using Eq. A-9a we find for $a \leq r \leq r'$

$$R_n(x) = \oint_{\pi D_2} \{ I_n(x) K_n(x') + M_n K_n(x) K_n(x') \} e^{-i[n\theta' + l z']} \quad (A-11)$$

and if $r \geq r'$ from Eq. II-15c

$$R_n(x) = E K_n(x) \quad (A-12)$$

Substituting Eq. A-9c into Eq. A-12 for $r \geq r'$

$$R_n(x) = \oint_{\pi D_2} \{ I_n(x') K_n(x) + M_n K_n(x') K_n(x) \} e^{-i[n\theta' + l z']} \quad (A-13)$$

We can combine Eq. A-11 and A-13 by writing

$$R_n(\lambda r) = \oint_{\pi D_2} \{ I_n(\lambda r_1) K_n(\lambda r_2) + M_n K_n(\lambda r_1) K_n(\lambda r_2) \} e^{-i[n\theta' + l z']} \quad (A-14)$$

Here $r \geq a$ and

$r_<$ is the minimum of (r, r')

$r_>$ is the maximum of (r, r')

For completeness, we note that A given Eq. A-1 can be written using Eq. A-3 and A-9a as

$$A = \frac{q_0 \{ I_n(\lambda a) K_n(\lambda r') + M_n K_n(\lambda a) K_n(\lambda r') \}}{\pi D_2 I_n(\lambda a)} e^{-i[n\theta' + \lambda z']} \quad (A-15)$$

if $r \leq a$, Eq. II-15a gives

$$R_n(\lambda r) = A I_n(\lambda r) \quad (A-16)$$

Placing Eq. A-15 into Eq. A-16 for $0 \leq r \leq a$

$$R_n(\lambda r) = \frac{q_0 \{ I_n(\lambda a) I_n(\lambda r) K_n(\lambda r') + M_n I_n(\lambda r) K_n(\lambda a) K_n(\lambda r') \}}{\pi D_2 I_n(\lambda a)} e^{-i[n\theta' + \lambda z']} \quad (A-17)$$

This completes our calculation of $R_n(\lambda, r)$ for all values of r .

Appendix B: Proof ψ_T Reduces to ψ_{DH} in Absence of the Low Dielectric Cylinder

The solution to Eq. II-28

$$\psi_S = \frac{2q_0}{\pi D_2} \int_0^\infty dl \cos[l(z-z')] \left\{ I_0(\lambda r_2) K_0(\lambda r_1) + \sum_{n=1}^\infty I_n(\lambda r_2) K_n(\lambda r_1) \cos n(\theta - \theta') \right\} \quad (B-1)$$

corresponds to the Green's function of

$$(\nabla^2 - \kappa^2) \psi_S = -\frac{4\pi q_0}{D_2} \delta(r - r') \quad (B-2)$$

in the absence of the dielectric cylinder. Consequently, we shall demonstrate that the rhs of Eq. B-1 equals the screened coulomb potential, i.e.,

$$\psi_S = \frac{q_0 e^{-\kappa |r - r'|}}{D_2 |r - r'|} \quad (B-3)$$

In cylindrical coordinates, $|r - r'|$ may be expressed as

$$|\underline{r}-\underline{r}'|^2 = r^2 + r'^2 - 2rr'\cos(\theta-\theta') + (z-z')^2$$

(B-4)

Defining, $w^2 = r^2 + r'^2 - 2rr'\cos(\theta-\theta')$, it can be shown that,¹⁹

$$K_0(\lambda w) = I_0(\lambda r) K_0(\lambda r') + 2 \sum_{n=1}^{\infty} I_n(\lambda r) K_n(\lambda r') \cos n(\theta-\theta')$$

(B-5)

Thus, substituting $K_0(\lambda w)$ into Eq. B-1

$$\Psi_T(M_n=0) = \Psi_S = \frac{2q_0}{\pi D_2} \int_0^{\infty} d\ell \cos \ell(z-z') K_0(\lambda w)$$

(B-6)

Let $\ell' = \ell K^{-1}$

$$\Psi_S = \frac{2q_0 K}{\pi D_2} \int_0^{\infty} d\ell' \cos[\ell' K(z-z')] K_0((\ell'^2 + 1)^{1/2} K w)$$

(B-7)

Now, by Bateman¹⁹ we have

$$\int_0^{\infty} dx \cos xy K_0(\alpha(x^2 + \beta^2)^{1/2}) = \frac{\pi e^{-\beta(y^2 + \alpha^2)^{1/2}}}{2 (y^2 + \alpha^2)^{1/2}}$$

(B-8)

Here $y = K(z - z')$, $\alpha = \chi \omega$, $\beta = 1$; using the appropriate values of α , y and β in Eq. B-8, we have

$$\psi_s = \frac{q_0 e^{-K[\omega^2 + (z - z')^2]^{1/2}}}{D_2 (\omega^2 + (z - z')^2)^{1/2}}$$

(B-9a)

which by Eq. B-4 gives

$$\psi_T(M_h=0) = \psi_s = \frac{q e^{-\chi |r - r'|}}{D_2 |r - r'|}$$

(B-9b)

Therefore, we have demonstrated the validity of Eq. B-3.

Appendix C: Derivation of Asymptotic Large Z Limit of ψ_T

We demonstrate that if $Kr_s \ll 1$, ψ_b vanishes much faster than

$$\frac{q_b e^{-\lambda|z-z'|}}{D_2 |z-z'|} \quad \text{in the limit of large } (Z-Z').$$

$$\psi_b = \frac{2g}{\pi D_2} \int_0^\infty d\ell \cos \ell z_\infty \left\{ M_0 K_0(\lambda r) K_0(\lambda r') + 2 \sum_{n=1}^\infty M_n K_n(\lambda r) K_n(\lambda r') \cos n\theta'' \right\}$$

(C-1a)

$$\theta'' = \theta - \theta', \quad z_\infty = |z - z'|$$

$$\psi_s = \frac{q_b e^{-\lambda|r-r'|}}{D_2 |r-r'|} \quad (C-1b)$$

Following Lighthill,²⁰ ψ_b is in the limit $Z-Z' \gg a$ the cosine transform of the rhs of Eq. C-1 with the bracketed term replaced by its asymptotic value near $\ell=0$. We then consider, M_n near $\ell=0$, where by Eq. II-25

$$M_n = \frac{D_1 \ell I_n(\lambda a) I_n'(\ell a) - D_2 \lambda I_n'(\lambda a) I_n(\ell a)}{D_2 \lambda K_n'(\lambda a) I_n(\ell a) - D_1 \ell I_n'(\ell a) K_n(\lambda a)} \quad (C-2)$$

For $n \neq 0$, it is possible to write²¹

$$x K_n'(x) = -n K_n(x) - x K_{n-1}(x)$$

(C-3)

Now by Abramowitz and Stegun¹⁵ (their Eq. 9.69), $n \neq 0$ and for small x

$$K_n(x) \sim \frac{(n-1)!}{2} \left(\frac{x}{2}\right)^{-n} \quad (C-4a)$$

$$x K_n'(x) \sim -\frac{n!}{2} \left(\frac{x}{2}\right)^{-n} - (n-2)! \left(\frac{x}{2}\right)^{-n+2} \quad (C-4b)$$

$$x K_n'(x) \sim -n K_n(x) \quad (C-5)$$

in the limit of small x .

Similarly,²¹ if $x \ll 1$

$$x I_n'(x) \sim n I_n(x) \quad (C-6)$$

Then using Eq. C-5 and C-6 and the fact that $D_2 \gg D_1$,

$$M_n \sim \frac{-D_a I_n(\lambda a) I_n(\lambda a)}{-D_a I_n(\lambda a) K_n(\lambda a)} \quad (C-7a)$$

$$M_n \sim \frac{I_n(\lambda a)}{K_n(\lambda a)} \quad (C-7b)$$

Substituting Eq. C-7b into Eq. C-1 we have

$$\lim_{z \rightarrow a} \psi_b = \frac{2q}{\pi D_a} \int_0^{\infty} d\lambda \cos \lambda z_{\infty} \left[M_0 K_0(\lambda r_z) K_0(\lambda r'_z) + \sum_{n=1}^{\infty} \frac{I_n(\lambda a) K_n(\lambda r_z) K_n(\lambda r'_z) \cosh n \theta''}{K_n(\lambda a)} \right] \quad (C-8)$$

A particularly simple case is obtained if $r_z = a$. This corresponds to either the location of the point charge at $r' = a$ or the measurement of the potential at $r = a$ due to a charge at r' , not necessarily at $r = a$. Furthermore, since the major contribution to ψ_b comes from the $\lambda = 0$ component of the bracketed term and because $K_n(\lambda r) K_n(\lambda r')$ is a strictly decreasing function of r and r' , we expect $\psi_b(r_z = a) > \psi_b(r_z > a)$ for a fixed value of r_z . For the same value of r , the boundary correction to the potential due to a point charge immersed in an ionic solution is smaller than the correction from a point charge on the cylinder. Con-

versely, the boundary correction to the potential on the cylinder due to a point charge in solution should be larger than the correction the same radial distance from the point charge but further from the cylinder.

Now for small x ,¹⁵

$$I_n(x) \sim (x/2)^n / n!$$

(C-9a)

and if $\lambda r_2 \ll 1$ we may approximate

$$\frac{I_n(\lambda a) K_n(\lambda r_2)}{K_n(\lambda a)} \sim \lambda^n \left(\frac{a^2}{2r_2} \right)^n$$

(C-9b)

$$\sim I_n \left(\lambda \frac{a^2}{r_2} \right)$$

(C-9c)

r_2 rather than r_1 is chosen to guarantee that Eq. C-9c is a valid approximation to Eq. C-9b.

Using Eq. C-9a-c in Eq. C-8,

$$\psi_b = \frac{2q}{\pi D_2} \int_0^\infty dl \cos l z_\infty \left[I_0(\lambda b) K_0(\lambda r_2) + 2 \sum_{n=1}^\infty I_n(\lambda b) K_n(\lambda r_2) \cos n\theta \right] \quad (C-10)$$

$$+ \frac{2q}{\pi D_2} \int_0^\infty dl \cos l z_\infty \left[M_0 K_0(\lambda r_2) K_0(\lambda r_1) - I_0(\lambda b) K_0(\lambda r_2) \right]$$

and

$$b = a^2/r_>$$

The first term in brackets on rhs of Eq. C-10 is given by Eq. B-5

$$K_0(\lambda \bar{w}) = I_0(\lambda b) K_0(\lambda r_>) + 2 \sum_{n=1}^{\infty} I_n(\lambda b) K_n(\lambda r_>) \cos n\theta''$$

$$\bar{w} = b^2 + r_>^2 - 2 b r_> \cos \theta''$$

(C-11)

and as in Eq. B-8

$$\frac{2}{\pi} \int_0^{\infty} d\lambda \cos \lambda z_{\infty} K_0(\lambda \bar{w}) = \frac{e^{-K(z_{\infty}^2 + \bar{w}^2)^{1/2}}}{(z_{\infty}^2 + \bar{w}^2)^{1/2}}$$

(C-12)

Moreover,

$$M_0 = \frac{D_1 \ell I_0(\lambda a) I_1(\ell a) - D_2 \lambda I_1(\lambda a) I_0(\ell a)}{-D_2 \lambda K_1(\lambda a) I_0(\ell a) - D_1 \ell K_0(\lambda a) I_1(\ell a)} \quad (C-13)$$

In the limit of small λ , to lowest order

$$M_0 \sim \frac{I_1(\lambda a)}{K_1(\lambda a)} \quad (C-14)$$

The second bracketed term on the rhs of Eq. C-10 is therefore

$$M_0 K_0(\lambda r_z) K_0(\lambda r_7) - I_0(\lambda b) K_0(\lambda r_z) =$$

$$K_0(\lambda r_z) \left[\frac{I_1(\lambda a) K_0(\lambda r_z)}{K_1(\lambda a)} - I_0(\lambda b) \right] \quad (C-15a)$$

We now rewrite C-15a as follows, if we denote lhs of Eq. C-15a by Δ

$$\Delta = \frac{I_1(\lambda a) K_0(\lambda r_z)}{I_1(\lambda r_7) K_1(\lambda a)} \left[K_0(\lambda r_7) I_1(\lambda r_7) + I_0(\lambda r_7) K_1(\lambda r_7) \right]$$

$$- \frac{I_1(\lambda a) K_0(\lambda r_z) I_0(\lambda r_7) K_1(\lambda r_7) - I_0(\lambda b) K_0(\lambda r_z)}{I_1(\lambda r_7) K_1(\lambda a)} \quad (C-15b)$$

The bracketed term on the rhs of Eq. C-15b is the Wronskian

$$\Delta = \frac{I_1(\lambda a) K_0(\lambda r_z)}{I_1(\lambda r_7) K_1(\lambda a) \lambda r_7} - \frac{I_0(\lambda b) K_0(\lambda r_z)}{I_1(\lambda r_7) K_1(\lambda a)}$$

$$- \frac{I_1(\lambda a) I_0(\lambda r_7) K_1(\lambda r_7) K_0(\lambda r_z)}{I_1(\lambda r_7) K_1(\lambda a)} \quad (C-15c)$$

Using the asymptotic forms of $I_1(x)$ and $K_1(x)$ in Eq. C-15c, we obtain

$$\Delta \sim -H_0(\lambda r_c) \quad (C-15d)$$

Placing Eq. C-15d into Eq. C-10 and integrating

$$\lim_{z_\infty \rightarrow \infty} \psi_b = \frac{q_b}{b_2} \left\{ e^{\frac{-x \sqrt{z_\infty^2 + \bar{\omega}^2}}{\sqrt{z_\infty^2 + \bar{\omega}^2}}} - e^{\frac{-x \sqrt{z_\infty^2 + r_c^2}}{\sqrt{z_\infty^2 + r_c^2}}} \right\} \quad (C-16)$$

However, $|z-z'| > \bar{\omega}$, so we can linearize the exponential about $K(z-z')$; expanding terms to lowest order we obtain

$$\lim_{z_\infty \rightarrow \infty} \psi_b = \frac{q_b}{b_2} \left\{ \frac{e^{-x z_\infty}}{2 z_\infty^2} (x + \bar{z}_\infty^{-1}) (2 b r_c \cos(\theta - \theta') - b^2) \right\} \quad (C-17)$$

with $z_\infty = |z-z'|$.

Moreover,

$$\lim_{z_\infty \rightarrow \infty} \psi_s = \frac{q}{b_2} \left\{ \frac{e^{-x z_\infty}}{z_\infty} - \frac{e^{-x z_\infty}}{2 z_\infty^2} (x + \bar{z}_\infty^{-1}) (r^2 + r'^2 - 2 r r' \cos(\theta - \theta')) \right\} \quad (C-18)$$

Combining Eq. C-17 and C-18, we have

$$\lim_{z_{\infty} \rightarrow \infty} \psi_T = q_b \left\{ \frac{e^{-xz_{\infty}}}{\bar{z}_{\infty}} + \frac{e^{-xz_{\infty}}}{2\bar{z}_{\infty}^2} (x + \bar{z}_{\infty}^{-1}) (-r^2 - r'^2 - b^2 + 2\cos(\theta - \theta') [br_z + rr']) \right\}$$

(C-19)

We can now demonstrate in the vicinity of the charge, $|\theta - \theta'|$ small, the above expression is an increasing (nondecreasing) function of r when $a \leq r \leq r'$

Let

$$f(r) = -r^2 - r'^2 - b^2 + 2\cos(\theta - \theta') [br_z + rr']$$

(C-20)

If $a \leq r \leq r'$

$$f(r) = -r^2 - r'^2 - a^4/r'^2 + 2 \left(\frac{a^2}{r'} + rr' \right) \cos(\theta - \theta')$$

(C-21a)

$$f'(r) = -2r + 2 \left[\frac{a^2}{r'} + r' \right] \cos(\theta - \theta')$$

(C-21b)

In the vicinity of the point charge $\theta = \theta'$, this is an increasing function.

However, when $|\theta - \theta'| > \arccos(rr'/(a^2 + r'^2))$, this will be a decreasing function. Physically, when $|\theta - \theta'| \leq \arccos[rr'/(a^2 + r'^2)]$, increasing r moves us closer to the point charge. When $|\theta - \theta'| > \arccos[rr'/(a^2 + r'^2)]$ increasing r moves us further from the point charge and the potential decreases.

When $r \geq r'$

$$f(r) = -r^2 - r'^2 - \frac{a^4}{r^2} + 2 \cos(\theta - \theta') \left[\frac{a^2 r'}{r} + rr' \right] \quad (C-22a)$$

$$f'(r) = -2r + \frac{2a^4}{r^3} + 2 \cos(\theta - \theta') \left[-\frac{a^2 r'}{r^2} + r' \right] \quad (C-22b)$$

Clearly the sum of the first two terms on the rhs of Eq. C-22b are negative semidefinite. The sum of the two terms, $\frac{-a^2 r'}{r^2} + r'$, is positive semidefinite. Hence,

$$\begin{aligned} f'(r) &\leq -2r + \frac{2a^4}{r^3} - \frac{2a^2 r'}{r^2} + 2r' \\ &\leq 2(-r + r') + \frac{2a^2}{r^2} (a^2 - r') \leq 0 \end{aligned} \quad (C-23)$$

which is strictly less than or equal to zero. Hence $f'(r)$ is a decreasing (nonincreasing) function of r when $r \geq r'$.

Appendix D: Asymptotic Forms of h_n for Large n

In this appendix, we present the asymptotic forms of h_n for large n to higher order and demonstrate that $\lim_{z \rightarrow 0} \psi_T$ is independent of K .

We consider the $K=0$ case first. By Eq. II-36

$$h_n = \frac{-K_n(y|z)I_n(y|z)}{y|z \{ D_2 K'_n(y|z)I_n(y|z) - D_1 K_n(y|z)I'_n(y|z) \}} \quad (D-1)$$

The uniform asymptotic approximation to the I_n, K_n for large n is given by

$$I_n(nx) = \frac{e^{n\gamma}}{\sqrt{2\pi n} (1+x^2)^{1/4}} \left[1 + \frac{u_1(t)}{n} + \frac{u_2(t)}{n^2} + \dots \right] \quad (D-2a)$$

$$K_n(nx) = \sqrt{\frac{\pi}{2n}} \frac{e^{-n\gamma}}{(1+x^2)^{1/4}} \left[1 - \frac{u_1}{n} + \frac{u_2}{n^2} - \dots \right] \quad (D-2b)$$

$$I'_n(nx) = \frac{e^{n\gamma} (1+x^2)^{1/4}}{\sqrt{2\pi n} x} \left[1 + \frac{v_1(t)}{n} + \frac{v_2(t)}{n^2} + \dots \right] \quad (D-2c)$$

$$K'_n(nx) = \sqrt{\frac{\pi}{2n}} \frac{e^{-n\gamma} (1+x^2)^{1/4}}{x} \left[1 - \frac{v_1(t)}{n} + \frac{v_2(t)}{n^2} - \dots \right] \quad (D-2d)$$

$$t = (1+x^2)^{-1/2} ; \quad \gamma = (1+x^2)^{1/2} + \ln(x/(1+\sqrt{1+x^2})) \quad (D-2e)$$

The $u_i(t)$ and $v_i(t)$ are given in Abramowitz and Stegun sections 9.3.9, 9.3.10, 9.3.13, and 9.3.14.¹⁶

Substitution of Eq. D-2a-d into Eq. D-1 yields

$$h_n = \frac{(1+w^2)^{-1/2}}{n(D_1+D_2)} \left\{ 1 + \frac{D_2-D_1}{(D_2+D_1)} \left(\frac{u_1-v_1}{n} \right) \right\}^{-1} \quad (D-3)$$

$$w = y(|z|n)^{-1}$$

or by Eq. II-35

$$H_n(x=0) = \frac{z}{(D_1 + D_2)^0} \int_0^\infty d\omega \frac{\cos \omega n z}{(1 + \omega^2)^{1/2}} \left[1 - \frac{(D_2 - D_1)(u_1 - v_1)}{n(D_2 + D_1)} + \dots \right] \quad (D-4)$$

Now,

$$u_1 = u_1(t) = t(3 - 5t^2)/24 \quad (D-5a)$$

$$v_1 = v_1(t) = (-9t + 7t^3)/24 \quad (D-5b)$$

$$t = 1/\sqrt{1 + \omega^2} \quad (D-5c)$$

Placing the values of u_1 and v_1 in Eq. D-4, we find

$$H_n(x=0) = \frac{z}{(D_1 + D_2)} \left\{ K_0(nz) - \frac{(D_2 - D_1)}{2n(D_2 + D_1)} \int_0^\infty d\omega \frac{\omega^2 \cos \omega n z}{(1 + \omega^2)^2} \right\} \quad (D-6a)$$

$$H_n(x=0) = \frac{z}{(D_1 + D_2)} \left\{ K_0(nz) - \frac{(D_2 - D_1)}{(D_2 + D_1)} \left(\frac{\pi}{8n} \right) (1 - n|z|) e^{-n|z|} \right\} \quad (D-6b)$$

If $K \neq 0$, then Eq. II-34c gives

$$h_n(K \neq 0) = \frac{-K_n(\alpha) I_n(y|z)}{\{D_2 \alpha K_n'(\alpha) I_n(y|z) - D_1(y|z) K_n(\alpha) I_n'(y|z)\}} \quad (D-7)$$

with $\alpha = (Y^2/Z^2 + K^2)^{1/2}$ and K is in units of a^{-1} .

For large n and to lowest order in Eq. D2a-d, Eq. D-7 becomes

$$h_n(K) = n^{-1} \{ D_2 (1+w^2 + K^2/n^2)^{1/2} + D_1 (1+w^2)^{1/2} \}^{-1} \quad (D-8)$$

Clearly provided that we are interested in small to moderate z , (large w), and large n , the contribution of K to h_n to lowest order in the various I_n and K_n is negligible. In fact, substitution of higher order terms in Eqs. D-2a-d, reveals that h_n is independent of K for large n and small z .

Thus,

$$\lim_{z \rightarrow 0} z \psi_T = \frac{4q}{\pi} \int_0^\infty dn H_n \quad (D-9)$$

with H_n given by Eq. D-8 is to an excellent approximation independent of K .

Appendix E: Details of the Contour Deformation to Obtain H_n

In the following, the derivation of Eq. III-2 is discussed in some detail. From Eq. II-32 and II-34,

$$h_n(\lambda, \lambda_0) = \frac{-K_n(\lambda r) I_n(\lambda_0)}{\{D_2 \lambda K_n'(\lambda) I_n(\lambda_0) - D_1 \lambda_0 K_n(\lambda) I_n'(\lambda_0)\}} \quad (E-1)$$

$$\text{with } \lambda = (\ell^2 + K^2)^{\frac{1}{2}}$$

$$\lambda_0 = (\ell^2 + K_0^2)^{\frac{1}{2}} \quad K_0 \rightarrow 0$$

$$a \equiv 1$$

and

$$\frac{2}{\pi} H_n = \frac{2}{\pi} z \int_0^{\infty} d\ell \cos \ell z h_n(\lambda, \lambda_0) \quad (E-2)$$

As mentioned in the body of the thesis, the asymptotic forms for the Bessel functions in the right half of the λ and λ_0 planes give adequate convergence at infinity for the $h_n(\lambda, \lambda_0)$. Assuming there are no poles, an assumption justified at the end of this appendix, we can deform the contour to run along the two sides of the positive imaginary axis. Let

$$\ell^- = R e^{i\pi/2 \ominus} \quad (E-3a)$$

$$\ell^+ = R e^{i\pi/2 \oplus} \quad (E-3b)$$

- and + refer to that portion of the branch cut in the right or left upper quadrants respectively. Whereupon, if $R < K$

$$\lim_{\lambda_0 \rightarrow 0} \lambda_0^- \text{ is positive imaginary} = iR \quad (\text{E-4a})$$

$$\lim_{\lambda_0 \rightarrow 0} \lambda_0^+ \text{ is negative imaginary} = -iR \quad (\text{E-4b})$$

With $h_n(\lambda_0, \lambda)$ defined from Eq. E-2, we have if $K > R$

$$\pi^{-1} H_n(K > R) = \frac{iZ}{\pi} \int_0^K dR e^{-R|Z|} \{ h_n(iR, \sqrt{K^2 - R^2}) - h_n(-iR, \sqrt{K^2 - R^2}) \} \quad (\text{E-5a})$$

Similarly when $R > K$

$$\pi^{-1} H_n(R > K) = \frac{iZ}{\pi} \int_K^\infty dR e^{-R|Z|} \{ h_n(iR, i\sqrt{R^2 - K^2}) - h_n(-iR, -i\sqrt{R^2 - K^2}) \} \quad (\text{E-5b})$$

At this point we need the recursion relationships of the I_n and K_n and the transformations from real to imaginary arguments.¹⁶

$$I_n'(x) = I_{n+1}(x) + \frac{n}{x} I_n(x) \quad (\text{E-6a})$$

$$K_n'(x) = -K_{n+1}(x) + \frac{n}{x} K_n(x) \quad (\text{E-6b})$$

$$I_n(iR) = (i)^n J_n(R) \quad (\text{E-7a})$$

$$iR I_n'(iR) = (i)^n [n J_n(R) - R J_{n+1}(R)] \quad (\text{E-7b})$$

$$K_n(isr) = \left(\frac{\pi}{2}\right) (-i)^{n+1} [J_n(sr) - i Y_n(sr)] \quad (\text{E-8a})$$

$$iS K_n'(is) = (-i)^{n+1} \frac{\pi}{2} \left[-s \{ J_{n+1}(s) - i Y_{n+1}(s) \} + n \{ J_n(s) - i Y_n(s) \} \right] \quad (\text{E-8b})$$

with

$$s = \sqrt{R^2 - K^2}$$

The $J_n(X)$ and $Y_n(X)$ are Bessel functions of the first and second kind respectively.

It immediately follows from Eq. E-5a that

$$\pi^{-1} H_n(X > R) = -\frac{2z}{\pi} \int_0^X dR e^{-R|z|} h_n(iR, \sqrt{X^2 - R^2})$$

(E-9a)

If we employ Eq. E7a-7b in Eq. E-9a, we obtain

$$h_n(iR, \sqrt{X^2 - R^2}) = \frac{-K_n(r\sqrt{X^2 - R^2}) (i)^n J_n(R)}{[D_2 \sqrt{X^2 - R^2} (i)^n J_n(R) K'_n(rt) - D_1 (i)^n Y_n(R) K_n(rt)]}$$

(E-9b)

Here $t = \sqrt{X^2 - R^2}$

$$\gamma_n(R) = nJ_n(R) - RJ_{n+1}(R)$$

Clearly in Eq. E-9b all $(i)^n$ cancel out, and $h_n(iR, \sqrt{X^2 - R^2})$ has no imaginary part. Otherwise stated,

$$H_n(K > R) = 0 \text{ for all } n.$$

From Eq. E-5b, it is evident that

$$\pi^{-1} H_n(R > X) = -\frac{2z}{\pi} \int_K^\infty dR e^{-R|z|} h_n(iR, iS)$$

(E-10a)

Let us explicitly examine $h_n(iR, iS)$

$$h_n(iR, iS) = \frac{-J_n(R)[J_n(Sr) - iY_n(Sr)]}{D(R, S)} \quad (E-10b)$$

$$D(R, S) = D_2 J_n(R) \{ -S[J_{n+1}(S) - iY_{n+1}(S)] + n[J_n(S) - iY_n(S)] \} \\ - D_1 \{ [nJ_n(R) - R J_{n+1}(R)] [J_n(S) - iY_n(S)] \} \quad (E-10c)$$

We have used Eq. E6a-E8b in Eq. E-10b and E-10c. Consequently, on consideration of the imaginary part of Eq. E-10b, we have

$$\text{Im } h_n(iR, iS) = \frac{-(BC - AE)}{C^2 + E^2} \quad (E-11a)$$

with

$$A = J_n(R) J_n(Sr) \quad (E-11b)$$

$$B = -J_n(R) Y_n(Sr) \quad (E-11c)$$

$$C = D_2 J_n(R) S J_n'(S) - D_1 J_n(S) R J_n'(R) \quad (E-11d)$$

$$E = -D_2 J_n(R) S Y_n'(S) + D_1 Y_n(S) R J_n'(R) \quad (E-11e)$$

$$BC-AE \rightarrow \frac{2D_2}{\pi} J_n^2(R) \text{ as } r \rightarrow a \equiv 1$$

Consequently, by Eq. 10-a

$$\pi^{-1} H_n = \frac{2|z|}{\pi} \int_0^\infty dR e^{-R|z|} \frac{BC-AE}{C^2+E^2} \quad (E-12)$$

As a check on Eq. E-12, if $K=0$ and $r=1$, then ψ_T given by

$$\psi_T = \frac{1}{\pi z} \left\{ H_0 + 2 \sum_{n=1}^{\infty} H_n \cos n\theta \right\} \quad (E-13a)$$

should reduce to

$$\psi_T = \frac{1}{D_2 \sqrt{z^2 + 2(1 - \cos \theta)}} \quad (\text{E-13b})$$

Setting $K=0$, i.e. $S=R$, and $D_1=D_2$, Eq. 11-a-d reduce to

$$A = J_n^2(R) \quad (\text{E-14a})$$

$$B = -J_n(R) Y_n(R) \quad (\text{E-14b})$$

$$C = 0 \quad (\text{E-14c})$$

$$E = -\frac{2D_2}{\pi} \quad (\text{E-14d})$$

We have used the Wronskian of Y_m and J_m to obtain Eq. E-14d. Moreover, by Eq. E-14a-d,

$$\frac{BC - AE}{C^2 + E^2} = -\frac{A}{E} \quad (\text{E-15a})$$

$$\frac{BC - AE}{C^2 + E^2} = \frac{\pi J_n^2(R)}{2 D_2}$$

(E-15b)

Substituting Eq. E-15b into Eq. E-12 and reversing the order of summation and integration in Eq. E-13a, we find

$$\psi_T(x=0) = \int_0^\infty \frac{dR e^{-R|z|}}{D_2} \left\{ J_0^2(R) + 2 \sum_{h=1}^\infty J_h^2(R) \cos h\theta \right\}$$

(E-16)

By Watson,¹⁸

$$J_0(\bar{w}) = J_0^2(R) + 2 \sum_{h=1}^\infty J_h^2(R) \cos h\theta$$

(E-17a)

$$\bar{w} = \sqrt{2(1 - \cos\theta)} R$$

(E-17b)

and

$$\psi_T = D_2^{-1} \int_0^\infty dR e^{-R|z|} J_0(R \sqrt{2(1 - \cos\theta)})$$

(E-18a)

The integral in Eq. E-18a is immediately recognized to give

$$\Psi_T(K=0) = \frac{1}{D_a \sqrt{z^2 + 2(1 - \cos \theta)}} \quad (E-18b)$$

which is in agreement with Eq. E-13b.

We now return to the question of the possible poles of the h_n in the z plane. We are indebted to Professor Ira Bernstein for suggesting the lines of our argument.

In Eq. II-13, let $D(r)$ be replaced by a continuous function of arbitrary steepness and the interval $(0, \infty)$. At the right boundary $R_n(r) = h_n(r)$ vanishes, and at the left $\frac{dh_n}{dr}$ vanishes. Then

$$(\mathcal{L} + \ell^2) h_n = \frac{\delta(r-a)}{r D(r)} = S(r) \quad (E-19a)$$

with

$$\mathcal{L} h_n = -\frac{1}{r D(r)} \left(\frac{\partial}{\partial r} r D(r) \frac{\partial h_n}{\partial r} \right) + \left(K^2(r) + \frac{n^2}{r^2} \right) h_n \quad (E-19b)$$

The operator \mathcal{L} is self adjoint and positive definite for a scalar product defined with a weight function $rD(r)$. Consequently, \mathcal{L} has a complete set of eigenfunctions f_i and positive eigenvalues λ_i ; the source and Greens function may be expanded as follows

$$S(r) = \sum_i s_i f_i ; \quad h_n = \sum_i \frac{s_i f_i}{l^2 + \lambda_i} \quad (\text{E-20})$$

it follows that h_n can have only imaginary poles. These will generate a branch cut as the limits on r are extended to zero and infinity.

Appendix F: Derivation of $R_n(\lambda'r)$

In this appendix, we derive the explicit form of $R_n(\lambda'r)$ appropriate to a point charge immersed in a cylindrically, symmetric low dielectric constant region. As is given by Eq. IV-2

$$R_n(\lambda'r) = \begin{cases} A I_n(\lambda r) & r \leq a \\ B I_n(\lambda r) + C K_n(\lambda r) & a \leq r \leq r' \\ D I_n(\lambda r) + E K_n(\lambda r) & r' \leq r \leq c \\ F K_n(\lambda r) & c < r \end{cases} \quad (F-1)$$

$\lambda^2 = \ell^2 + K^2$ as previously indicated.

The following boundary conditions hold:

$$(i) \quad A I_n(\lambda a) = B I_n(\lambda a) + C K_n(\lambda a) \quad (F-2)$$

$$(ii) \quad A \ell I_n'(\lambda a) = B \lambda I_n'(\lambda a) + C \lambda K_n'(\lambda a) \quad (F-3)$$

Eq. F-2 and F-3 allow us to determine

$$A = \frac{B \lambda I_n'(\lambda a) + C \lambda K_n'(\lambda a)}{\ell I_n'(\lambda a)} \quad (F-4)$$

and

$$B = M_n C$$

(F-5a)

where

$$M_n = \frac{\lambda I_n(la) I_n'(\lambda a) - l I_n'(la) I_n(\lambda a)}{l K_n(\lambda a) I_n'(la) - \lambda K_n'(\lambda a) I_n(la)} \quad (F-5b)$$

$$(iii) \quad D I_n(\lambda c) + E K_n(\lambda c) = F K_n(\lambda c) \quad (F-6)$$

$$(iv) \quad D_1 \{ D I_n'(\lambda c) + E K_n'(\lambda c) \} = D_2 F K_n'(\lambda c) \quad (F-7)$$

whence,

$$F = \frac{D_1 \{ D I_n'(\lambda c) + E K_n'(\lambda c) \}}{D_2 K_n'(\lambda c)} \quad (F-8)$$

and

$$D = (D_1 - D_2) \left[\frac{K_n'(\lambda c) K_n(\lambda c) E}{D_2 I_n(\lambda c) K_n'(\lambda c) - D_1 I_n'(\lambda c) K_n(\lambda c)} \right] \quad (F-9)$$

defining

$$Q_n = \frac{K_n'(\lambda c) K_n(\lambda c)}{\{ D_2 I_n(\lambda c) K_n'(\lambda c) - D_1 I_n'(\lambda c) K_n(\lambda c) \}} \quad (F-10)$$

$$D = Q_n E \quad (F-11)$$

Moreover,

$$(v) \quad B I_n(\lambda r') + C K_n(\lambda r') = D \underline{I}_n(\lambda r') + E K_n(\lambda r') \quad (F-12a)$$

By Eq. F-5a and F-11, we have

$$B I_n(\lambda r') + M_n B K_n(\lambda r') = M_n E I_n(\lambda r') + E K_n(\lambda r') \quad (F-12b)$$

$$(vi) \lim_{\epsilon \rightarrow 0} x \frac{dR_n}{dx} \bigg|_{x'-\epsilon}^{x'+\epsilon} = \frac{-q}{\pi D_1} e^{-i[n\theta' + l z']} = f(\theta', z') \quad (F-13)$$

More explicitly, $x' = \lambda r'$

$$x' \{ Q_n E I_n(x') + E K_n(x') - B I_n(x') - M_n B K_n(x') \} = f(\theta', z') \quad (F-14)$$

and by Eq. F-12a

$$B = \frac{Q_n E I_n(x') + E K_n(x')}{I_n(x') + M_n K_n(x')} \quad (F-15)$$

Combining Eq. F-12b and F-14, we find

$$E = \frac{q}{\pi D_1} \left\{ \frac{I_n(x') + M_n K_n(x')}{(1 - M_n Q_n)} \right\} e^{-i[n\theta' + l z']} \quad (F-16)$$

By Eq. F-15

$$B = \frac{q \{ Q_n I_n(x') + \kappa_n(x') \} e^{-i[n\theta' + \ell z']}}{\pi D_1 (1 - M_n Q_n)} \quad (F-17)$$

Moreover, from Eq. F-5a

$$C = M_n B$$

so that

$$C = \frac{q M_n \{ Q_n I_n(x') + \kappa_n(x') \} e^{-i[n\theta' + \ell z']}}{\pi D_1 (1 - M_n Q_n)} \quad (F-18)$$

Similarly, by Eq. F-11

$$D = E Q_n \text{ or}$$

$$D = \frac{q Q_n \{ I_n(x') + M_n \kappa_n(x') \} e^{-i[n\theta' + \ell z']}}{\pi D_1 (1 - M_n Q_n)} \quad (F-19)$$

and using Eq. F-8 and F-10

$$F = \frac{q_0}{\pi D_2} \left\{ \frac{Q_n I_n(\lambda r') I_n'(\lambda c) + Q_n M_n K_n(\lambda r') I_n'(\lambda c)}{(1 - M_n Q_n) K_n'(\lambda c)} \right\} e^{-i[n\theta' + \ell z']} \\ + \frac{q_0}{\pi D_2} \left\{ \frac{I_n(\lambda r') K_n'(\lambda c) + M_n K_n(\lambda r') K_n'(\lambda c)}{(1 - M_n Q_n) K_n'(\lambda c)} \right\} e^{-i[n\theta' + \ell z']}$$

(F-20)

Thus by Eq. F-1 we have

$a \leq r \leq r'$

$$R_n(\lambda' r) = \frac{q_0}{\pi D_1} \left\{ \frac{Q_n I_n(\lambda r') I_n(\lambda r) + K_n(\lambda r') K_n(\lambda r)}{(1 - M_n Q_n)} \right\} e^{-i[n\theta' + \ell z']} \\ + \frac{q_0}{\pi D_1} \left\{ \frac{M_n Q_n I_n(\lambda r') K_n(\lambda r) + M_n K_n(\lambda r) K_n(\lambda r')}{(1 - M_n Q_n)} \right\} e^{-i[n\theta' + \ell z']} \quad (F-21)$$

$r' \leq r \leq c$

$$R_n(\lambda' r) = \frac{q_0}{\pi D_1} \left\{ \frac{Q_n I_n(\lambda r') I_n(\lambda r) + Q_n M_n I_n(\lambda r) K_n(\lambda r')}{(1 - M_n Q_n)} \right\} e^{-i[n\theta' + \ell z']} \\ + \frac{q_0}{\pi D_1} \left\{ \frac{I_n(\lambda r') K_n(\lambda r) + M_n K_n(\lambda r') K_n(\lambda r)}{(1 - M_n Q_n)} \right\} e^{-i[n\theta' + \ell z']} \quad (F-22)$$

$r \geq c$

$$\begin{aligned}
 R_n(\lambda'r) = & \frac{q}{\pi D_2} \left\{ \frac{Q_n I_n(\lambda r') I_n'(\lambda c) K_n(\lambda r) + Q_n M_n K_n(\lambda r) K_n(\lambda r') I_n'(\lambda c)}{(1 - M_n Q_n) K_n'(\lambda c)} \right\} e^{-i[n\theta + \ell z']} \\
 & + \frac{q}{\pi D_2} \left\{ \frac{I_n(\lambda r') K_n(\lambda r) + M_n K_n(\lambda r') K_n(\lambda r)}{(1 - M_n Q_n)} \right\} e^{-i[n\theta + \ell z']} \quad (F-23)
 \end{aligned}$$

Note that if $\lambda = \lambda$, $D_1 = D_2$, $M_n = Q_n = 0$, all the above cases reduce to

$$R_n(\lambda'r) = I_n(\lambda r_<) K_n(\lambda r_>)$$

which when inserted in Eq. IV-1 will generate the spherically symmetric screened coulomb potential.

Appendix G : Equivalence of G_T and ψ_T for a Point Charge on a Salt
Excluding Cylinder

We demonstrate that if $r'=c=a$, Eq. IV-4 reduces to the case of a point charge on a salt excluding, low dielectric constant cylinder, i.e.,

$$R_n(\lambda r) e^{i(n\theta' + lz')} = \frac{q}{\pi D_2} \left\{ I_n(\lambda c) K_n(\lambda r) + \bar{M}_n K_n(\lambda c) K_n(\lambda r) \right\} \quad (G-1)$$

Here

$$\bar{M}_n = \frac{D_1 l I_n'(lc) I_n(\lambda c) - D_2 \lambda I_n'(\lambda c) I_n(lc)}{D_2 \lambda K_n'(\lambda c) I_n(lc) - D_1 l K_n(\lambda c) I_n'(lc)} \quad (G-2)$$

Extensive use will be made of the Wronskian

$$x \left\{ K_n(x) I_n'(x) - K_n'(x) I_n(x) \right\} = 1 \quad (G-3)$$

It is more convenient to rewrite Eq. G-1 in the following form

$$\begin{aligned}
 R_n(\lambda r) e^{i[n\theta + \ell z']} &= \frac{q \kappa_n(\lambda r)}{\pi D_2 W} \left\{ D_2 \lambda \kappa_n'(\lambda c) I_n(\ell c) I_n(\lambda c) - D_1 \ell \kappa_n(\lambda c) I_n'(\ell c) I_n(\lambda c) \right\} \\
 &+ \frac{q \kappa_n(\lambda r)}{\pi D_2 W} \left\{ D_1 \ell \kappa_n(\lambda c) I_n'(\ell c) I_n(\lambda c) - D_2 \lambda \kappa_n(\lambda c) I_n'(\lambda c) I_n(\ell c) \right\}
 \end{aligned}
 \tag{G-4a}$$

$$W = D_2 \lambda \kappa_n'(\lambda c) I_n(\ell c) - D_1 \ell \kappa_n(\lambda c) I_n'(\ell c)$$

$$R_n e^{i[n\theta + \ell z']} = \frac{-q \kappa_n(\lambda r) I_n(\ell c)}{\pi \left\{ D_2 \lambda c \kappa_n'(\lambda c) I_n(\ell c) - D_1 \ell c \kappa_n(\lambda c) I_n'(\ell c) \right\}}
 \tag{G-4b}$$

Now, setting $c=r'=a$ in Eq. IV-4 we obtain

$$R_n(\lambda r) e^{i[n\theta + \ell z']} = f(r) \tag{G-5a}$$

$$\begin{aligned}
 f(r) &= q \kappa_n(\lambda r) \frac{\{ Q_n I_n'(\lambda c) I_n(\lambda c) + Q_n I_n'(\lambda c) \kappa_n(\lambda c) \}}{\pi D_2 (1 - M_n Q_n) \kappa_n'(\lambda c)} \\
 &+ q \kappa_n(\lambda r) \frac{\{ I_n(\lambda c) + M_n \kappa_n(\lambda c) \}}{\pi D_2 (1 - M_n Q_n)}
 \end{aligned}
 \tag{G-5b}$$

$$f(r) = \frac{q_b \kappa_n(\lambda r) \{ D_2 I_n(\lambda c) [I_n(\lambda c) \kappa_n'(\lambda c) - I_n'(\lambda c) \kappa_n(\lambda c)] \}}{\pi D_2 (1 - M_n Q_n) T}$$

$$+ \frac{q_b \kappa_n(\lambda r) \{ D_2 M_n \kappa_n(\lambda c) [I_n(\lambda c) \kappa_n'(\lambda c) - \kappa_n(\lambda c) I_n'(\lambda c)] \}}{\pi D_2 (1 - M_n Q_n) T} \quad (G-5c)$$

$$T = D_2 I_n(\lambda c) \kappa_n'(\lambda c) - D_1 I_n'(\lambda c) \kappa_n(\lambda c)$$

$$f(r) = \frac{-q_b \kappa_n(\lambda r) \{ I_n(\lambda c) + M_n \kappa_n(\lambda c) \}}{\pi D_2 (1 - M_n Q_n) \{ D_2 I_n(\lambda c) \kappa_n'(\lambda c) - D_1 I_n'(\lambda c) \kappa_n(\lambda c) \}} \quad (G-6)$$

We now examine the denominator of Eq. G-6, D_e

$$D_e = \pi \lambda c \left\{ D_2 \lambda I_n(\lambda c) \kappa_n'(\lambda c) \frac{1}{\lambda c} - D_1 \frac{\ell}{\lambda c} I_n'(\lambda c) \kappa_n(\lambda c) \right\} \gamma^{-1} \quad (G-7a)$$

$$\gamma = \ell \kappa_n(\lambda c) I_n'(\lambda c) - \lambda \kappa_n'(\lambda c) I_n(\lambda c)$$

$$D_e = \pi \left\{ D_2 \lambda I_n(\lambda c) \kappa_n'(\lambda c) - D_1 \ell I_n'(\lambda c) \kappa_n(\lambda c) \right\} \gamma^{-1} \quad (G-7b)$$

Using Eq. G-7b in Eq. G-6; we have

$$f(r) = \frac{-q \kappa_n(\lambda r) \{ I_n(\lambda c) + [\lambda I_n(lc) I_n'(\lambda c) - l I_n(\lambda c) I_n'(lc)] \delta^{-1} \}}{\pi \{ D_2 \lambda I_n(lc) \kappa_n'(\lambda c) - D_1 l I_n'(lc) \kappa_n(\lambda c) \}} \quad (G-8)$$

Examining the numerator of Eq. G-8 we have

$$N = -q \kappa_n(\lambda r) \{ l \kappa_n(\lambda c) I_n'(lc) I_n(\lambda c) - \lambda \kappa_n'(\lambda c) I_n(lc) I_n(\lambda c) \\ - l I_n(\lambda c) I_n'(lc) \kappa_n(\lambda c) + \lambda \kappa_n(\lambda c) I_n'(lc) I_n(lc) \}$$

$$N = -q \kappa_n(\lambda r) \{ \lambda I_n(lc) [I_n'(\lambda c) \kappa_n(\lambda c) - \kappa_n'(\lambda c) I_n(\lambda c)] \} \quad (G-9a)$$

$$N = -q \kappa_n(\lambda r) I_n(lc) c^{-1} \quad (G-9b)$$

Substituting Eq. G-9b into Eq. G-8 we obtain

$$f(r) = \frac{-q \kappa_n(\lambda r) I_n(lc)}{\pi \{ D_2 \lambda \kappa_n'(\lambda c) I_n(lc) - D_1 l c I_n'(lc) \kappa_n(\lambda c) \}} \quad (G-10)$$

which is identical to Eq. G-4b. Therefore, we have demonstrated the equivalence of Eq. IV-4 to Eq. II-24 when $r'=c=a$.

Appendix H: Derivation of Asymptotic Large Z Limit of G_T

In this appendix, we evaluate $G_T(r, r')$ in the limit of large $Z-Z'$.

When $r < c$, by Eq. IV-9

$$G_b = \frac{2q}{\pi D_1} \int_0^\infty dl \cos l z_\infty \left[Q_0 I_0(\lambda r) I_0(\lambda r') + 2 \sum_{n=1}^\infty Q_n I_n(\lambda r) I_n(\lambda r') \cos n(\theta'') \right]$$

$$z_\infty = |z - z'|, \quad \theta'' = \theta - \theta' \quad (H-1)$$

For $r > c$, it follows from Eq. IV-10

$$G_b = \frac{2q}{\pi D_2} \int_0^\infty dl \cos l z_\infty \left\{ \frac{Q_0 I_0(\lambda r') I_1(\lambda c) K_0(\lambda r)}{-K_1(\lambda c)} + \sum_{n=1}^\infty \frac{Q_n I_n(\lambda r') I_n'(\lambda c) K_n(\lambda r) \cos n\theta''}{K_n'(\lambda c)} \right\} \quad (H-2)$$

where

$$Q_n = \frac{(D_1 - D_2) K_n'(\lambda c) K_n(\lambda c)}{\{ D_2 I_n(\lambda c) K_n'(\lambda c) - D_1 I_n'(\lambda c) K_n(\lambda c) \}} \quad (H-3)$$

The $r < c$ case is treated first.

If $n \neq 0$.

$$Q_n I_n(\lambda r') I_n(\lambda r) = \frac{(D_1 - D_2) K_n'(\lambda c) K_n(\lambda c) I_n(\lambda r) I_n(\lambda r')}{\{D_2 I_n(\lambda c) K_n'(\lambda c) - D_1 I_n'(\lambda c) K_n(\lambda c)\}} \quad (H-4)$$

As derived explicitly in Appendix C if $x \ll 1$

$$x K_n'(x) \sim -n K_n(x)$$

$$x I_n'(x) \sim n I_n(x)$$

Hence, when $kc \ll 1$ and $n \neq 0$

$$Q_n I_n(\lambda r) I_n(\lambda r') \sim \frac{(D_1 - D_2) K_n^2(\lambda c) I_n(\lambda r) I_n(\lambda r')}{\{D_2 I_n(\lambda c) K_n(\lambda c) + D_1 I_n(\lambda c) K_n(\lambda c)\}} \quad (H-5a)$$

$$D_2 \gg D_1$$

$$Q_n I_n(\lambda r) I_n(\lambda r') \sim \frac{(D_1 - D_2) K_n(\lambda c) I_n(\lambda r r' / c)}{(D_2 + D_1)} \quad (H-5b)$$

For $n=0$

$$Q_0 I_0(\lambda r) I_0(\lambda r') = \frac{(D_1 - D_2) \{ K_1(\lambda c) K_0(\lambda c) I_0(\lambda r) I_0(\lambda r') \}}{\{ D_2 K_1(\lambda c) I_0(\lambda c) + D_1 I_1(\lambda c) K_0(\lambda c) \}} \quad (H-6a)$$

$$\sim \frac{(D_1 - D_2) K_0(\lambda c) I_0(\lambda d)}{D_2} \quad (H-6b)$$

$d = rr'/c$. Employing Eq. H-5b and H-6b in Eq. H-1,

$$\lim_{z_\infty \rightarrow \infty} G_b = \frac{2q}{\pi D_1} \int_0^\infty d \cos \theta z_\infty [\kappa_0(\lambda) \rho_d - \kappa_0(\lambda c) I_0(\lambda d)] \frac{[D_1 - D_2]}{(D_2 + D_1)} \quad (H-7a)$$

$$+ \frac{2q}{\pi D_1} \int_0^\infty d \cos \theta z_\infty \left[\frac{D_1 - D_2}{D_2} \right] \kappa_0(\lambda c) I_0(\lambda d)$$

with $z_\infty = |z - z'|$, $\rho_d = (c^2 + d^2 - 2cd \cos(\theta - \theta'))^{1/2}$

$$\lim_{z_\infty \rightarrow \infty} G_b = \frac{q(D_1 - D_2)}{D_1(D_1 + D_2)} \frac{e^{-\lambda(z_\infty^2 + \rho_d^2)^{1/2}}}{(z_\infty^2 + \rho_d^2)^{1/2}} +$$

$$\frac{q(D_1 - D_2)}{D_2(D_1 + D_2)} \frac{e^{-\lambda(z_\infty^2 + c^2)^{1/2}}}{(z_\infty^2 + c^2)^{1/2}} \quad (H-7b)$$

Consequently it follows from Eq. H-7b that if $Kr_s \ll 1$

$$\lim_{z_\infty \rightarrow \infty} G_T = \frac{q e^{-x z_\infty}}{D_2 z_\infty} - \frac{q e^{-x z_\infty}}{2 D_1 z_\infty^2} (x + z_\infty^{-1}) (r^2 + r'^2 - c^2 - \frac{r^2 r'^2}{c^2}) + \frac{q e^{-x z_\infty}}{2 D_2 z_\infty^2} (x + z_\infty^{-1}) (4 r r' \cos \theta'' - r^2 - r'^2 - \frac{r^2 r'^2}{c^2}) \quad (H-8)$$

The second term on the right hand side represents the influence of the low dielectric region on G_T . It is trivially demonstrated that

$$G_{\text{low dielectric}}(r, r') = - \frac{q e^{-x z_\infty}}{2 D_1 z_\infty^2} (x + z_\infty^{-1}) (r^2 + r'^2 - c^2 - \frac{r^2 r'^2}{c^2}) \quad (H-9)$$

is a monotone decreasing function of r and r' . Moreover, since

$$G_{\text{low dielectric}}(r, r') = 0 \text{ when } r = r' = c; \quad G_{\text{low dielectric}}(r, r') > 0 \text{ if } r, r' \leq c$$

Physically, this agrees with the notion that as we move either the test or point charge from the low dielectric region to the high dielectric region the potential must decrease as a function of r and r' . The third term on the rhs of Eq. H-8 accounts for that portion of the higher order terms in the potential characteristic of a point charge in bulk solvent; it is a non-increasing function of r and r' .

We now examine the $r \geq c$ case. From Eq. F-2

$$\frac{Q_n I_n(\lambda r) I_n'(\lambda c) K_n(\lambda r)}{K_n'(\lambda c)} = \frac{(D_1 - D_2) K_n(\lambda c) K_n(\lambda r) I_n(\lambda c) I_n(\lambda r')}{\{D_2 I_n(\lambda c) K_n'(\lambda c) - D_1 I_n'(\lambda c) K_n(\lambda c)\}} \quad (\text{H-10})$$

Let $Kr_s \ll 1$ and if $n \neq 0$,

$$\frac{Q_n I_n(\lambda r) I_n'(\lambda c) K_n(\lambda r)}{K_n'(\lambda c)} \sim \frac{(D_2 - D_1) I_n(\lambda r') K_n(\lambda r)}{D_2} \quad (\text{H-11})$$

When $n=0$

$$\frac{Q_0 I_0(\lambda r') I_1(\lambda c) K_0(\lambda r)}{-K_1(\lambda c)} = \frac{(D_2 - D_1) K_0(\lambda c) I_1(\lambda c) I_0(\lambda r') K_0(\lambda r)}{D_2 I_0(\lambda c) K_1(\lambda c)} \quad (\text{H-12})$$

It can be shown that if $Kr_s \ll 1$, it follows from Eq. H-11 and H-2 that

$$\lim_{z \rightarrow \infty} G_b(r, z, c) = \frac{Q_0 (D_2 - D_1)}{D_2} \int_0^{\infty} d\lambda \cos \lambda z_{\infty} [K_0(\lambda r') - K_0(\lambda r)]$$

$$r = (r'^2 + r^2 - 2rr' \cos \theta)''^{1/2} \quad (\text{H-13a})$$

$$\lim_{z_{\infty} \rightarrow \infty} \psi_b(r, z, c) = \frac{q e^{-\kappa z_{\infty}}}{2 D_2 z_{\infty}^2} (\kappa + z_{\infty}^{-1}) (2 r r' \cos \theta'' - r'^2)$$

(H-13b)

and $r \geq c$

$$\lim_{z_{\infty} \rightarrow \infty} G_T(r, z, c) = \frac{q e^{-\kappa z_{\infty}}}{D_2 z_{\infty}} + \frac{q e^{-\kappa z_{\infty}}}{2 D_2 z_{\infty}^2} (\kappa + z_{\infty}^{-1}) (4 r r' \cos \theta'' - r^2 - 2 r'^2)$$

(H-13c)

The second term on the rhs takes account of both the radial variation at large z_{∞} and the boundary perturbation term. Note that for fixed r , it is a strictly decreasing function of r' . As one moves the charge outside the dielectric region the potential must decrease. When viewed from outside the cylinder, in the asymptotic limit, the point charge appears to be immersed in bulk solvent. Whether increasing r results in an increase or decrease in the potential (for r values near r'), depends on the angular separation between the test and point charge. See the discussion at the end of Appendix C for an analogous situation.

Appendix J : Formal Calculation of $\Delta\psi^{line}$

We explicitly calculate $\Delta\psi^{line}$ due to an infinite line of charge embedded on the surface of a low dielectric cylinder.

It immediately follows from Eq. V-6a with $p=\infty$ and $\theta=0$ that

$$\Delta\psi^{line} = 2\beta \left\{ \frac{\kappa_0(\lambda a)}{D_2 \lambda a \kappa_1(\lambda a)} + 2 \sum_{n=1}^{\infty} \Delta h_n^{line} \right\} \quad (J-1)$$

where

$$\Delta h_n^{line} = \lim_{p \rightarrow \infty} \{ h_n(2\pi n/p) - h_n^0(2\pi n/p) \} \quad (J-2a)$$

any by Eq. II-34a

$$h_n(x) = \frac{-\kappa_n(\lambda a) I_n(x)}{[D_2 \lambda a \kappa'_n(\lambda a) I_n(x) - D_1 x I'_n(x) \kappa_n(\lambda a)]} \quad (J-2b)$$

$$h_n^0(x) = \frac{-\kappa_n(x) I_n(x)}{\{D_2 x I_n(x) \kappa'_n(x) - D_1 x \kappa_n(x) I'_n(x)\}} \quad (J-2c)$$

It follows from our discussion in Appendix C that

$$\lim_{x \rightarrow 0} x I_n'(x) = n I_n(x) \quad (\text{J-3a})$$

$$\lim_{x \rightarrow 0} x K_n'(x) = -n K_n(x) \quad (\text{J-3b})$$

Inserting J-3a and J-3b into Eq. J-2c, we have

$$\lim_{x \rightarrow 0} h_n^0(x) = \lim_{x \rightarrow 0} \frac{-K_n(x) I_n(x)}{[-D_2 n K_n(x) I_n(x) - D_1 n I_n(x) K_n(x)]} \quad (\text{J-4a})$$

$$\lim_{x \rightarrow 0} h_n^0(x) = \frac{1}{n(D_2 + D_1)} \quad (\text{J-4b})$$

Similarly,

$$\lim_{x \rightarrow 0} h_n(x) = \lim_{x \rightarrow 0} \frac{-K_n(\lambda a) I_n(x)}{\{D_2 \lambda a K_n'(\lambda a) I_n(x) - D_1 n I_n(x) K_n(\lambda a)\}} \quad (\text{J-5a})$$

$$\lim_{x \rightarrow 0} h_n(x) = \frac{-K_n(\lambda a)}{\{D_2 \lambda a K_n'(\lambda a) - D_1 n K_n(\lambda a)\}} \quad (\text{J-5b})$$

For arbitrary values of Ka ,

$$Ka \kappa'_n(Ka) = -n \kappa_n(Ka) - Ka \kappa_{n-1}(Ka) \quad (J-5c)$$

Hence,

$$\lim_{Ka \rightarrow 0} h_n(x) = \left\{ (D_2 + D_1)n + D_2 Ka \frac{\kappa_{n-1}(Ka)}{\kappa_n(Ka)} \right\}^{-1} \quad (J-5d)$$

Thus

$$\Delta \psi^{line} = a\beta \left\{ \frac{\kappa_0(Ka)}{D_2 Ka \kappa_1(Ka)} + 2 \sum_{n=1}^{\infty} \Delta h_n^{line} \right\} \quad (J-6a)$$

where

$$\Delta h_n^{line} = \left\{ \left[(D_2 + D_1)n + D_2 Ka \frac{\kappa_{n-1}(Ka)}{\kappa_n(Ka)} \right]^{-1} - [n(D_2 + D_1)]^{-1} \right\} \quad (J-6b)$$

Note that $\lim_{Ka \rightarrow 0} \frac{Ka \kappa_{n-1}(Ka)}{\kappa_n(Ka)} \rightarrow 0$ as $Ka \rightarrow 0$; i.e. $\Delta h_n \rightarrow 0$ as $Ka \rightarrow 0$.

Appendix K: Discrete Charge Wormlike Model with No Rearrangements or Fluctuations

The discrete model with no charge rearrangements or fluctuations is treated. Using the approximations employed in case (i), the potential energy, V' , at a given charge site is

$$V' = \frac{q^2}{D} \sum_{j=1}^{\infty} \frac{e^{-x_j a/\alpha}}{24R_c^2(0)} \{ ja/\alpha + \kappa^2 j^2 a^2 \alpha^{-2} \} \quad (K-1)$$

Equation K-1 is essentially the discrete version of Eq. VIII-14. Here a single sum is employed to correct for over counting.

Consider the sum

$$\psi(\kappa a \alpha^{-1}) = \sum_{j=1}^N e^{-x_j a \alpha^{-1}} = \frac{(1 - e^{-\kappa a \alpha^{-1}(N+1)})}{(1 - \exp(-\kappa a \alpha^{-1}))} - 1$$

In the limit that $N \rightarrow \infty$

$$\psi(\kappa a \alpha^{-1}) = (1 - \exp\{-\kappa a \alpha^{-1}\}) - 1 \quad (K-2)$$

Furthermore,

$$-\frac{d\psi}{dx} = \sum_{j=1}^{\infty} (ja\alpha^{-1}) e^{-j\kappa a\alpha^{-1}} = \frac{a\alpha^{-1} e^{-\kappa a\alpha^{-1}}}{(1 - \exp(-\kappa a\alpha^{-1}))^2} \quad (\text{K-3})$$

$$\frac{d^2\psi}{dx^2} = \frac{a^2 \alpha^{-2} \exp(-\kappa a\alpha^{-1})}{(1 - \exp(-\kappa a\alpha^{-1}))^2} + \frac{2a^2 \alpha^{-2} e^{-2\kappa a\alpha^{-1}}}{(1 - e^{-\kappa a\alpha^{-1}})^3} \quad (\text{K-4})$$

Substituting the expressions of Eq. K-3 and K-4 into Eq. K-1, we obtain

$$V' = \frac{q^2}{24R_c^2(0)} \left\{ \frac{(a\alpha^{-1} + \kappa a^2 \alpha^{-2}) e^{-\kappa a\alpha^{-1}}}{(1 - e^{-\kappa a\alpha^{-1}})^2} + \frac{2\kappa a^2 \alpha^{-2} e^{-2\kappa a\alpha^{-1}}}{(1 - e^{-\kappa a\alpha^{-1}})^3} \right\} \quad (\text{K-5})$$

To pass from the discrete to the continuum model, we must let $\kappa a\alpha^{-1} \rightarrow 0$ subject to the constraint that aq/a remains fixed. Since V' is the potential energy experienced by a point charge on a segment of length $a\alpha^{-1}$, the potential energy per unit length, V , equals $V'aq\alpha^{-1}$. Expanding the exponentials in Eq. K-5

$$V = \frac{\alpha^2 q^2}{24R_c^2(0)} \left\{ \frac{(1 - \kappa^2 a^2 \alpha^{-2})}{\kappa^2} + \frac{2(1 - 2\kappa a\alpha^{-1})}{\kappa^2} \right\} \quad (\text{K-6})$$

and

$$\lim_{x\alpha^{-1} \rightarrow 0} V = \frac{\alpha^2 \Gamma_0^2}{8x^2 D R_c^2(0)}$$

(K-7)

In exact agreement with Eq. VIII-19.

REFERENCES

1. J. G. Kirkwood and F. H. Westheimer, J. Chem. Phys., 6, 506 (1938).
2. F. H. Westheimer and J. G. Kirkwood, J. Chem. Phys., 6, 513 (1938)
3. E. P. Buff, N. S. Goel and J. R. Clay, J. Chem. Phys., 63, 1367 (1975).
4. D. L. Beveridge and G. W. Schnuelle, J. Phys. Chem., 79, 2562 (1975).
5. F. R. Harris and S. A. Rice, J. Chem. Phys., 25, 955 (1935).
6. T. L. Hill, Arch. Biochem. Biophys., 57, 229 (1955).
7. G. Manning, J. Chem. Phys., 51, 924, 3249 (1969).
8. G. Manning and A. Holtzer, J. Phys. Chem., 77, 2206 (1973).
9. G. Manning, Biophys. Chem., 7, 95 (1977).
10. J. H. Bailey, Biopolymers, 12, 1705 (1973).
11. K. Iwasa, J. Chem. Phys., 62, 2967 (1975).
12. A. D. MacGillvray and J. J. Winkleman, J. Chem. Phys., 45, 2184 (1966.)
13. A. D. MacGillvray, J. Chem. Phys., 56, 80, 83 (1972).
14. A. D. MacGillvray, J. Chem. Phys., 57, 4071, 4075 (1972).
15. M. Abramowitz, I. A. Stegun, "Handbook of Mathematical Functions", Dover Publications, Inc., New York, N.Y., 1972. Their notation for the various Bessel functions is employed throughout the thesis.
16. L. D. Landau, E. M. Lifshitz, "Electrodynamics of Continuous Media", Addison-Wesley Publishing Company, Inc., Reading, Mass., 1960, p. 40.
17. J. L. Kraut, "Fundamentals of Mathematical Physics", McGraw-Hill, New York, N. Y., 1967.
18. G. N. Watson, "Theory of Bessel Functions", Cambridge University Press, London, England, 1966, Chapter 11.
19. A. Erdelyi, ed., "Tables of Integral Transforms: Bateman Manuscript Project", Mac-Graw-Hill, New York, N. Y., 1954, Vol. I, p. 56.
20. M. J. Lighthill, "Fourier Analysis and Generalized Functions", Cambridge University Press, London, England, 1973.
21. H. B. Dwight, "Tables of Integrals and Other Mathematical Data", The Macmillan Co., New York, N. Y., 1957, Chapter 10.
22. See Appendix K for a discussion of the applicability of a continuous versus a discrete charge distribution.

23. I Noda, T. Tsuge, M. Nagasawa, J. Phys. Chem., 74, 710 (1970).
24. Z. Alexandrowicz, J. Chem. Phys., 47, 4377 (1967).
25. We shall discuss excluded volume theory in greater detail in the following chapter.
26. A. Takahashi and M. Nagasawa, J. Am. Chem. Soc., 86, 548 (1964).
27. H. Eisenberg and D. Woodside, J. Chem. Phys., 36, 1844 (1962).
28. T. Kurucsev, Rev. Pure and Appl. Chem., 14, 147 (1964).
29. S. A. Rice and M. Nagasawa, "Polyelectrolyte Solutions", Academic Press, New York, N. Y., 1961, p. 416.
30. H. Yamakawa, "Modern Theory of Polymer Solutions", Academic Press, New York, N. Y., 1969, Section 9c.
31. Recently, it has come to our attention that there is an alternative derivation of Eq. VIII-21 as presented in Appendix K. See T. Odijk, J. Poly. Sci., 15, 477 (1977).
32. See discussion preceding Eq. VIII-25. In fact, even if we do not make the assumption that $\gamma(s) \sim \gamma(s')$, the results of case (iii) will still hold.
33. F. Oosawa, Biopolymers, 9, 677 (1970).
34. In the derivation of this equation we have assumed R_c^{-2} is constant. If it isn't, the integrals in Eq. VIII-38 could be broken up into pieces where R_c^{-2} is constant. The essential results still remain the same.
35. R. Feynmann, "Statistical Mechanics. A Set of Lectures", W. A. Benjamin, Inc., Reading, Mass., 1974.
36. M. Nagasawa and A. Holtzer, J. Am. Chem. Soc., 86, 538 (1966).
37. J. Hermans, J. Am. Chem. Soc., 88, 2416 (1966).
38. M. Nagasawa, T. Murase and A. Kondo, J. Phys. Chem., 69, 4005 (1965).
39. N. S. Schneider and P. Doty, J. Phys. Chem., 58, 762 (1954).
40. S. A. Rice and F. E. Harris, J. Phys. Chem., 58, 733 (1954).
41. N. Saito, K. Takahashi and Y. Yunoko, J. Phys. Soc. Jap., 22, 219 (1967).
42. See Reference 7 for justification of this approximation.
43. L. M. Gross and U. P. Strauss in "Chemical Physics of Ionic Solutions", B. E. Conway and R. G. Barradas, Eds., John Wiley & Sons, Inc., New York, N. Y., 1966, p. 347.

44. M. Nagasawa and A. Takahashi, in M. B. Huglin, ed., "Light Scattering from Polymer Solutions", Academic Press; New York, N. Y., 1972, Chapter 16.
45. M. Fixman, J. Chem. Phys., 41, 3772 (1964).
46. J. Skolnick and M. Fixman, Macromolecules, 10, 944 (1977). See also Chapter 3.
47. T. Odijk, J. Polym. Sci., (Phys. Ed.), 15, 477 (1977).
48. G. Weill, "Persistence Length of DNA as a Function of Ionic Strength and the Problem of the Electrostatic Contribution to Persistence Lengths". Preprint.
49. T. Odijk and M. Mandel, "The Influence of Chain Flexibility on the Colligative Properties of Polyelectrolyte Solutions", Preprint.
50. T. Odijk and A. C. Houwaart, "On the Theory of the Excluded Volume Effect of a Polyelectrolyte in a 1-1 Electrolyte Solution", Preprint, J. Poly. Sci., (Phys. Ed.).
51. See Chapter 2.
52. L. Kotin and M. Nagasawa, J. Chem. Phys., 36, 873 (1962).
53. L. Onsager, Ann. N. Y. Acad. Sci., 51, 627 (1949).
54. H. Yamakawa and G. Tanaka, J. Chem. Phys., 55, 3188 (1971).
55. G. E. Boyd and D. P. Wilson, J. Phys. Chem., 80, 805 (1975).
56. J. Skerjanc, Biophys. Chem., 1, 376 (1974).
57. T. Orofino and P. J. Flory, J. Phys. Chem., 63, 283 (1959).